Diploma Thesis

Retention of Western Baltic Herring Larvae within the Main Spawning Area

Robert Bauer

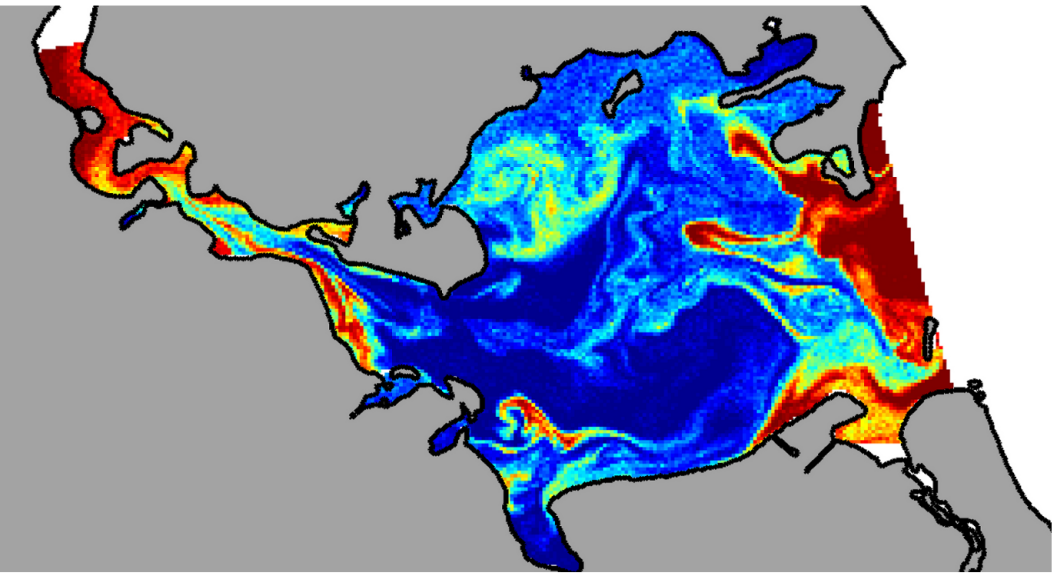

Johann Heinrich von Thünen-Institut

Leibniz Institute for Baltic Sea Research Warnemünde

First Examiner:

PD Dr. Cornelius Hammer

Institute of Baltic Sea Fisheries

Alter Hafen Süd 2

18069 Rostock

Germany

Second Examiner:

Prof. Dr. Hans Burchard

Leibniz Institute for Baltic Sea Research

Seestraße 15

18119 Warnemünde

Germany

"Essentially, all models are wrong, but some are useful."

(George Edward Pelham Box)

Contents

List of Abbreviations

2-D two-dimensional

3-D three-dimensional

BSH German Federal Maritime and Hydrographic Agency

BSM Baltic Sea Model

CW calendar week

DaMSA Danish Maritime Safety Administration

DWD German Weather Service

GETM General Estuarine Transport Model

GSA Greifswalder Bodden - Strelasund area

GWB Greifswalder Bodden

GWBM Greifswalder Bodden Model

IBM Individual Based Model

MOM Modular Ocean Model

MSL mean sea level

PNR point of no return

POP persistent organic pollutant

RHLS Rügen Herring Larvae Survey

SLD Sea level deviation

VM vertical migration

VPA Virtual Population Analysis

WBSM Western Baltic Sea Model

WBSS Western Baltic Spring Spawning Herring

Abstract

During 2004-2008, recruitment success of Western Baltic Spring-Spawning herring (WBSS) has shown an unprecedented decline. The reasons for this development are currently unknown. Among others, larval drift is one crucial factor that is known to affect larval survival and therefore could influence recruitment success. This might be of particular importance for WBSS which spawn in semi-enclosed waters that are assumed to provide more suitable conditions for larval survival than the surrounding open Baltic Sea.

Within this study, the risk of herring larval dispersal from the Greifswalder Bodden (GWB), the main spawning area of WBSS to the adjacent Baltic Sea has been analyzed. Larval drift was simulated by a two-dimensional Lagrangian particle tracking model which was forced by depth-integrated flow fields derived from a high resolution three-dimensional hydrodynamic model. Drift patterns under constant and real wind conditions were investigated. Focus was set on the WBSS spawning seasons in 2008 and 2009, two years with contrasting recruitment success. Finally, a retention index was defined which estimates the percentage of remained larvae during both years, based on calculated retention probabilities of virtual cohorts and larval abundances found in the GWB during the Rügen herring larvae survey in 2008 and 2009.

The results impressively demonstrate that for all scenarios tested, a significant proportion of larvae remained in the GWB. Intra- and inter-annual differences in the amount of removed larvae were low. Taken together, larval drift can not explain the observed recruitment failure of WBSS in 2008. By contrast, results suggest that larval retention is a crucial and stable feature of the life strategy of WBSS.

Zusammenfassung

Der Rekrutierungserfolg des frühjahrslaichenden Herings der westlichen Ostsee (WBSS) verzeichnete von 2004 bis 2008 einen dramatischen Rückgang. Die Ursachen dieser Entwicklung sind bislang noch nicht geklärt. Ein Prozess der sich entscheidend auf das Überleben von Fischlarven auswirken kann, stellt die Verdriftung von Larven aus nahrungsreichen Gebieten dar. Die Verdriftung mag dabei insbesondere für den Rekrutierungserfolg des WBSS von Bedeutung sein, welche maßgeblich die inneren Küstengewässer der Ostsee zum Laichen aufsuchen. Diese Gebiete gelten im Vergleich zur offenen Ostsee als besonders produktiv.

Im Rahmen dieser Arbeit wurde das Risiko der Verdriftung von Heringslarven aus dem Greifswalder Bodden (GWB), dem Hauptlaichgebiet des WBSS, hin zur umliegenden Ostsee untersucht. Die Verdriftung von Heringslarven wurde dabei mit Hilfe eines zweidimensionalen Lagrange'schen Modells zur Verfolgung von passiven Teilchen simuliert, welches auf tiefen-integrierte Strömungsfelder eines dreidimensionalen hydrodynamischen Modells zurückgreift. Modellsimulationen wurden sowohl für konstante als auch für reale Windverhältnisse durchgeführt. Letztere stammen aus den Jahren 2008 und 2009, zwei Jahre mit besonders gegensätzlichem Rekrutierungserfolg. Zuletzt wurde ein Retentionsindex definiert, welcher, basierend auf der berechneten Retentionswahrscheinlichkeit virtueller Kohorten und dem verzeichnetem Larvenaufkommen in den Modelljahren, den Anteil im Bodden verbliebener Larven beschreibt.

Die Ergebnisse zeigen eindrucksvoll, dass bei allen untersuchten Szenarien ein signifikanter Anteil an Larven im GWB verblieb. Inner- und zwischenjährliche Unterschiede in der Menge verdrifteter Larven sind sehr gering. Zusammengefasst kann die Verdriftung der Heringslarven zur offenen Ostsee nicht den verzeichneten Rekrutierungseinbruch des WBSS im Jahr 2008 erklären. Dagegen legen die Ergebnisse den Schluss nahe, dass die Retention der Heringslarven ein grundlegendes und stabiles Merkmal in der Lebenstrategie des WBSS darstellt.

1 Introduction

1.1 Western Baltic Spring-Spawning Herring

The name "herring" refers to the family Clupeidae, which represents a basal group within the Teleostei. This family consists of 188 mainly planktivorous marine species, although some predatory and many freshwater or anadromous species exist (Nelson, 2006). Many of its members form large pelagic schools and are of higher ecological and commercial importance. This applies especially to the two species of the genus Clupea, the Pacific herring (*Clupea pallasii*) and the Atlantic herring (*Clupea harengus*).

Atlantic herring is widely distributed throughout the continental shelves on both sides of the North Atlantic. Spawning seasons and grounds differ among populations. Often autumn and spring spawners are separated. While the North Sea stocks are dominated by autumn spawners, Norwegian and Baltic stocks comprise mainly spring spawners. However, autumn spawners were abundant within the Baltic until the 1960s (Anwand, 1962; Rechlin, 1991, 2000). In addition, Baltic herring stocks differ from their relatives in other regions in some morphological and physiological characteristics (Klinkhardt, 1996). Baltic herring possess a smaller number of vertebrae and reach a smaller size at age. In addition, Baltic stocks mature at younger age and at lower salinities. Though, these characteristics are not consistent within the Baltic herring stocks, showing a gradual trend with increasing distance from the North Sea. Currently, 5 different assessment units are distinguished by fishery management within the Baltic Sea (ICES, 1998): I.) The Western Baltic herring (ICES Subdivisions 22-24), II.) the Central Baltic herring (ICES Subdivisions 25-27, 28.2, 29 & 32), III.) the Gulf of Riga herring (ICES Subdivision 28.1), IV.) the Bothnian Sea herring (ICES Subdivision 30) and V.) the Bothnian Bay herring (ICES Subdivision 31). Together with sprat, these herring stocks represent the main pelagic fish resources of the Baltic Sea. Thereby, herring stocks may consist different sub-populations. Thus, Western Baltic herring is further separated in spring and autumn spawners.

Annual migrations between feeding, spawning and overwintering areas are quite common among herring populations. During the summer months, Western Baltic Spring-Spawning herring (WBSS) migrate to the Skagerrak and the adjacent parts of the North Sea (Figure 1). The Skagerrak and the Kattegat also serve as nursery grounds for North Sea autumn spawners (ICES, 2007). Therefore, mixing of two distinct stocks occurs within this area, which makes stock assessment difficult (Gröger & Gröhsler, 2001). Common techniques used to separate these stocks are otolith microstructure analyses and counting the number of vertebrae (ICES, 1998; s.a.).

After overwintering in the Sound, the Belts and the Western Baltic Seas, WBSS move to their spawning grounds (Nielsen et al., 2001). Like many other herring populations, WBSS spawn in shallow coastal waters. Thereby, spawning of WBSS clearly concentrates during March until May (Klinkhardt, 1996; Jørgensen et al., 2005; Hammer et al., 2009) within the Greifswalder Bodden, the supposed main spawning area (Biester, 1989; ICES, 1998). However, spawning occurs throughout the coastal regions and estuaries of the Western Baltic Sea, with other important spawning grounds being the Kiel Fjord, the inshore Bay of the River Trave and the River Schlei (Kändler, 1952; Rechlin & Bagge, 1996; Klenz, 2000). Generally, herring spawns

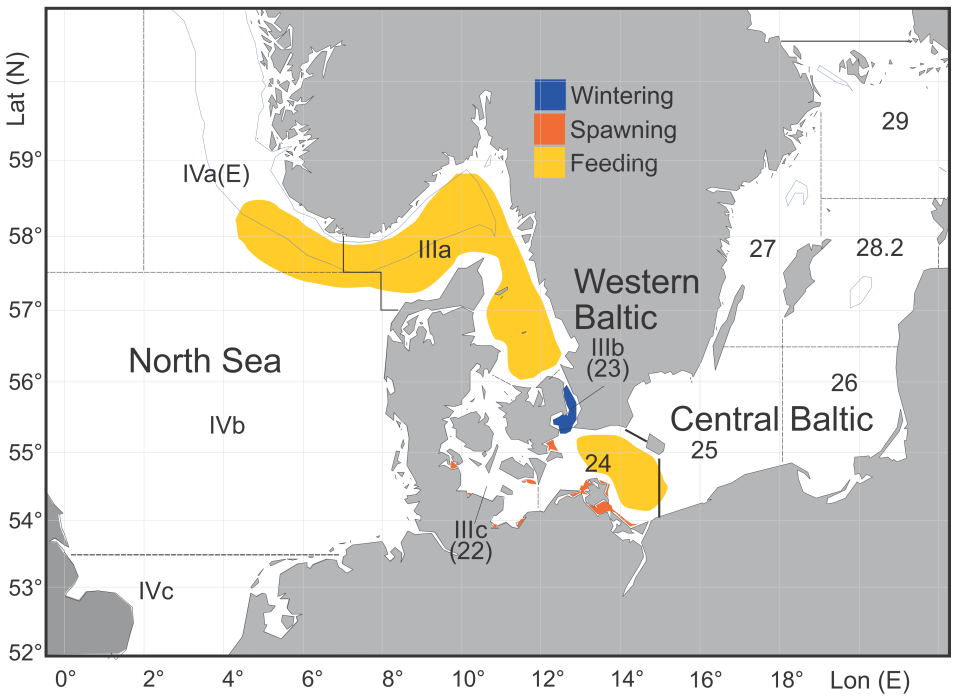

Figure 1: Distribution area of Western Baltic Spring-Spawning herring (WBSS). Wintering, spawning and feeding grounds are colored. Arabic and Roman numerals denote ICES subdivisions. (vTI-OSF, Zimmermann with kind regards)

in batches with older and larger individuals arriving first at the spawning grounds (Lambert, 1987; Klinkhardt, 1996). Unlike most other herring, WBSS do not spawn on stones or gravel. By contrast, eggs are deposited on sea-grass (e.g. *Zostera marina*) and other submerged macrophytes, often in multiple layers (Scabell & Jönsson, 1984; Klinkhardt & Biester, 1985; Scabell, 1988). The number and size of eggs depends on the size, condition and the race of females. WBSS deposit between 11 000 and 80 000 eggs (Anwand, 1962) of 1 to 1.4 mm in diameter, with more and larger eggs being laid by earlier arriving larger females (Puttler, 1972; Hammer et al., 2009). The incubation period is correlated with temperature. Blaxter & Hempel (1963) quoted its range from 7.5 days at 14°C to 24 days at 5°C. The hatching size of herring larvae ranges on average between 5 and 7 mm (Klinkhardt, 1996) and is also related to temperature. Newly hatched larvae are still keeping a yolk sac. This energy source lasts for several days, depending on its size and the environmental temperature. For WBSS larvae at a temperature of 8°C, the yolk sac is resorbed at around 6.5 days after hatching (Klinkhardt, 1996). At higher incubation temperatures of 9-12°C the yolk sac is exhausted after 5–6 days (Puttler, 1972). Generally, yolk-sac absorption is completed earlier by smaller larvae hatched from smaller eggs in the later season due to higher temperature-dependent metabolic rates and smaller yolk reserves (Puttler, 1972; Hammer et al., 2009). Although still carrying this energy source, larvae start feeding on zooplankton before complete yolk resorption. Though, larval food consumption is strongly restricted by mouth width and limited visual perception. As a result, larvae can only consume small, closely located zooplankton. Like all life stages of herring, herring larvae are opportunistic feeders. They prey upon a broad range of planktonic organisms such as diatoms, tintinnids and mollusc larvae, but mainly on calanoid nauplii and

copepodites. In addition, even protozoans are assumed to be an important food source of first feeding larvae (Spittler et al., 1990).

Early larval stages exhibit only a low tolerance against starvation. In this context, Blaxter & Hempel (1963) defined the "point of no return" (PNR) at which starving larvae are no longer able to recover. The time to reach the PNR is related to the larval stage as well as the metabolic rate and thus temperature. According to Yin & Blaxter (1987) starving yolk sac larvae reach the "point of no return" 3 – 5 days after yolk resorption, while 46-day-old Baltic herring larvae endure starvation 6-7 days. Growth rates of herring larvae range from 0.2 to 0.4 mm per day depending on the herring stock, temperature and food availability (Klinkhardt, 1996). Normally, 16-18 weeks after hatching larvae reach a size of 25-35 mm. At this stage, the lateral line canals and the auditory bulla-swim bladder system develop (Hoss & Blaxter, 1979; Blaxter et al., 1983), larvae start metamorphosing into juveniles (Klinkhardt, 1996).

Early juveniles form large schools in coastal waters (Klinkhardt, 1996). Growth rates of juveniles are high during summer and fall. Hence, spring-hatched juveniles can measure up to 100 mm by their first winter (Klinkhardt, 1996). For overwintering, juveniles move to deeper waters. The following spring, 2-year-old juveniles migrate to the feeding grounds where mixing with adults occurs.

The age of maturity differs strongly among herring stocks, ranging from 2-6 years. As other small-sized herring, Baltic herring are reported to mature earlier, often after 2 years.

1.2 Stock Development of WBSS

Spawning stock biomass (SSB) of WBSS has been decreasing since the early 1990s (ICES, 2011; Figure 2). Stock development, often expressed by changes in SSB, is attributed to individual growth and mortality of adults as well as to the recruitment of new year classes into the SSB. Although growth and mortality patterns can often be estimated with some precision, stock development remains difficult to assess due to recruitment variability. This applies especially for low-trophic species such as herring.

Estimates of WBSS recruitment are available since 1991 (ICES, 2007, 2011), whereby the range of recruitment at age 0 was between 3 and 6.5 x 10^9 until 2004 (Figure 2). However, in subsequent years recruitment of WBSS dropped sharply, annually decreasing by 15-35% (ICES, 2011). Amongst others, these recruitment estimates are based on annual larval abundances recorded during the Rügen Herring Larvae Survey (RHLS). This survey is conducted weekly during the WBSS spawning season within the GWB and the Strelasund since 1992, determining the abundance of larvae that have reached 20 mm (Oeberst et al., 2009b). Estimated larval abundance correlates significantly with the abundance of age 1 herring, derived from acoustic surveys, and VPA[1]-derived estimates of age 0 recruitment (Oeberst et al., 2009b). This confirms the importance of the GWB and the Strelasund, which are considered as the main spawning area of WBSS (Biester, 1989; ICES, 1998). Furthermore, year-class strength of WBSS appears to be determined during early-life stages (ICES, 2007; Oeberst et al., 2009b), which applies also to other fish stocks.

[1]VPA: Virtual population analysis is a model technique used in fisheries to assess the status and development of fish stocks.

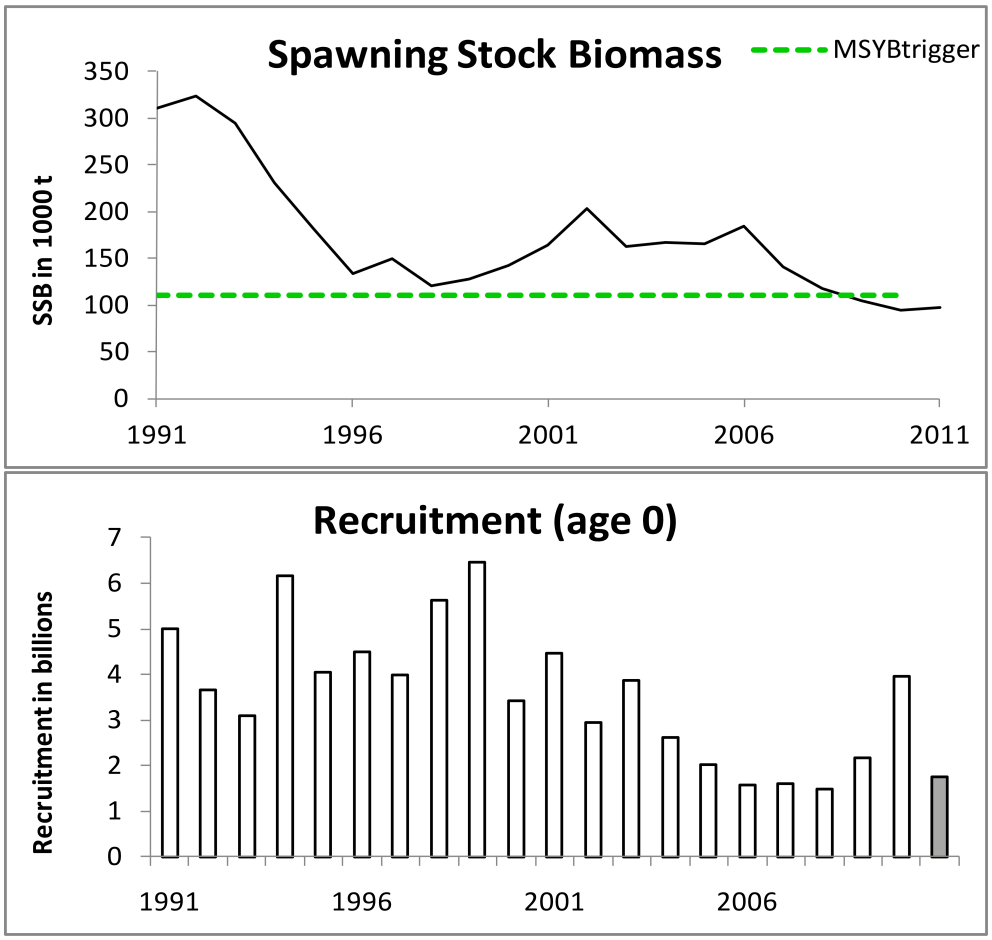

Figure 2: Development of SSB and recruitment of WBSS since 1991. Recruitment in 2011 (grey bar) represents a preliminary estimate based on the average long term recruitment. The dashed green line denotes the triggered biomass that can produce the maximum sustainable yield (MSY). Source: ICES (2011)

1.3 Recruitment Variability

Recruitment variability can be caused by changes in SSB, reduced fecundity of adults and variation in early life stage mortality affecting eggs and larvae. Given the size of the SSB, further information of the age structure and related fecundity, the total number of produced eggs can be roughly estimated. However, the spawner-recruit relationships are commonly not proportional as indicated. Thus, recruitment variability is often insufficiently explained by changes in spawning stock biomass (SSB). This emphasizes that recruitment is mainly determined during the early life history of fish.

Early life stages of fish are affected by high natural mortalities. Mass mortality of herring eggs has been observed in thick egg patches due to insufficient oxygen supply (Klinkhardt & Biester, 1984; Messieh & Rosenthal, 1989). In addition, egg mortality of Baltic herring has been shown to be related to the spawning substrate with highest mortalities being reported for eggs attached to filamentous brown algae and red algae (Aneer, 1985, 1987; Rajasilta et al., 1989, 2006). Predation is another factor that is known to cause high egg mortality rates. Potential predators of herring eggs include invertebrates, fish, marine mammals and birds

(Palsson, 1984; Scabell, 1988). Among the diverse egg predators documented for WBSS, the three-spined stickleback (*Gasterosteus aculeatus*) and the long-tailed duck (*Clangula hyemalis*) were observed to consume large proportions of deposited eggs (Scabell, 1988).
Mortality rates remain high for early larval stages. In this context, Hjort (1914) stated that larval survival and hence recruitment is primarily determined by food supply during the time of first feeding when larval resistance to starvation is lowest. This hypothesis, also known as "critical period" hypothesis, was taken up and refined by numerous researchers. Cushing (1975) described a connection between spawning time and the production cycles of phyto- and zooplankton. According to his match-mismatch hypothesis, the appearance of larval densities must match the abundance peak of associated prey organisms to ensure larval survival. Thereby, larvae rely not only on the quantity but also on the quality of food, precisely its composition and size (Busch, 1996). Moreover, Cushing (1975) considered larval survival to be not only dependent on food supply, accounting for predation effects. Early-hatched larvae within the spawning season match the early production cycle and hence may find enough food to survive. However, growth is not at its optimum due to lower prey abundances and temperatures. As a consequence, larvae are exposed longer to predation and thus high mortality rates, reducing their probability of survival.
Appropriate nursery conditions can be accomplished by high density patches of prey organisms in which larvae can feed effectively. Investigating recruitment variability of anchovy (*Engraulis mordar*) off the Californian coast, Lasker (1978) found these patches to be formed after calm oceanic conditions, when the upper water column is relatively stable. In contrast, strong winds and strong coastal upwelling events cause the patches to disperse, resulting in too low concentrations for larval survival (Lasker, 1975, 1978, 1981). Thus, it is obvious that the occurrence of larvae and associated prey organisms must coincide in both space and time to maintain larval survival. Furthermore, the importance of atmospheric and physical oceanographic conditions for larval survival becomes evident. However, oceanic conditions do not only control the development and distribution of zooplankton.
In addition, swimming abilities of young larvae are insufficiently developed. However, apart from physiological factors, swimming performance of larvae is strongly influenced by the viscosity of the surrounding regime (Fuiman & Batty, 1997; Hunt von Herbing, 2002; Hunt von Herbing & Keating, 2003). Swimming speeds of early larval stages ($<$ 14 mm) can reach several cm/sec (e.g. 4.3 cm/sec for 13.5 mm herring larvae; von Westernhagen & Rosenthal, 1979), but are usually of much smaller magnitude (Klinkhardt, 1996). Moreover, especially yolk sac larvae are not capable to swim continuously for a longer time period (Klinkhardt, 1996). Instead impulsive motion or jump-swimming is common. Thus, being capable of only restricted locomotion, the spatial distribution of larvae is strongly affected by the hydrodynamics of their environment.
The passive transport of larvae by water currents is generally defined as larval drift. Larval drift can occur from spawning grounds to nursery areas via a residual current (Cushing, 1975) as suggested by the "migration triangle" hypothesis (Harden Jones, 1968). Perhaps the most striking example of this concept is the drift of the larvae (leptocephali) of the European Eel (*Anguilla anguilla*) from the spawning grounds in the Sargasso Sea to the European coastal waters. Thereby, moving with the North Atlantic Drift takes approx. 10 months (Bonhommeau

et al., 2009, 2010). Larval drift over large distances is also reported for several herring stocks, particularly of the eastern Atlantic such as stocks off the British Isles (Bückmann et al., 1950; Cushing, 1986). In contrast, larval retention has been demonstrated, amongst others, for the Norwegian Spring-Spawning herring (Sætre et al., 2002), the British Columbia Pacific herring (Hay & McCarter, 1991, 1997) and the Gulf of St. Lawrence Spring-Spawning herring (Henri et al., 1985). Associated retention areas are often highly productive and hence assumed to exhibit more favorable feeding conditions than the surrounding environment. Thus, in that case, retention most likely benefits larval survival while the drift away from favorable habitats reduces the probability to survive the pronounced "critical period" in the life history of fish (Sætre et al., 2002).

In this context, Iles & Sinclair (1982) have suggested that retention areas are particularly important for herring stocks. However, according to their interpretation larval retention does not necessarily imply that larvae have to remain stationary. Instead, larvae can drift over large distances, as shown for Norwegian Spring-Spawning herring larvae but are aggregated within a stable physical oceanographic system, such as the Norwegian coastal current (Sinclair, 1988). Being geographically stable from year-to-year, these "retention systems" are assumed to represent a crucial feature of herring stocks. In fact, Iles & Sinclair (1982) considered the number of distinct herring stocks to be determined by the number of geographically stable larval retention areas. Although the hypothesis of Iles & Sinclair (1982) has received great attention and lead to a many discussions (Sinclair, 1988), it is difficult to test this hypothesis.

1.4 The Greifswalder Bodden

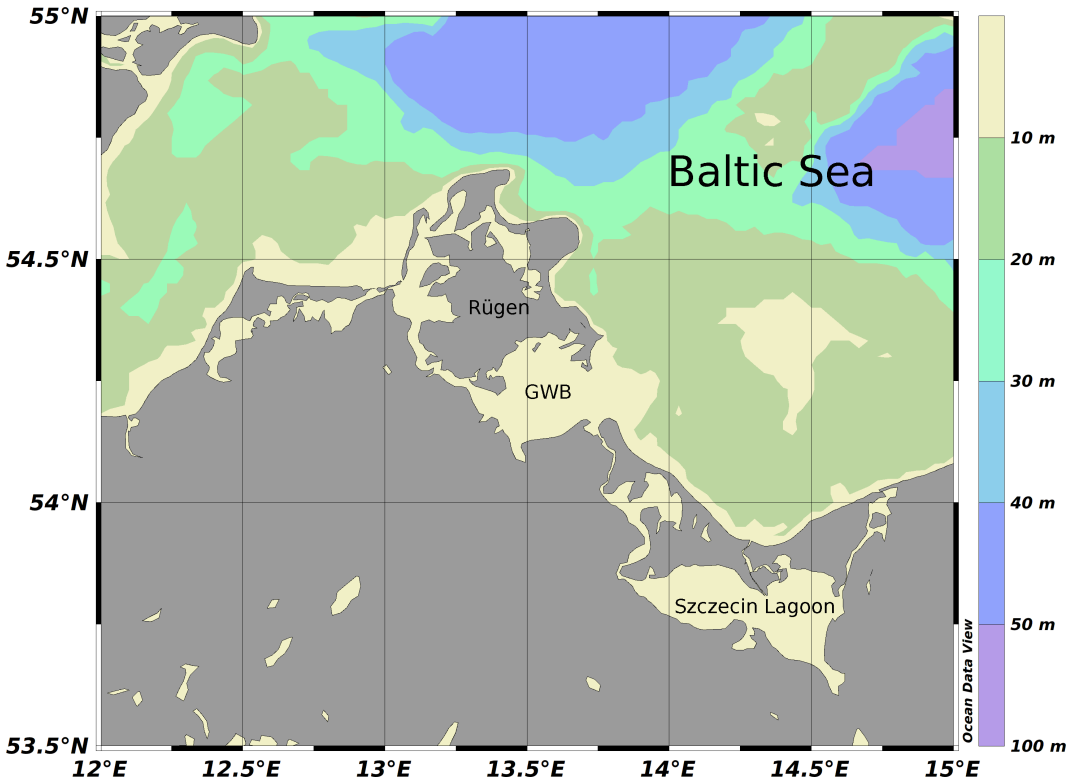

Figure 3: The eastern part of the German Baltic coast, showing the Island of Rügen and the Greifswalder Bodden (GWB). The map was produced by using Ocean Data View (ODV) (Schlitzer, 2010)

The eastern part of the German Baltic coast is characterized by a jagged coastline consisting of several peninsulas, islands and lagoons. This area serves as feeding and breeding ground for numerous species, with particularly the lagoons being of high ecological value. The largest lagoon in this region is the Greifswalder Bodden (GWB) covering a total surface area of 514 km^2(Correns, 1979; Vietinghoff et al., 1995; Schiewer, 2008a). Like adjacent lagoons, the GWB is relatively shallow with an average depth of about 5.6 m and a maximum depth of 13.5 m (Correns, 1979; Stigge, 1989; Vietinghoff et al., 1995; Birr, 1997; Schiewer, 2008a). The sea-bed of the western part is almost of constant depth. However, the bathymetry of the GWB is not uniform. The eastern part of the lagoon consists of several shoals and deeper holes. Differences are also apparent in the sediment distribution (Katzung, 2004). The deeper grounds of the western basin are generally covered with muddy sediments. The sediments of shallow areas like the shoals and the extended shorelines are dominated by sand (Figure 4).

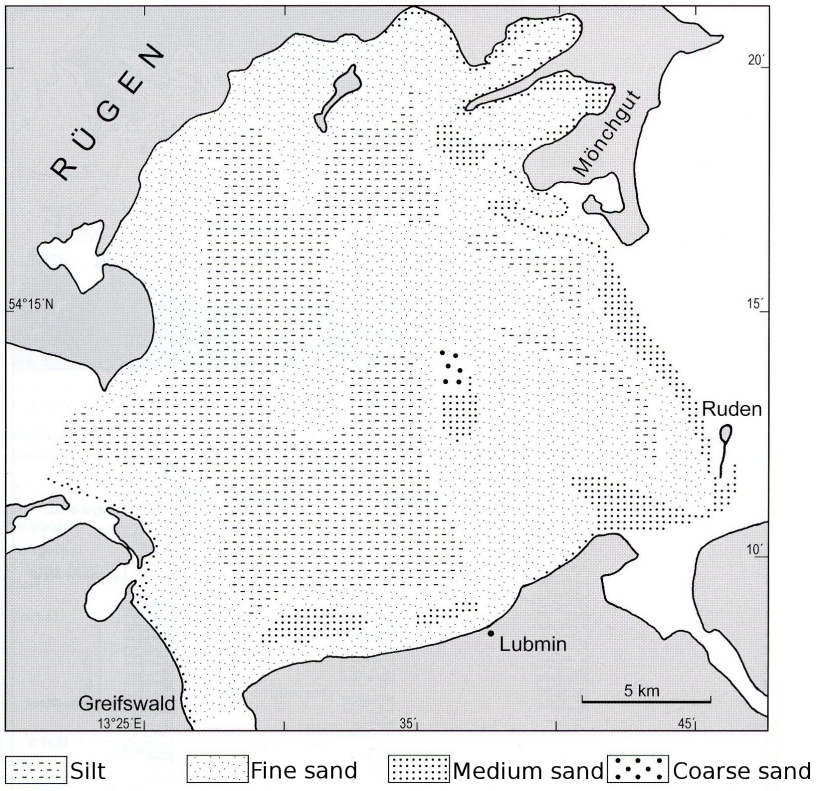

Figure 4: Surface sediment distribution in the GWB. Figure adopted from Katzung (2004).

The GWB has two connections to the open Baltic Sea. A large but shallow opening is located on the eastern edge of the lagoon. An additional connection to the Baltic Sea is provided by the Strelasund, a narrow channel on the western side which connects the GWB with a chain of other lagoons. Particularly due to its large direct connection, water exchange with the Baltic Sea is less restricted than at adjacent lagoons where connections are either extremely narrow or indirect. Thus, the total volume of the GWB is is assumed to be replaced 8 (Stigge, 1989) to 12 (Jönsson et al., 1998; Schiewer, 2008a) times a year. However, it remains unclear whether the whole water body is replaced or if the water exchange is restricted to the boundaries of the GWB. Moreover, exchange rates were reported to range between 10-200% per month. This high variability was attributed to changes in flow fields (Jönsson et al., 1998).

According to Jönsson et al. (1998) three main flow patterns can be distinguished for the GWB (Figure 5). I) A water inflow at both sides and an outflow at the south of the Isle of Ruden, at the eastern opening of the GWB; II) an inflow of water at the eastern opening which extends to the Strelasund; and III) a strong eastward flow through the whole GWB. Thereby, monthly water exchange rates of these flow fields accounted for 0-10%, 10-25% and 50-200% of the total GWB volume, respectively. In this context, Lampe (1994) stated that the residual flow in the GWB is directed to the east. This indicates that large parts of the GWB are assumed to be involved in the water exchange with the Baltic Sea.

Unlike wind fields, freshwater runoff has no significant influence on the water balance and circulation patterns, accounting only for 0.3% of the total water balance (Lampe, 1994). This is due to the small watershed of the GWB which measures only 665 km^2 (Schiewer, 2008a). Low

freshwater discharges enter the lagoon mainly from the brooks Ryck and Ziese at its southern part. Additional runoff comes from the Peene Strom which carries slightly brackish water from the Szczecin Lagoon. Evaporation and precipitation are also of minor importance (Correns, 1978), each accounting only for 1-2% of the water balance of the GWB (Lampe, 1994).

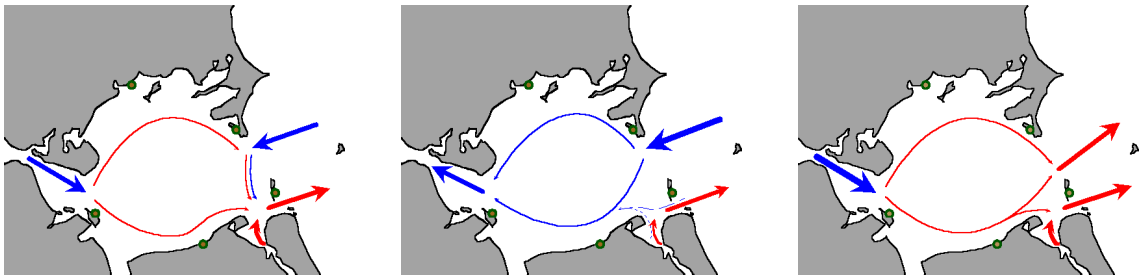

Figure 5: Schematic representation of main flow patterns in the GWB described by Jönsson et al. (1998).

The lagoon has brackish water due to its connections to the Baltic Sea. The salinity of the GWB ranges between 5.3 and 12.2 PSU, but is on average 7.4 PSU which is almost equal to the surface salinity of the surrounding Pomeranian Bay (Stigge, 1989; Buckmann et al., 1998). High salinities are caused by the inflow of higher saline waters from the Darss sill via the Strelasund (Stigge, 1989). Due to its overall low depth, no thermoclines and haloclines can establish (Wasmund & Kell, 1991). Locally salinity stratification can occur at the mouth of the Peene Strom: Strong easterly winds can push freshwater from the Peene Strom into the lagoon, causing a stratification that can last for several weeks (Buckmann et al., 1998; Meyer et al., 1998).

The ecosystem of the GWB has undergone substantial changes during the second half of the 20th century (Vietinghoff et al., 1994). By the 1930s, nearly 90% of the lagoon's sea floor was covered by macrophytes (Seifert, 1938; Blümel et al., 2002). Anthropogenic eutrophication, starting in the 1950s, has caused the system to switch to a phytoplankton-dominated state (Munkes, 2005). As a result, macrophyte depth limits and coverage showed a significant decline. Estimates of the total coverage during the 1980s and 1990s range between 11 and 16%. External nutrient loads were reduced strongly during the early 1990s (e.g. Phosphate by 70%) (Bachor, 2005b; Munkes, 2005). However, results from an extensive macrophyte monitoring in 2009, consisting of aerial photography, video transect surveys and SCUBA surveys, suggest no significant changes in depth limits and coverage during the last two decades (Messner & Von Oertzen, 1990, 1991; Rambow, 1994; Hübel et al., 1995; Vietinghoff et al., 1995; Bartels & Klüber, 1999). Instead, phytoplankton production is still stimulated by nutrient loads from runoff, especially from the highly eutrophic Peene Strom (Bachor, 2005b) and from internal loadings (Munkes, 2005). In this context, Munkes (2005) stated that the restoration of macrophyte vegetation is hampered by an increased turbidity and associated reduced light levels. Both factors are caused by the resuspension of particulate matter and phytoplankton production. Overall, the GWB is still considered to be eutrophic (Westphal & Lenk, 1998; Bachor, 2005a). Other lagoons of the surrounding area are highly eutrophic or even hypereutrophic due to their restricted water exchange (Bachor, 2005a).

1.5 The Aim of the Study

Retention areas have been suggested to represent crucial features in the biology of herring stocks. This might particularly apply to WBSS who spawn in semi-enclosed coastal waters. Generally, larval retention within the distinct spawning ground of WBSS, the GWB, is assumed to favor larval survival due to the high productivity of these areas. Though, the high inter-annual variability in water exchange rates, shown by earlier studies (Stigge, 1989; Jönsson et al., 1998), led to the question whether the GWB acts as retention area for WBSS larvae. Moreover, these results suggest that larval drift out of the supposed retention areas could have contributed to the recruitment variability and recent recruitment decline of WBSS.

Based on these considerations the following hypotheses were established:

1. The GWB acts as retention area for WBSS larvae. Most of the larvae hatched in the GWB remain in this area until they have passed the critical period of development.
2. Larval retention mainly depends on prevailing wind fields and spawning site locations
3. The risk of larval removal from the GWB is highly variable during the WBSS spawning season and between years
4. The variability of larval drift pattern contributes to the observed inter-annual variations in recruitment success and year-class strengths

The aim of this study is to address these hypotheses.

2 Material and Methods

2.1 Circulation Model

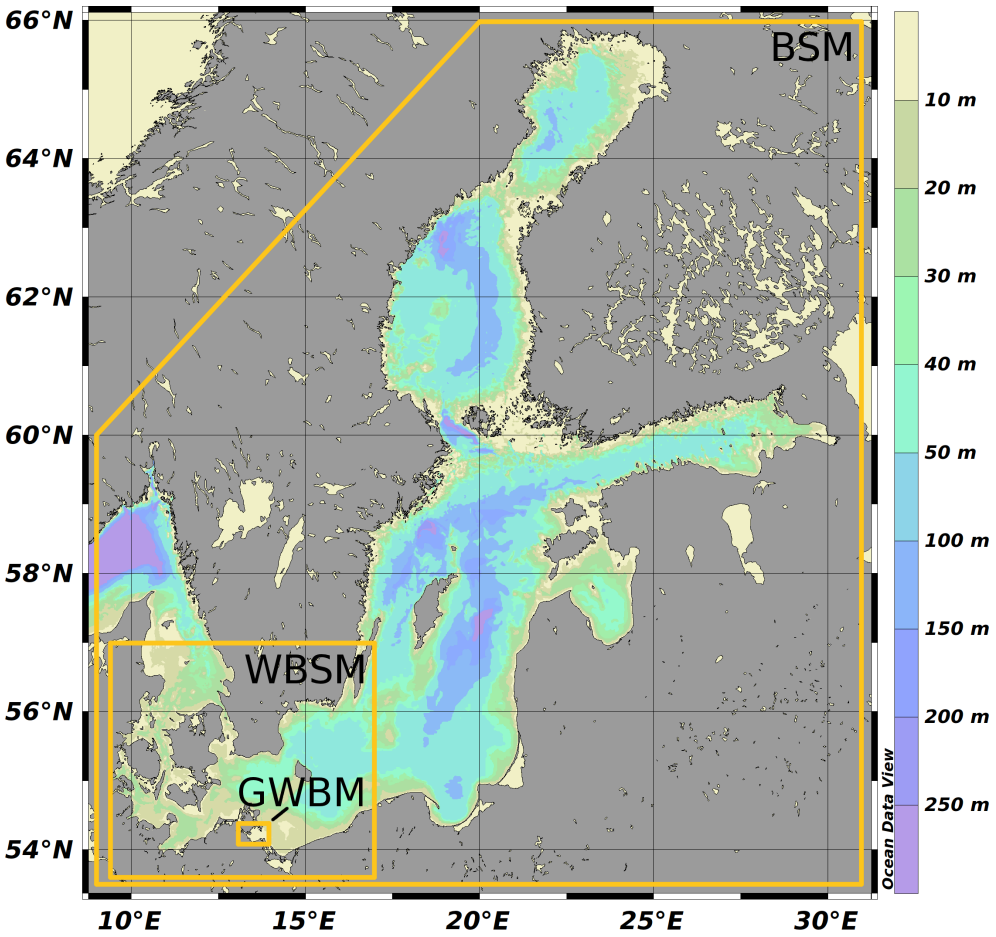

Figure 6: Overview of the nested circulation model domains. (BSM: Baltic Sea Model; WBSM: Western Baltic Sea Model; GWBM: Greifswalder Bodden Model). A more detailed view of the GWBM domain is given in figure 10. The map was produced by using Ocean Data View (ODV) (Schlitzer, 2010).

A threefold nested model approach was used to simulate flow fields in the GWB, the Strelasund and the surrounding Baltic Sea. The outermost model domain encompasses the entire Baltic Sea and parts of the North Sea (Figure 6). Circulation patterns in this area are simulated using the hyrodynamic, three-dimensional (3-D) Modular Ocean Model (MOM, Griffies et al. (2004)). The spatial resolution used for model domain of this Baltic Sea model (BSM) is relatively high, with a horizontal grid spacing of 1 nm and 77 vertical geopotential layers, giving a total number of 666 x 723 grid points (Fennel et al., 2010). A detailed description of this model is given in Fennel et al. (2010).

In addition, the 3-D numerical hydrodynamic General Estuarine Transport Model (GETM) has been applied for both nested models, the Western Baltic Sea model (WBSM) and the GWB model (GWBM). This model was developed by Burchard & Bolding (2002), especially to simulate estuarine and shallow water circulations. So far GETM has been successfully implemented for the simulation of a variety of different regions so far, including the Western

Baltic Sea (Burchard et al., 2005, 2009; Hofmeister et al., 2010) and the GWB (Burchard et al., 2008). In the latter case, Burchard et al. (2008) used GETM to investigate possible effects of cooling water discharges from an intended power plant at Lubmin within the GWB. The applied GETM models were run on an equidistant, spherical grid associated with an adaptive sigma coordinate system[2], developed by Hofmeister et al. (2010). However, both nested models differ in their numerical setup in several ways. The first embedded, central domain covers the Western Baltic Sea (WBSM, figure 6) with a horizontal resolution of 600 m and 50 vertical layers. The bathymetry of this area was obtained from the Danish Maritime Safety Administration (DaMSA, http://www.frv.dk). Lateral open boundary conditions were derived from MOM simulations of the BSM. Daily freshwater runoff of several rivers, which drain into the model domain (e.g. Oder, Trave, Warnow) were taken from the BSM setup (Fennel et al., 2010). Besides river runoff, the model is forced at the surface by prevailing wind fields, heating/cooling and fresh water fluxes (precipitation - evaporation). The applied atmospheric forcing consisted of 3 hourly data of air temperature, humidity, cloud cover, air pressure, precipitation and wind fields taken at 10 meters above mean sea level (MSL). These fields were provided by the German Weather Service (DWD, http://www.dwd.de). The spatial resolution of forcing fields was about 7 km. From the WBSM, four-hourly averaged temperature and salinity profiles along with hourly values of sea surface elevation and depth-averaged currents were extracted. These data served as boundary conditions for the nested GWBM.

The innermost model, the Greifswalder Bodden model (GWBM) covers the Strelasund, GWB and parts of the surrounding Baltic Sea (Figure 6 and 7). This domain exhibits the highest resolution (180 m horizontal grid spacing and 10 vertical layers). Associated bathymetric data were obtained from the Bundesamt für Seeschifffahrt und Hydrographie (German Federal Maritime and Hydrographic Agency, BSH, http://www.bsh.de). Although these data were provided with a high horizontal resolution of 90 m, grid resolution was reduced to 180 m for computational feasibility. The new bathymetry was interpolated and manually revised by using satellite imagery. Special focus was set on maintaining the fairways to the open Baltic and the Strelasund. Additional considerations were made to incorporate affects of macrophyte beds on current fields. In general, macrophyte beds are known to affect currents and sediment deposition through higher bottom frictions (Li et al., 2008). Hammer et al. (2009) investigated the spatial distribution of macrophytes within the GWB and the Strelasund using aerial photography. Bottom friction of areas which are according to Hammer et al. (2009) covered by macrophytes were increased by a factor of 10, from the default 1 mm to 1 cm. The lower depth limit of implemented macrophyte coverage is approx. 3 m (Figure 8). The coverage of deeper layers could not be detected by aerial photography due to low water transparency and associated low light penetration. However, additional investigations conducted by Hammer et al. (2009) using underwater videography and SCUBA diving suggest that the macrophyte distribution is strongly limited to the shallower and therefore coastal areas. The center of the lagoon is not covered by macrophytes. Freshwater fluxes within the model domain are generally weak with only the Peene Stream being of greater importance. Runoff from the Peene Stream was

[2]sigma coordinate system: In a sigma coordinate system, the water column is divided by a defined, fixed number of vertical layers. Thus, layer thickness is not uniform, but varies horizontally according to the total water depth of grid point.

provided by the WBSM. The applied atmospheric forcing was identical to those mentioned for the WBSM setup.

The model setup and simulations of hydrodynamical models were carried out by Dr. Ulf Gräwe (Leibniz Institute for Baltic Sea Research, Warnemünde - Germany). Calculated hourly sea surface elevation and depth integrated flow fields, including eddy viscosity of the whole GWBM model domain as well as 4 hourly 3-D velocity fields, temperature and salinity profiles of selected stations (Figure 10) were stored for further analyses, conducted by the author (s.b.).

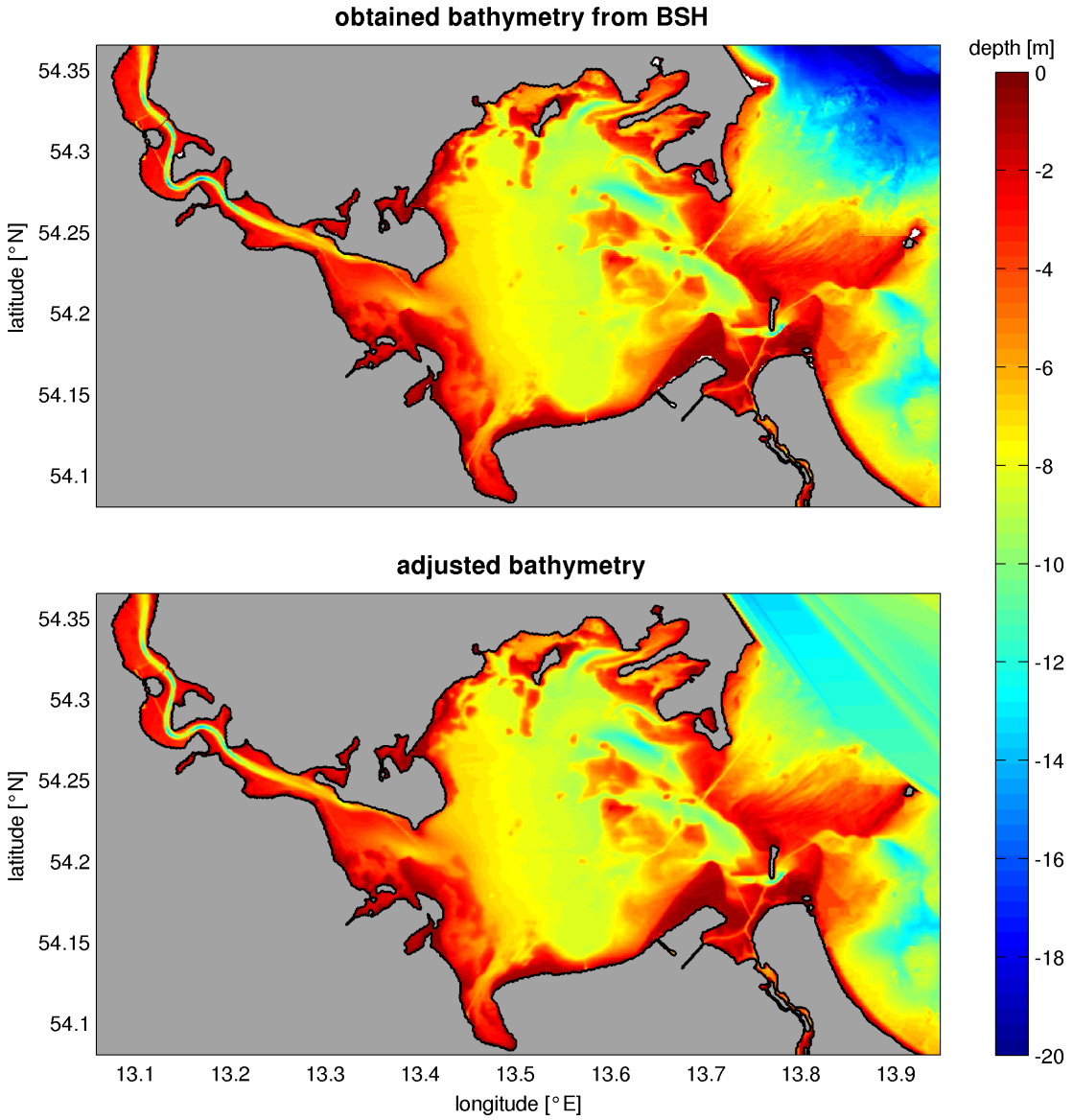

Figure 7: Obtained and adjusted bathymetry of the GWBM model domain. White spaces mark areas outside the model domain.

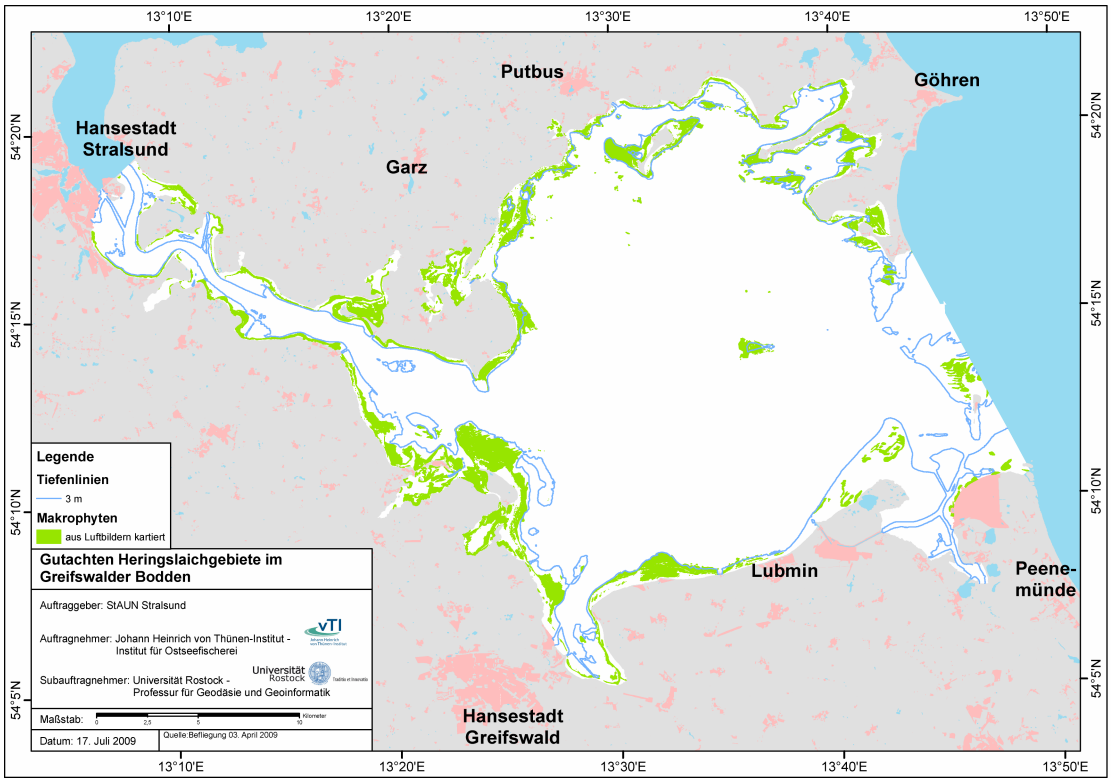

Figure 8: Macrophyte coverage (green) of the GWB and Strelasund, mapped by aerial photography. From Hammer et al. (2009). The blue contour line indicates the 3 m depth level.

2.2 Particle Tracking Model

General Description

In the present study, an offline[3], two-dimensional (2-D) Lagrangian particle tracking model developed by Gräwe & Wolff (2010) was used to simulate WBSS larval dispersal within the GWB and the Strelasund. The underlying assumption behind this application is that herring larvae behave like passive particle drifters, having no ability to swim against currents (s.a.). This simplified approach is further discussed below.

In general, the model is based upon an advection-diffusion equation, whereby advection accounts for the directed transport due to the velocity and diffusion for the undirected transport of particles as a result of turbulent mixing of the surrounding flow.

$$\partial_t(HC) = -\nabla\left(H\mathbf{U}C\right) + \nabla\left(KH\nabla C\right) \tag{1}$$

gives the advection-diffusion equation for a depth averaged concentration field $C = C\left(\mathbf{X}, t\right)$ of a passive tracer for the defined water column $H\left(\mathbf{X}, t\right)$, in dependence of the operating velocity $\mathbf{U}\left(\mathbf{X}, t\right) = \left(U\left(\mathbf{X}, t\right), V(\mathbf{X}, t\right)$ and the local eddy diffusivity $K\left(\mathbf{X}, t\right)$ at the position $\mathbf{X} = (x, y)$.

Within this partial differential equation (PDE) temporal changes of the concentration field are described from a fixed position which is called the Eulerian perspective. By contrast, the concentration field can also be specified from a transient point of view, the Lagrangian perspective that follows the flow and thus traces the movement of individual particles. Hence, the spatial position $\mathbf{X}$ is no longer interpreted as a fixed reference, but as another variable $\mathbf{X}\left(t\right)$ of drifting particles, which varies with time. In order to switch perspectives, equation 1 can be transformed to

$$d\mathbf{X}\left(t\right) \overset{\hat{I}to}{=} \left(\mathbf{U} + \frac{K}{H}\nabla H + \nabla K\right)dt + \sqrt{2K}d\mathbf{W}\left(t\right). \tag{2}$$

For further details see Arnold (1974).

As an additional term this equation contains a normally distributed random variable $\mathbf{W}\left(t\right)$, called Wiener noise increment, which possess a mean of $\bar{\mathbf{W}}\left(t\right) = 0$ and a standard deviation of $\sigma = \sqrt{|t - s|}$ that reaches $\sqrt{dt}$. This variable accounts for the random movement of particles. The turbulent diffusivity $K\left(X, t\right)$ was parameterized by means of the Smagorinsky approach (Smagorinsky, 1963):

$$K = c\,\Delta x\,\Delta y\,\sqrt{\left(\partial_x U\right)^2 + \left(\partial_y V\right)^2 + 0.5\left(\partial_y U + \partial_x V\right)^2}, \tag{3}$$

where Δx, $\triangle y$ denotes the grid spacing and c_s represents the Smagorinsky constant. In the present study, the default value of c_s was set to 0.1 which is commonly used in literature. However, since $K\left(X, t\right)$ is spatially highly variable, particles tend to move to regions of lower diffusivity. The term ∇K equalizes this erroneous behavior (Hunter et al., 1993; Heemink & Blokland, 1995; Spagnol et al., 2002; Visser, 2008) and is thus added to the equation 2.

[3] offline particle tracking model: offline particle tracking models require stored flow fields as forcing, thus running separately from circulation models (North et al., 2009).

Generally, equation 2 can further be simplified, by substituting its deterministic part $a = \mathbf{U} + \frac{K}{H}\nabla H + \nabla K$ and its stochastic part $b = \sqrt{2K}$, leading to

$$d\mathbf{X}(t) = a(\mathbf{X})\,dt + b(\mathbf{X})\,d\mathbf{W}(t). \tag{4}$$

This equation can be solved by different numerical schemes (Gräwe, 2011). Within the present study the Heun-Scheme, a first order explicit predictor–corrector method was applied to solve the Langevin equation. Gräwe (2011) has shown that this scheme provides accurate results and is considered as highly efficient. Further explanations of the model are given in Gräwe & Wolff (2010); Gräwe (2011).

General Model Setup

In order to analyze the larval removal from the GWB to the open Baltic Sea two boundaries were established to limit the area of the lagoon (Figure 10). The first boundary separates the lagoon from the open Baltic Sea along its eastern inlet, crossing the Isle of Ruden. The second boundary was set at the northwesterly opening of the Strelasund. This area is subsequently defined as GWB - Strelasund area (GSA). For each model run 100 particles, representing simulated WBSS larvae were equally distributed within every grid box of the GSA, resulting in a total amount of 1776700 released particles. Hence, the initial setup does not account for the importance of different potential spawning sites. Only two-dimensional (2-D) depth-integrated flow fields from the GWBM were used to drive the particle tracking model, although the GWBM was run in 3-D mode. Thereby, the main benefits of this simplified approach are the significantly reduced computational storage and effort. Generally, applying depth-integrated velocity fields seems reasonable when vertical mixing is strong. In this supposed case, particles are forced to move throughout the water column. Hence, they are exposed to a current regime that is comparable to the depth-integrated flow. Testing the validity of this assumption is subject of further analysis (s.b.). Flow fields cause a horizontal displacement of particles which are seeded within the model domain. To obtain velocities at a specific particle position, these gridded velocities are linearly interpolated by the model in space and time. Tracking time was subject to the experimental setup (s.b.). Particles were treated and tracked individually with particle positions being recorded every 6 hours. However, the particle tracking was spatially limited by the lateral boundaries of the GWBM (Figure 6, with a more detailed view in figure 10). Particles that have crossed these boundaries were excluded from further tracking, resulting in shorter tracking times.
The whole model setup information is contained in the configuration file “LADOS.inp” which is attached in the appendix.

2.3 Experiments at Constant Wind Conditions

Circulation patterns in coastal lagoons are mainly influenced by winds, tides and bathymetry (Miller et al., 1990). With a tidal range of 15 cm, the Baltic Sea is classified as a microtidal system (Schiewer, 2008b). Thus, effects of tidal forcing on the circulation of the GWB are relatively weak. Instead, the circulation of the lagoon is strongly influenced by prevailing wind fields (Jönsson et al., 1998; Stigge, 1989; Birr, 1988; Correns, 1977; Brosin, 1970). Hence, in a first approach circulation patterns and associated larval dispersal under different constant wind conditions were investigated.

Circulation Patterns

The effects of different wind conditions on flow fields were analyzed. Therefore, constant wind speeds (1, 3, 6 and 9 m s^{-1}) for cardinal (N, E, S, W) and inter-cardinal (NE, SE, SW, NW) wind directions were used as forcing for the GWBM, resulting in a total number of 32 scenarios. Surface and depth averaged flow fields were extracted from the model runs, thus consisting only of 2-D (u and v) velocity vectors. Absolute current speeds were determined using

$$spd = \sqrt{u^2 + v^2}. \tag{5}$$

On this basis, average absolute current speeds were calculated for the GWB and the Strelasund. Spatial patterns of current speeds and directions were examined for each flow field and compared with each other. Special focus was set on changes related to wind direction and speeds.

Larval Drift

To evaluate the effects of different wind-forcing on larval drift, particle-tracking analyses were conducted based on obtained simulated steady-state flow fields (s.a.). For each model run, particles were seeded in the GSA as mentioned above. The tracking time was set to 31 days, which was assumed to approximately coincide with the critical period of larval survival.
The percentage of all particles retained within the GSA was calculated for each recorded time step, every 6h. The resulting time series was plotted to examine temporal course of particle removal in relation to the acting wind field (s.a.). It was expected that areas affected by larval drift differ with prevailing wind fields. Therefore, the mean residence time[4] and percentage of removed particles was calculated for each seeding location. In addition, the total percentage of removed particles was computed for several sub areas, for I) the entire GSA, II) the GWB, III) & IV) areas of the GWB exhibiting a lower depth than 6 and 3 m, respectively and V) the Strelasund. According to recent results from Hammer et al. (2009), these depth levels limit the total and main distribution area of macrophytes and thus spawning grounds within GWB. Location and extent of defined sub-areas are shown in figure 9. The boundary between the GWB and the Strelasund was chosen according to previous studies (Jönsson et al., 1998; Meyer et al., 1998; Buckmann et al., 1998).

[4] mean residence time: average time that particles spent within a certain area (in this case the GWB and the GWB)

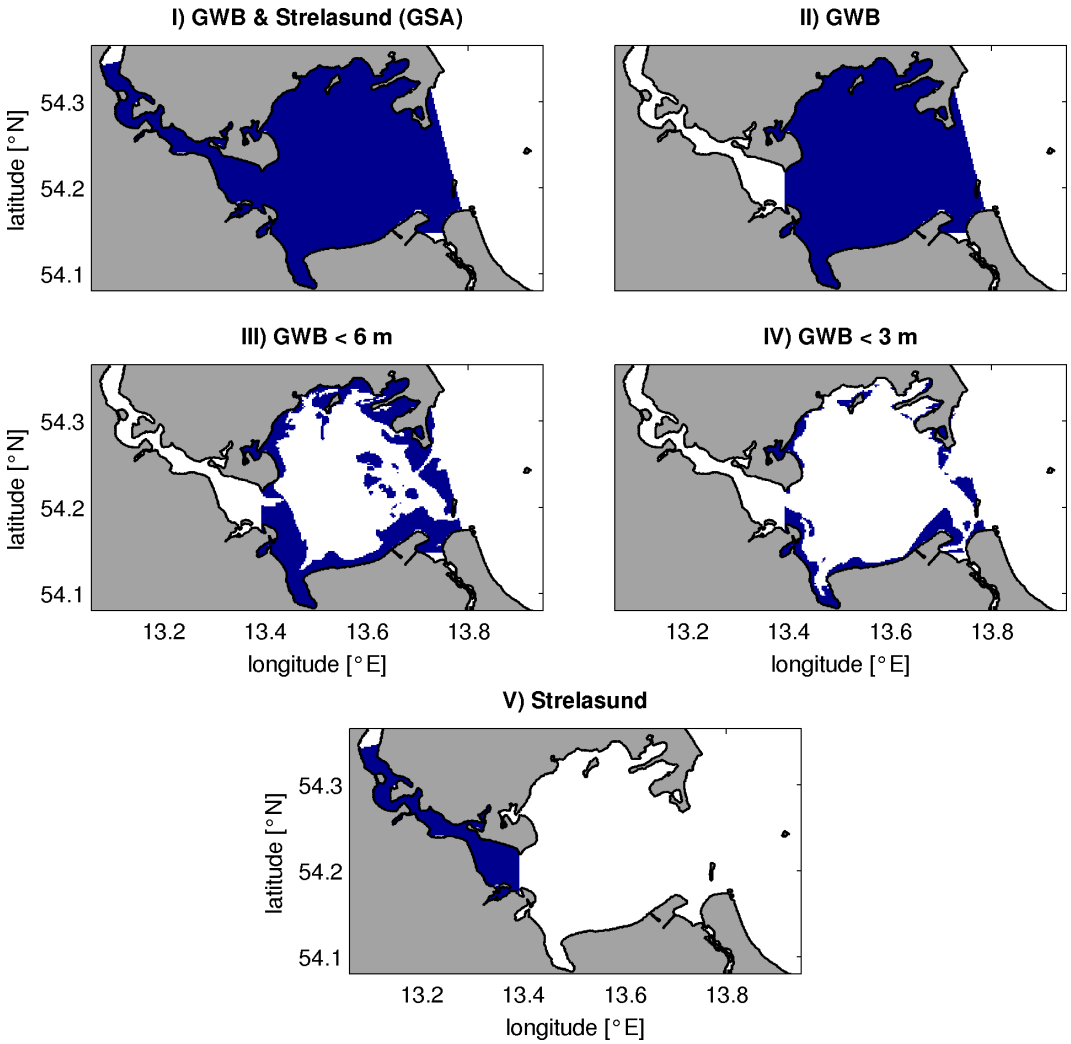

Figure 9: Sub areas of particle drift analyses. I) GWB and the Strelasund (GSA), II) GWB, III) areas of the GWB with a lower depth than 6 m and IV) areas of the GWB with a lower depth than 3 m and V) the Strelasund.

Analyses on the Numerical Setup

As mentioned above, the applied particle tracking model is based on a advection-diffusion equation (equation 4). In the present study, the Heun-Scheme was used to solve this equation. Besides, the Smagorinsky constant (c_s) which influences the turbulence dissipation and thus the eddy diffusivity was set to 0.1. However, results could differ for other numerical schemes and diffusivities. To investigate potential differences caused by the numerical setup, model runs were conducted using two other numerical schemes, the first-order Milstein-Scheme and the Platen-Scheme, which is of second-order (Gräwe, 2011; Kloeden & Platen, 1999). In addition, effects related to different values of c_s (0.05 and 0.2) were investigated. Thereby, model runs were forced with flow fields obtained for NW winds with speeds of 6 m s^{-1}. As done in the previous analysis, particles were tracked for 31 days. For each setup, the percentage of removed particles was determined for several sub-areas (Figure 9). Results were compared with those of the default numerical setup (Heun-Scheme, c_s= 0.1).

2.4 Experiments at Real Wind Conditions

Within the previous analysis, potential flow fields and mechanisms influencing larval drift were examined based on constant wind forcing. However, steady forcing by constant winds is unlikely. Moreover, it can be assumed that circulation patterns of coastal lagoons are highly variable in space and time. In this context, Miller et al. (1990) declared *"The advective movement of water within the lagoon is the most rapidly fluctuating term, because shallow waters are highly responsive to temporal variations in wind stress and therefore most likely to affect particle transport. Significant changes in current patterns are commonly recorded over time scales on the order of a few hours. This is superimposed on to much slower variations in response to weather systems moving through the area, and to seasonally changing wind patterns."*. Hence, the next step has to be the investigation of circulation patterns, water exchange rates and larval drift under real wind conditions. For this purpose, atmospheric data of 2008 and 2009, two years with contrary recruitment success, have been selected as forcing for the GWBM.

Model Validation

To evaluate the accuracy of simulated flow fields, model results are typically compared with observed field data. Generally, this process is called model validation. Within the present approach, the results of the model were validated by comparing simulated and observed data of depth-integrated temperature and sea level deviation (SLD) of 2008 and 2009.
Temperature data of 2008 and 2009 were obtained from the Rügen Herring Larvae Survey (RHLS) for several survey stations (Figure 10). By default, temperature profiles are measured from approximately 1 m below surface to 1 m above bottom during each week of the survey. However, only surface and bottom temperature are stored electronically. In addition, only depth-averaged temperatures were available from simulated flow fields, although 3-D runs were conducted. Thus, in order to receive depth-averaged temperature for the intended comparison, the mean observed surface and bottom temperature were calculated. For each averaged survey record, depth-averaged temperature of the same day were selected from the closest grid point of simulated flow fields. The daily mean of simulated temperature was calculated. Pairwise comparisons of simulated and survey depth-averaged temperature data were statistically evaluated. Therefore, a linear regression was fit to the data.
Regarding the comparison of observed and model-simulated SLD, three stations were selected (Greifswald, Stralsund and Koserow, Figure 10). While the stations of Greifswald and Stralsund are located within the GWB model domain, Koserow is situated outside, approx. 7.2 km away from the south eastern corner of the GWB model domain. This station has been chosen to evaluate the accuracy of the coarse scaled Western Baltic Sea model, which provides boundary conditions such as sea level rise for the nested GWB model (s.a.). Hourly, observed sea level data, such as sea level rise, of each station were provided by the BSH. Model data with the same temporal resolution were derived from stations close to the measuring locations (less than 70 m distance). For each dataset the deviations from its longterm sea level were calculated, giving the observed and estimated SLD at each station. Differences in the SLD time series were evaluated. For this purpose, pairwise comparisons were applied to the data. To determine

the correlation of measured and modeled data a linear regression was conducted using the least squares method.

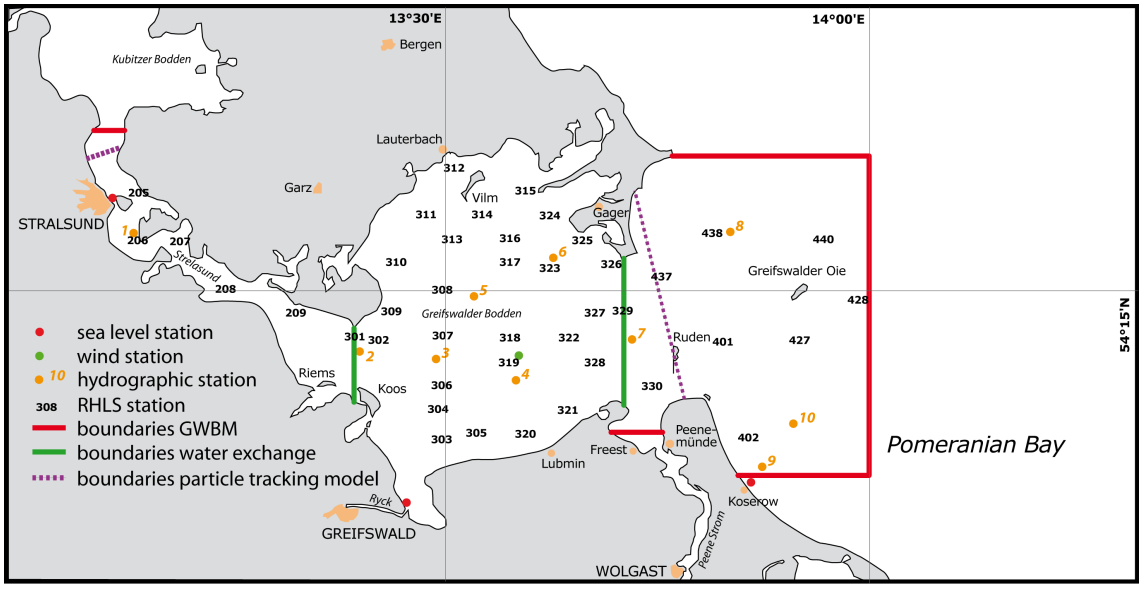

Figure 10: Overview of used stations and boundaries of conducted calculations and experiments. Figure adopted from Zimmermann.

Water Exchange

Time series of the water volume, volume changes and exchange rates for the GWB were investigated. Special focus was set on the duration and frequency of in- and outflow events. To calculate the volume of the GWB, the area of the GWB was limited by two boundaries (Figure 10). These boundaries were chosen according to a prior approach by Buckmann et al. (1998), who examined the water exchange rates of the GWB during several months in 1994 and 1995, based on simulation results. Thus, the intended direct comparison of the results of both studies was enabled. For each time step, the water volume of the GWB was determined by summarizing the volumes of all grid points of the restricted area:

$$V(t) = \sum_{i=1}^{n} V_i(t) \,. \tag{6}$$

Thereby, the volume of each included grid box i was calculated based on

$$V_i(t) = A\, z_i(t) \,. \tag{7}$$

The time dependent sea surface height $z_i(t)$ is denoted by

$$z_i(t) = h_i + \zeta_i(t) \,, \tag{8}$$

where h_i represents the long-term mean water level and $\zeta_i(t)$ the sea surface elevation at the time step t. Alongside, the surface area was set constant to $A = (180\ \mathrm{m})^2$, disregarding minor increments of grid box dimensions which are accompanied by higher latitudes.

Volume changes $\frac{dV}{dt}$ were calculated for subsequent hourly time steps. On this basis, positive and negative deviations of volume changes were summarized separately for each month, with their average being the monthly exchanged water volume. In addition, this amount was divided by the average water volume of the area to obtain monthly water exchange rates of the GWB.

Wind and Water Flow Patterns

Wind and water flow patterns during the WBSS spawning season of 2008 and 2009 were investigated. The purpose was to identify the main directions and duration of flow patterns. Simulated meteorological data were provided from the local operational model LM-E (Schulz, 2006) of the German Weather Service (DWD), encompassing the whole model domain of the GWB model. A station located within the center of the lagoon was selected in order to avoid influences of landmasses on wind fields (Figure 10). Obtained wind field data, taken at 10 meters above ground level, had a time resolution of 3 hours and was divided in u (east-west) and v (north-south) components. Wind time series were plotted. In addition, total frequencies of different wind directions during each month of the WBSS spawning season were examined by using wind rose plots (R package climatol). Therefore, wind directions in degrees were determined according to equation 9 and grouped by rounding to the next decade.

$$dir = \begin{cases} \left| \left(\arctan 2\left(v, u\right) - \frac{\pi}{2} \right) \frac{180}{\pi} \right| & if\ u \geqq 0 \mid v < 0 \\ 360 - \left| \left(\arctan 2\left(v, u\right) - \frac{\pi}{2} \right) \frac{180}{\pi} \right| & if\ u < 0\ \&\ v \geq 0 \end{cases} \tag{9}$$

It has been stated that the mean flow in the GWB is directed to the east (Lampe, 1994). This implies that an outflow would typically occur at the eastern opening. To test this hypothesis, depth integrated flow fields were investigated at the boundaries of the GWB. Focus was set on the frequency and duration of in- and outflow events. Therefore, two stations were selected, one at each boundary (Figure 10). Like wind data currents were given as u and v vectors. Thus, the current directions were calculated using equation 9 as previously described for the wind data. The zonal (east-west) flow was assumed to reflect in- and outflow events through the Strelasund and across eastern sill. Accordingly, the time series of zonal flow were investigated at both stations, neglecting the meridional component.

Spatio-Temporal Variability of Vertical Salinity, Temperature and Velocity Profiles

Apart from water exchange rates and flow fields, inflow events are characterized by temporal changes in vertical salinity and temperature profiles. Moreover, by investigating the variability of the vertical salinity and temperature structure at several stations, the spreading and thus the spatial distribution of inflows can be determined. Related analyses were conducted for 10 stations, covering areas of the central GWB as well as the Strelasund and the surrounding Baltic Sea (Figure 10).

Stratification can also occur as a result of water stagnation, especially at higher temperatures. Thereby, wind induced currents diminish with depth due to internal and bottom friction. Hence, an additional analysis was performed on the vertical consistency of current speeds at the selected stations. In addition, spatially dependent differences in current speeds were compared

with findings from analyses on flow fields under constant wind conditions. Like salinity and temperature data, current speeds were given for each sigma layer of the water column, albeit in u and v vectors. Absolute velocities were calculated using equation 5.

Directed and Turbulent Flow

Movement of particles within arbitrary fluids is determined by advective and diffusive processes. Thereby, advection represents the directed horizontal and vertical movement of particles due to the velocity of surrounding flow fields. Aside from that, the diffusion accounts for the random movement of particles, that is caused by Brownian motion and shear stress of circumjacent currents. Being linearly independent of each other, these terms can be considered separately. Consequently, it can be calculated how far particles get displaced from their original position due to these processes, during a determined period of time. To get an idea of their magnitude and spatially dependence, the local average advective and diffusive displacement distances (during 1 hour) were calculated for flow fields of 2008 and 2009, by using equations 10 and 11, respectively. Furthermore, the ratio of both processes were computed to investigate their spatial dominance in certain areas.

$$S_{Advection} = \sqrt{u^2 + v^2} \cdot 3600 \tag{10}$$

$$S_{Diffusion} = \sqrt{2K \cdot 3600} \tag{11}$$

Larval Drift

Larval drift during the spawning seasons of 2008 and 2009 was investigated. Therefore, a particle tracking was performed using the associated depth-integrated flow fields from the GWBM model. Thus, within the present approach vertical movement of particles is not taken into account. WBSS is known to spawn in batches, resulting in a continuous supply of larvae (s.a.). Hence, cohorts of particles were released, with one cohort being seeded at the beginning of every calendar week (CW) during the whole spawning season (March 1 - June 30, CW 10-27). For each cohort 100 particles were seeded within every grid point giving a total number of 1875000 released particles per cohort. As in the previous approaches it was considered to address tracking time to the critical period of larval survival. This period was assumed to be related to the time needed by larvae to reach a length of 20 mm. This limit was set based on the following considerations: The total amount of 20 mm herring larvae, caught in the GWB and the Strelasund during the RHLS, correlates well with the abundance of recruits at age 1 and 2, forming the basis of the N-20 recruitment index (Oeberst et al., 2009b; s.a.). Moreover, below this critical size, herring larvae are reported to show high mortality rates (Blaxter & Hempel, 1961). With approaching this length, larvae obtain a better resistance against starvation (Yin & Blaxter, 1987). At the same time, swimming performance of larvae improves. Thus, feeding success and the ability to avoid predators increases (Purcell et al., 1987, s.a.). In addition, locomotion becomes less restricted by viscosity (Fuiman & Batty, 1997; Gillis, 2003), making the assumption more unlikely that larvae behave like passive drifters.

In order to calculate the individual critical period for each seeded "larvae" the particle tracking scheme from Gräwe (2011) was extended by a "growth" module by Dr. Ulf Gräwe (Leibniz Institute for Baltic Sea Research, Warnemünde - Germany). This module calculates the "larval length" for each particle at every time step based on a initial length and on a mean daily growth model presented by Oeberst et al. (2009a):

$$G = 0.011 + 0.037\,T \qquad \left(r^2 = 0.51\right). \tag{12}$$

This growth model relies on depth integrated temperature data (temperature range: 5-20°C) and larval catches from the GWB and the Strelasund which were recorded during the RHLS in 1992-2006 (Oeberst et al., 2009a).

Larvae are assumed to become affected by currents soon after hatching. Hence, the initial length of simulated larvae was set to 6 mm which is within the range, but a bit smaller than the average hatching length of WBSS larvae in the GWB described by Klinkhardt (1996) (average 6.48 mm; range: 5.5-7.3 mm). Within the applied module, larval growth was determined by the ambient depth integrated temperature data along individual particle trajectories. Therefore, larval growth and thus the critical period and tracking time could differ by particle ("larvae"). The fate of each "larvae" was investigated, whether larvae have reached the final tracking length of 20 mm inside the GSA ("remained larvae") or not ("removed larvae"). It has to be emphasized that the larval position at any earlier time was ignored by this decision. Larvae could have been located outside of the GSA. As long as they have grew up the final millimeters inside the area, larvae were considered as "remained larvae".

The total amount of removed larvae was calculated for each cohort and each grid point, giving the temporally and spatially resolved probability to drift out to the Baltic Sea. Based on these results, the percentage of removed particles of each cohort was examined for several specified areas (Figure 9) and all spawning sites of WBSS reported by Scabell (1988) (Figure 24). Moreover, it was evaluated whether removed larvae have left the GSA through the Strelasund or the eastern sill of the GWB (Figure 10).

To visualize the time dependent removal of simulated larvae, the percentage of all particles retained within the GSA was calculated for each recorded time step (every 6h), whereas the time series was stopped at the average tracking time of each cohort.

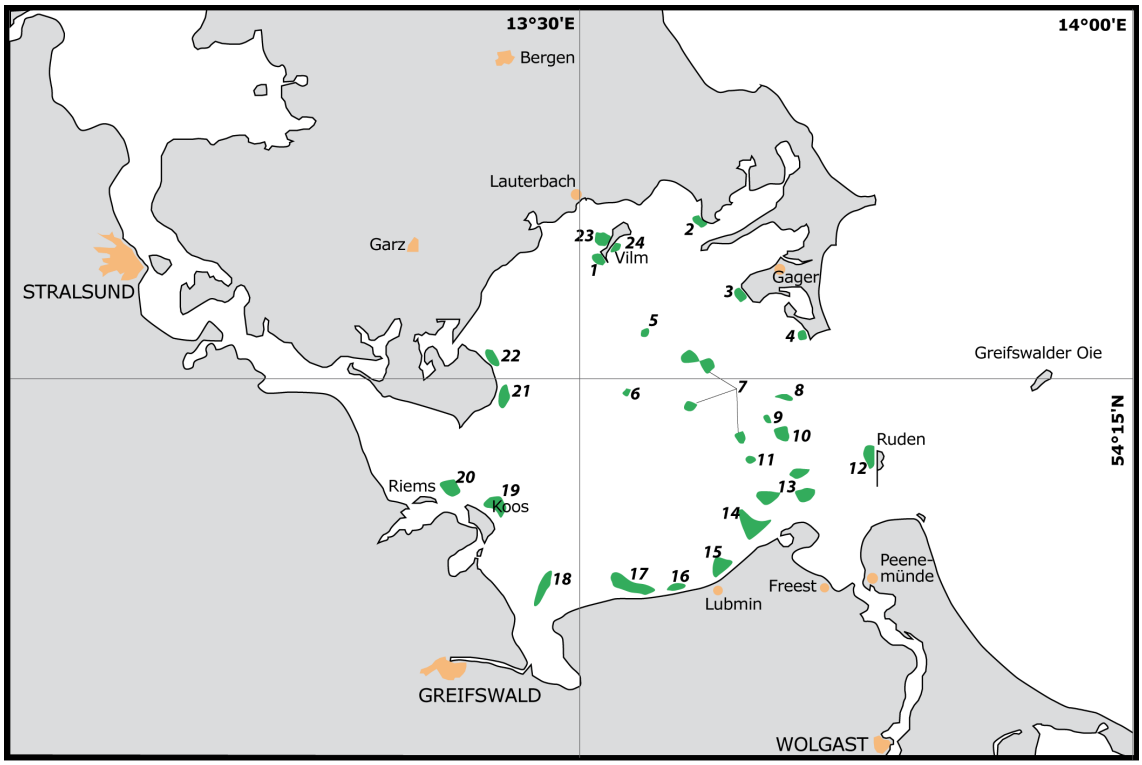

Figure 11: Overview of WBSS spawning sites in the GWB, reported by Scabell (1988). Figure adopted from Zimmermann.

2.5 Retention Index

A retention index was established to enable the quantification of the inter-annual variability of larval removal. Thereby, the annual retention index R_a was defined as the sum of cohort specific probability to remain in the GSA $P_{a,C}$, weighted by the cohort specific shares on annual larval abundances $\frac{N_{a,C}}{N_a}$:

$$R_a = \sum_{C=1}^{n} \left(P_{a,C} \frac{N_{a,C}}{N_a} \right). \tag{13}$$

The retention index was calculated for both model years and two larval size classes (larvae $\leqq$ 6 mm and larvae $\leqq$ 7 mm). The applied larval abundance data were obtained from the RHLS.

2.6 Supplementary Analyses

The temporal course of larval drift and flow fields was further analyzed. Larval drift was investigated by seeding 10000 particles in the center of the Strelasund and at 7 important spawning sites of WBSS reported by Scabell (1988) (Figure 11, selected spawning sites: 1, 3, 6, 12, 16, 18, 21). These particles were tracked at all obtained constant flow fields and at real wind conditions. For constant flow fields, tracking time was set to 31 days, as done in previous analyses. At real wind conditions, weekly cohorts of particles were tracked until the average number of particles have reached the critical length of 20 mm. The percentage of remained larvae was calculated at each time step. Thereby, contrary to the definition in previous analysis, larvae were only considered as removed larvae after passing the boundaries of the GWBM (Figure 10). For both setups, constant and real wind conditions, the spatial distribution of particles was plotted every 3 hours. In addition, monthly flow fields during the WBSS spawning season in 2008 and 2009 (March - July) were plotted every 3 hours.
Produced plots were combined to movie streams. In total 76 movies were created: 32 movies for larval drift at constant wind conditions, 2x18 movies for larval drift and 2x4 movies for flow fields at real wind conditions. These movie files are contained on the enclosed DVD.

3 Results

3.1 Experiments at Constant Wind Conditions

Circulation Patterns

Average current speeds within the GWB and the Strelasund for different wind fields are given in table 1 and 2, respectively. With the average current speeds being less than 0.2 m s^{-1} and maximum speeds not exceeding 0.7 m s^{-1} currents in the GWB and the Strelasund are relatively weak. However, current speeds depend on the forcing wind fields. Generally, current velocities increase with increasing wind speeds. Currents in the GWB are strongest at NW and N winds. By contrast, highest current speeds occur at NW and SE winds in the Strelasund. In general, currents in the Strelasund are twice as strong as in the GWB, unless the wind blows not from NE or SW. At these wind directions, flow through the Strelasund appears to be greatly hampered.

Surface and depth-integrated flow fields within the GWB and the Strelasund for constant wind speeds (6 m s^{-1}) and different wind directions are presented in figure 12 and 13, respectively. Circulation patterns of further investigated wind speeds (1, 3, 6 and 9 m s^{-1}) for several wind directions are shown in figures 43-50. Regarding spatial patterns, currents appear to be strongest in near coastal areas. In these areas wind forcing can easily extend to the bottom, setting the whole water column in motion. However, under calm wind conditions water flow throughout the lagoon and the Strelasund is negligible, even at the surface layer. Circulation patterns within the lagoon and the Strelasund differ for different wind conditions. In general, increasing wind speeds do not alter but intensify prevailing flow fields at equal wind directions. Opposite wind directions create inverse flow fields, particularly within the Strelasund. Westerly, northwesterly and northerly winds cause a significant inflow via the Strelasund. By contrast, at easterly, southeasterly and southerly winds strong directed outflow takes place. Thus, a funnel effect is quite apparent: Water speeds up rapidly as it is forced to move inside the narrow channel. The further flow is similar to that through a pipe. By reaching the mouth of the channel, the flow weakens. This effect is strongest at southeasterly and northwesterly winds when wind directions are perfectly aligned with the channel, while at southwesterly or northeasterly winds water exchange via the Strelasund is negligible and flow within the channel occurs partly bidirectional. It is remarkable, that the in- or outflowing water of the Strelasund recruits mainly from or to a near-coastal current in the southwestern part of the GWB. The flow is far less connected to the water masses of the central GWB.

The circulation patterns at the eastern inlet of the GWB with its pronounced sill are much more diverse. Although this inlet is relatively wide, a direct inflow is greatly hampered by the sill as indicated by depth averaged flow fields. This is particularly evident for westerly and easterly winds, where otherwise a strong water exchange could be expected. Instead, water out- and inflow is strongest at northwesterly and southeasterly winds, respectively. Despite a deeper fairway that breaks through this barrier, strongest flow occurs along the northerly or southerly coastline. The numerous grounds and shelves in the east of the lagoon cause a strong deflection of water flows and strong turbulences. Flow reversal in these areas is a frequent feature for several wind fields.

Currents in the central GWB, however, are relatively weak, despite being directly exposed to prevailing winds. Surface currents in this area are aligned with wind directions. By contrast, depth integrated flow fields show the rise of a counter current, especially at N and S winds. This current arises from the water flow along the coastline which hits reverse flowing or calmer waters, causing a deflection of the flow towards the center of the lagoon.

Table 1: Average current speeds [cm s^{-1}] in the GWB for depth-averaged flow at constant wind forcing.

wind speed	wind direction							
[m s^{-1}]	W	NW	N	NE	E	SE	S	SW
1	0.1	0.2	0.1	0.1	0.1	0.2	0.1	0.1
3	1.1	1.3	1.3	1.0	1.1	1.3	1.3	1.0
6	2.6	3.0	3.1	2.6	2.6	3.0	3.1	2.5
9	6.0	7.0	7.3	6.1	6.1	6.9	6.6	5.5

Table 2: Average current speeds [cm s^{-1}] in the Strelasund for depth-averaged flow at constant wind forcing.

wind speed	wind direction							
[m s^{-1}]	W	NW	N	NE	E	SE	S	SW
1	0.3	0.4	0.2	0.2	0.4	0.4	0.2	0.2
3	2.4	2.7	1.9	1.1	2.4	2.8	2.0	1.1
6	5.4	6.7	5.1	2.3	5.5	6.8	5.2	2.4
9	12.0	16.0	13.0	5.1	12.0	16.0	13.0	4.1

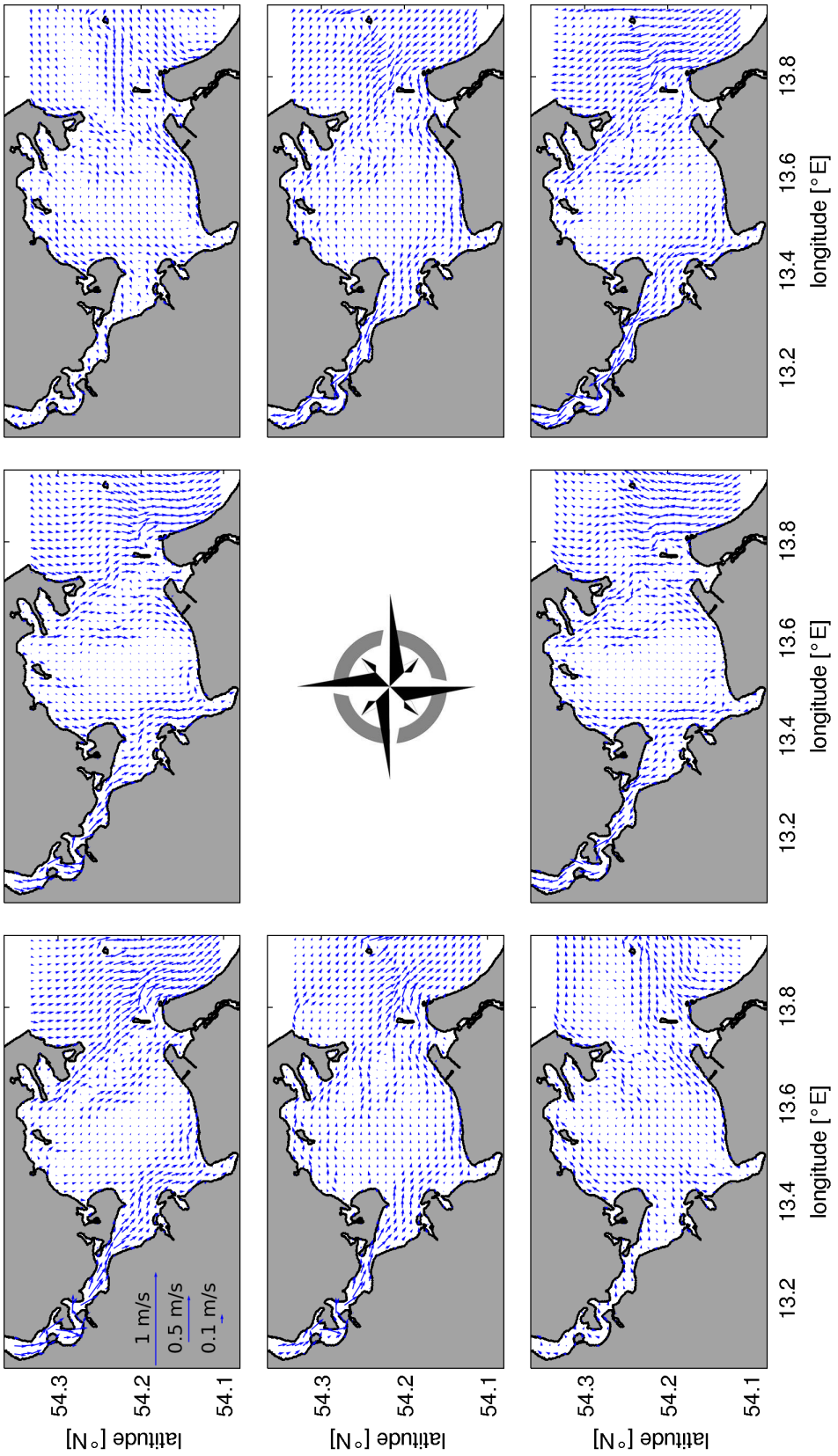

Figure 12: Simulated, surface flow fields for constant wind speeds (6 m s^{-1}) and different wind directions. Plot orientation with respect to the compass rose corresponds to the forcing wind direction (e.g. upper left plot refers to north-westerly winds). The vector length gives the current speed, vector direction relates to the current direction.

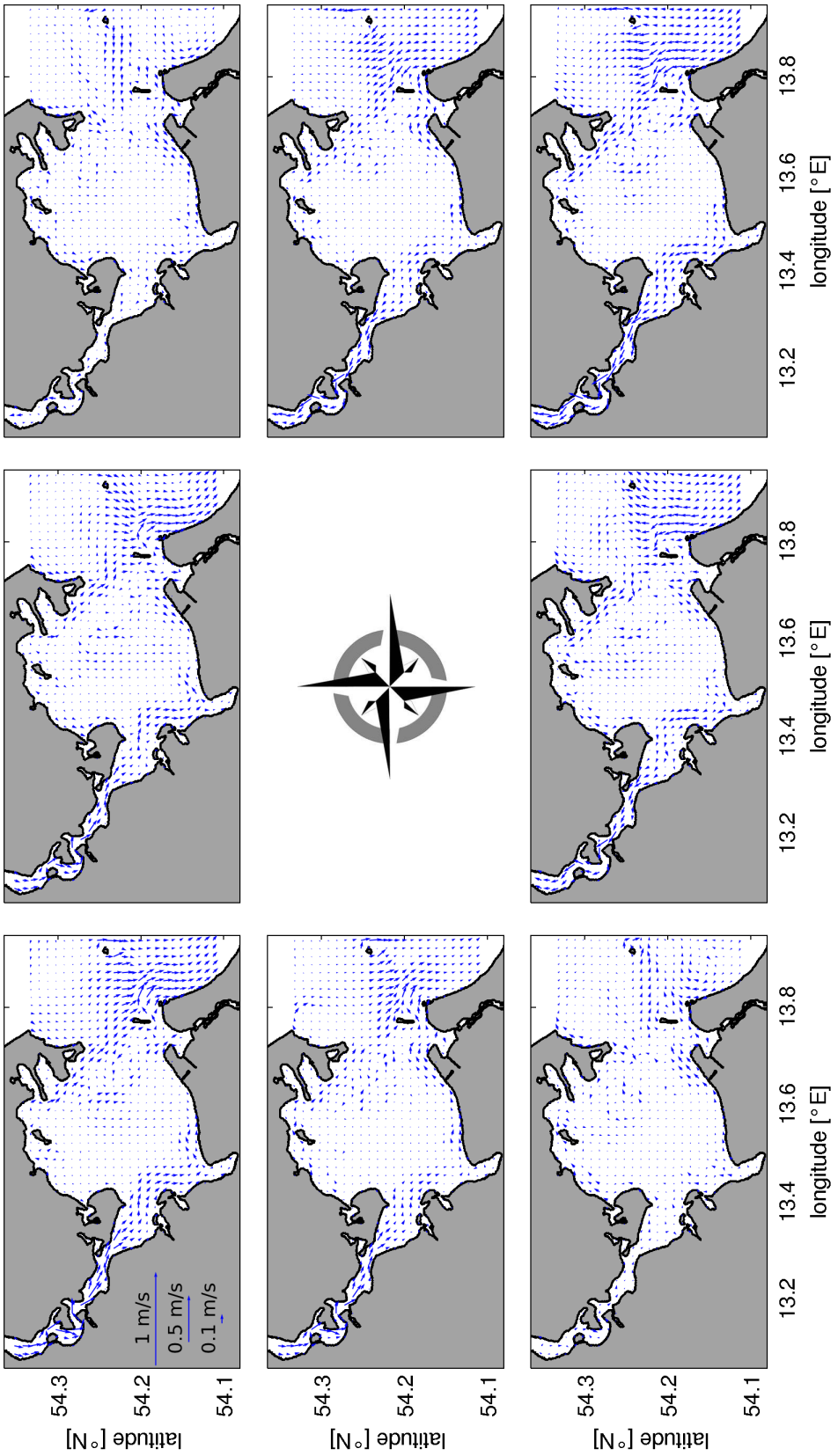

Figure 13: Simulated, depth averaged flow fields for constant wind speeds (6 m s^{-1}) and different wind directions. Plot orientation with respect to the compass rose corresponds to the forcing wind direction (e.g. upper left plot refers to north-westerly winds). The vector length gives the current speed, vector direction relates to the current direction.

Larval Drift

Weak winds have almost no impact on larval dispersal. Less than one third of all seeded particles were drifted to the open Baltic after 31 days of steady winds of 3 m s^{-1}, regardless the wind direction (Table 3). The percentage of removed particles was negligible for even lower wind speeds. Generally, higher wind speeds resulted in a greater proportion of removed particles. However, even after one month of enduring wind forcing of 9 m s^{-1} the percentage of remained particles was still above 20%. At SW and NE winds more than 50% of all seeded particles were retained. By contrast, retention was lowest at southeasterly and northwesterly winds. Thus, it is interesting to note, that at opposite wind directions almost the same amount of particles is drifted outside the lagoon.

In general, particles can leave the lagoon either across the large opening in the east or through the Strelasund to the west. As shown by the spatially resolved mean residence times (Figure 15 and figures 55-58), always one of these two paths is favored, depending on wind directions. Drift across the eastern boundary occurs mainly at westerly to northerly winds. On the other hand, flushing of particles through the Strelasund is clearly apparent at easterly, southeasterly and southerly winds, coinciding with results from flow field analyses. As a result, the risk to drift outside the lagoon is not uniform within the GWB and areas at risk differ with prevailing wind fields. Under low wind speeds only particles which were seeded very close to these boundaries are threatened to drift outside. With increasing wind speeds and time, areas at risk extend further into the lagoon and more particles get exposed (Table 3). Thereby often more particles of the inner basin are more affected than those of near-shore areas. In addition, the flushing effect of the Strelasund reveals itself also at opposite wind directions, although particles within the Strelasund are pushed towards inside the lagoon. Often the particle flow continues across the North - South axis of the central basin. This is particularly evident at N and NW winds. Taking this wind directions and of wind speeds of 3 m s^{-1}, none of the particles seeded in the Strelasund is affected by larval drift since the flow along this conveyor belt does not reach the Strelasund within the given tracking time of 31 days. However, at the same wind directions and greater wind speeds more than 45% of all particles seeded in the Strelasund cross the eastern boundary. On the other side, flushing and thus particle transport through the Strelasund is greatly hampered at SW and NE winds. Nevertheless, the Strelasund appears to be strongly affected by larval drift at several wind fields.

By contrast, large parts of the western and eastern central basin remain completely unaffected. Regarding nearshore areas, the north western part of the GWB as well as the isolated coves of the GWB and the Strelasund can be considered as retention areas. Particles originating from the northeasterly and southeasterly shoreline of the GWB are much more threatened to drift to the open Baltic, especially at westerly winds.

Table 3: Percentage of removed particles in relation to wind conditions and seeding location (sub area). Extent of defined sub-areas are shown in figure 9.

wind direction	speed	GSA	GWB total	GWB < 6 m	GWB < 3 m	Strelasund
W	1	5.7	6.7	11.4	11.5	0.2
	3	31.7	33.6	54.6	57.9	21.4
	6	48.9	50.1	70.2	72.4	42.8
	9	70.5	70.7	81.8	79.8	69.5
NW	1	6.0	7.1	10.3	8.5	0.2
	3	25.8	30.6	32.4	27.0	0.0
	6	53.0	53.9	54.3	45.4	48.6
	9	65.4	64.1	63.9	54.9	71.9
N	1	3.9	4.5	5.6	3.5	0.4
	3	18.5	21.9	26.4	23.6	0.0
	6	40.3	37.7	44.9	41.1	54.6
	9	57.1	55.1	61.5	55.2	67.7
NE	1	4.0	1.6	1.8	1.6	16.4
	3	18.4	8.4	12.8	11.6	72.4
	6	24.2	16.5	21.9	21.2	65.1
	9	40.9	35.7	41.0	39.4	68.6
E	1	6.6	1.9	2.9	3.4	31.7
	3	30.6	19.8	26.7	24.7	88.7
	6	50.5	43.1	49.9	47.9	90.2
	9	64.5	59.3	67.8	62.7	92.1
SE	1	7.8	3.5	5.8	7.0	31.0
	3	32.7	22.6	24.4	23.3	87.0
	6	60.4	55.2	53.8	50.6	88.4
	9	76.4	74.1	75.0	71.9	88.7
S	1	5.8	4.9	8.5	10.6	10.6
	3	26.9	15.9	23.2	25.8	86.0
	6	47.9	40.1	46.7	44.7	89.4
	9	56.1	49.8	55.3	54.0	89.7
SW	1	5.4	6.2	11.6	14.7	0.6
	3	16.8	19.3	28.9	35.7	3.2
	6	27.0	30.9	39.1	45.2	6.2
	9	43.7	47.8	54.1	56.2	21.7

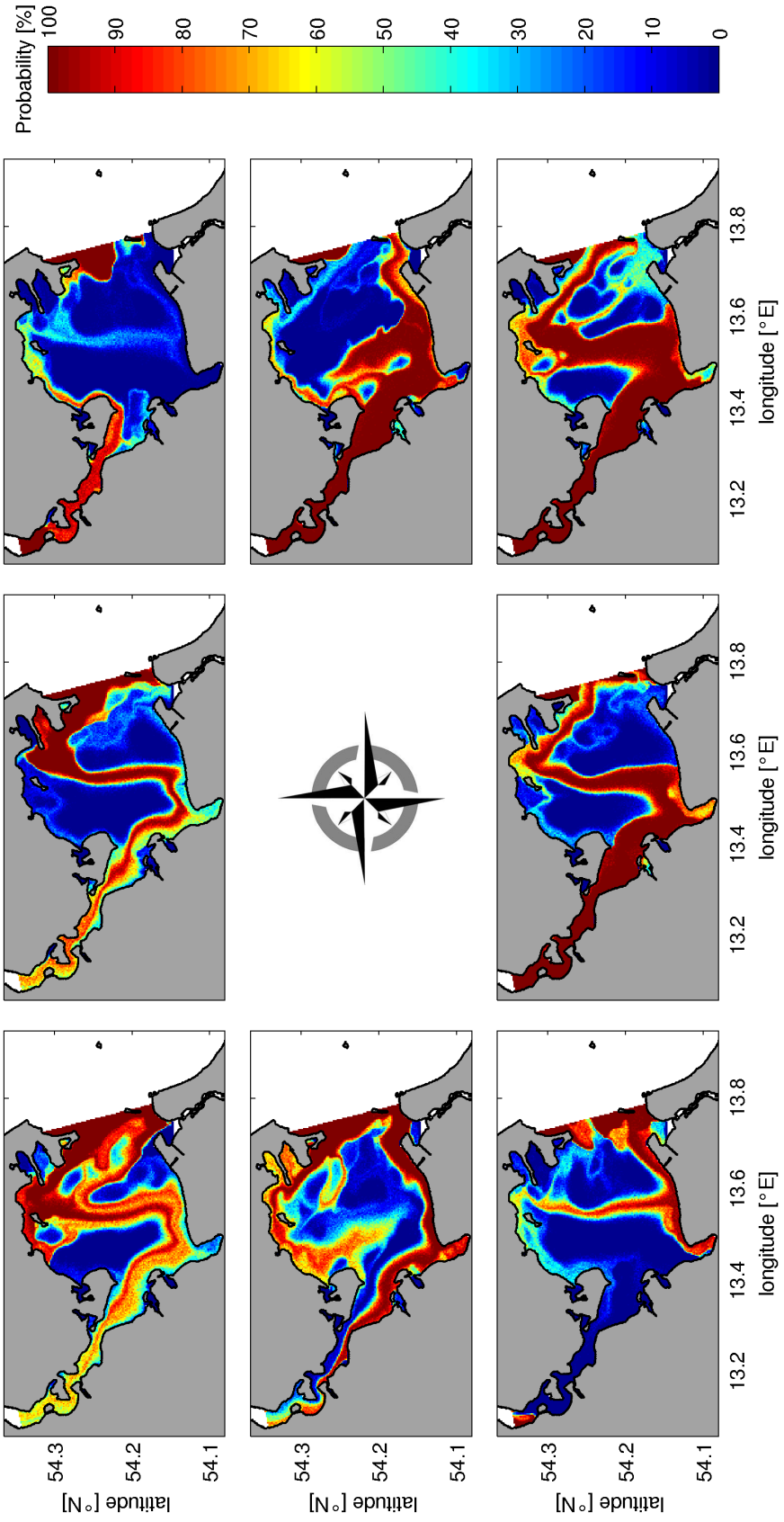

Figure 14: Spatially resolved probability to drift out of the lagoon, for particles exposed for 31 days to wind speeds of 6 m s^{-1}. Plot orientation with respect to the compass rose corresponds to the forcing wind direction (e.g. upper left plot refers to north-westerly winds).

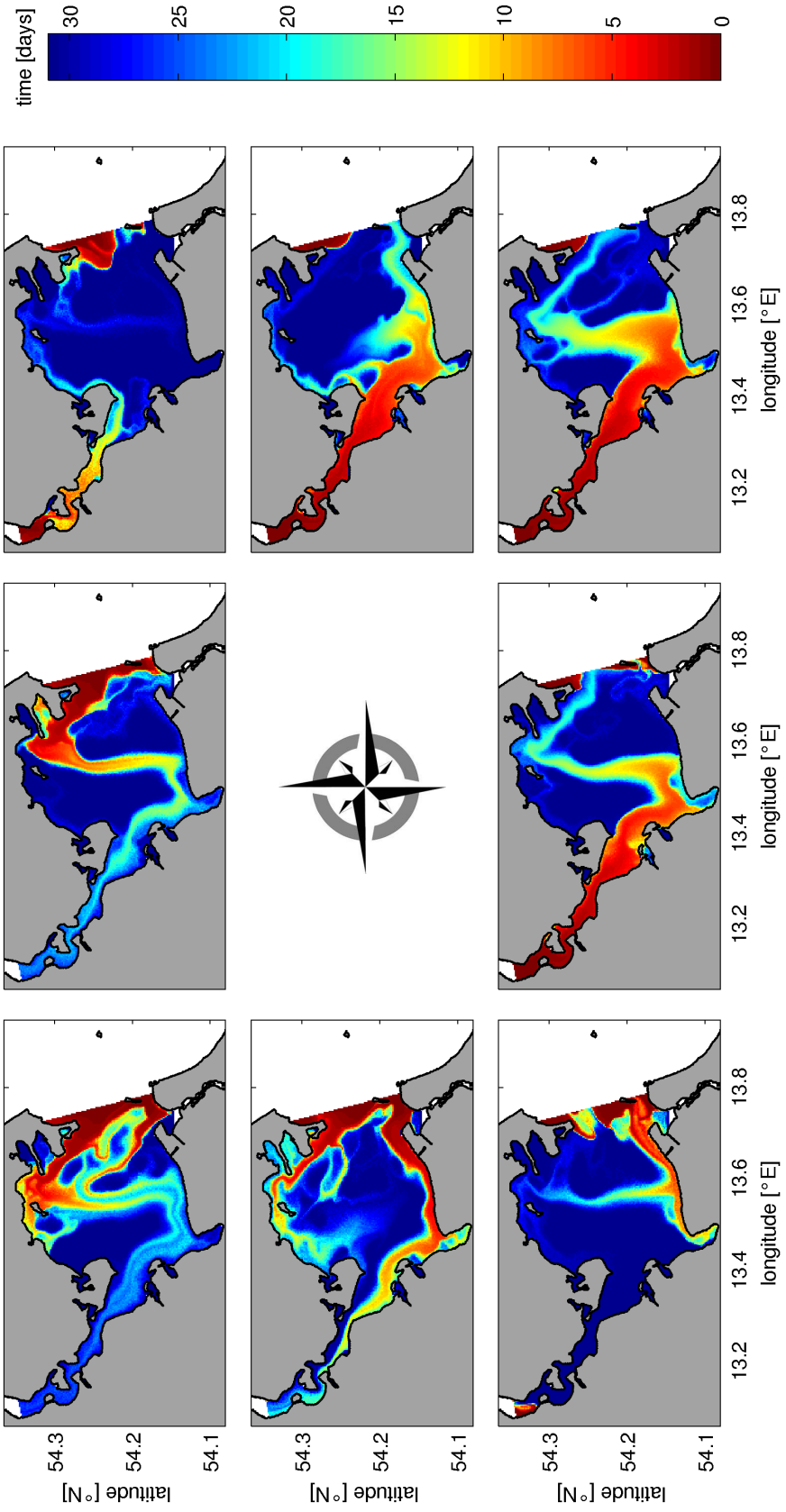

Figure 15: Spatially resolved residence time for particles exposed for 31 days to wind speeds of 6 m s^{-1}. Plot orientation with respect to the compass rose corresponds to the forcing wind direction (e.g. upper left plot refers to north-westerly winds).

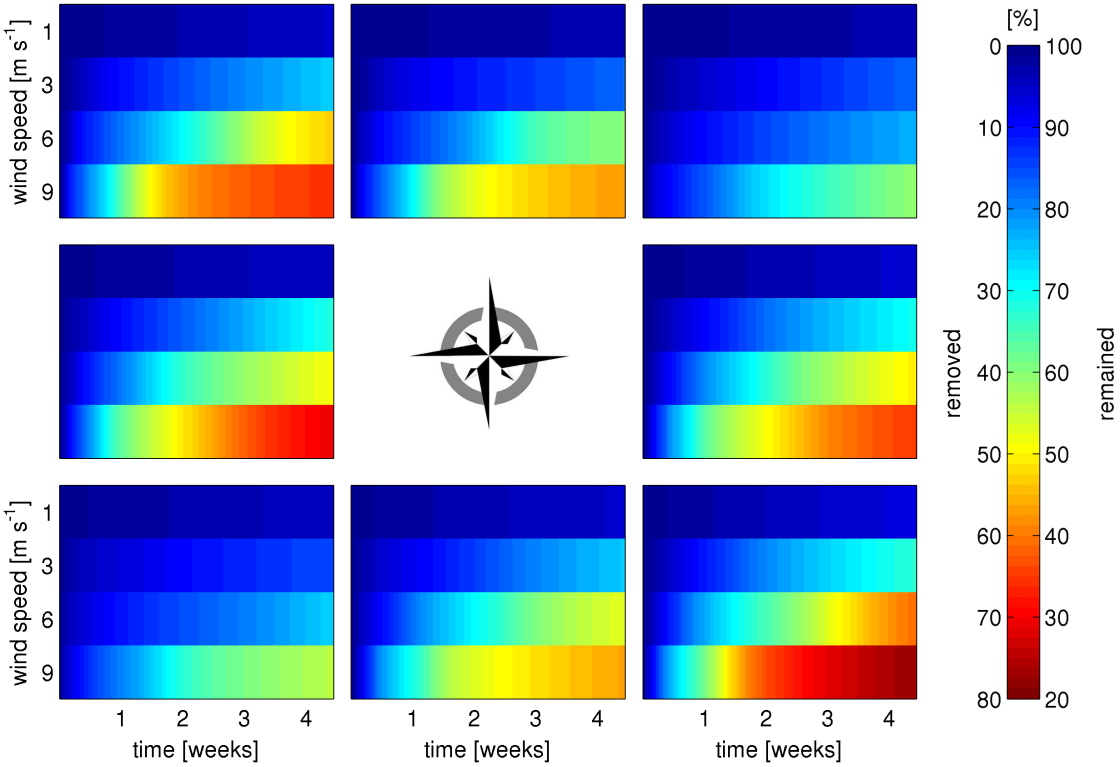

Figure 16: Time series of remained and removed particles in relation to wind conditions. Plot orientation with respect to the compass rose corresponds to the forcing wind direction (e.g. upper left plot refers to north-westerly winds).

Analyses on the Numerical Setup

The simulation results for the different numerical schemes and different levels of c_s are presented below. In general, the spatial patterns of the risk to drift outside the GSA were quite similar for the different numerical setups (Figure 17 and 18). Estimates differ locally. Thereby, turbulent effects increasing the risk to drift outside the GSA appear to be more pronounced for the Platen-Scheme and at higher levels of c_s. Though, estimated percentages of removed particles of several sub-areas (Table 4 and 5) show no large deviations. Estimates differ by less than 5 %.

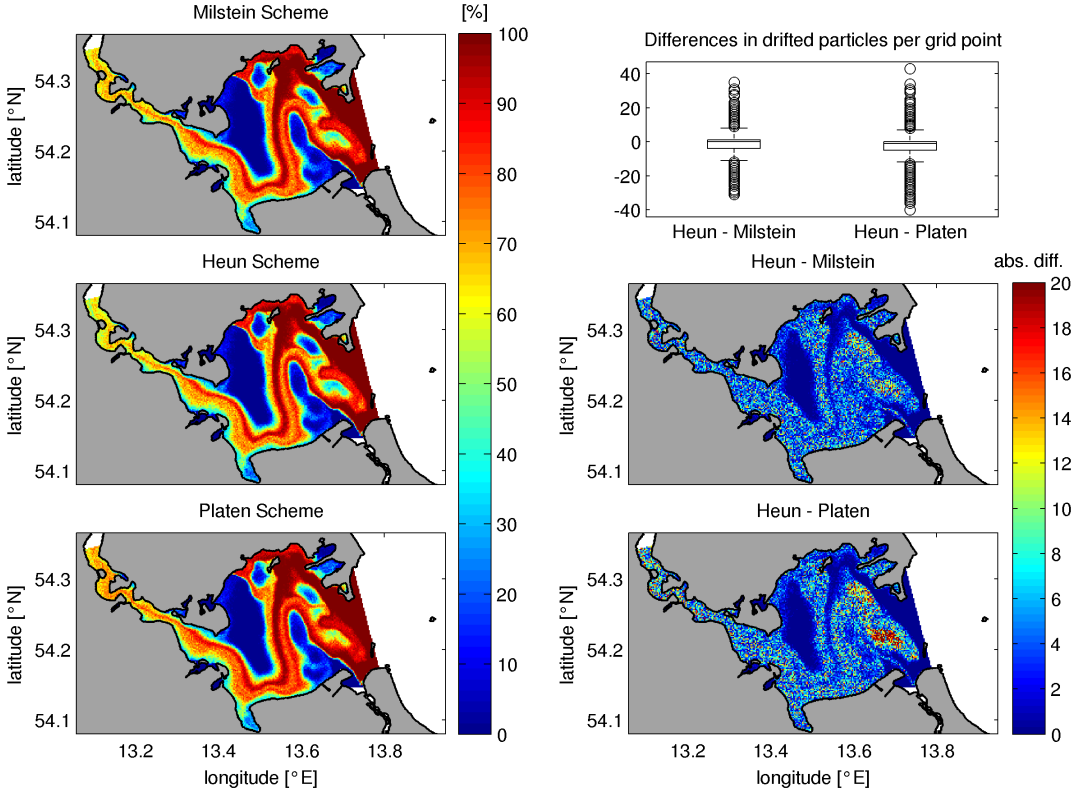

Figure 17: Influence of the applied numerical scheme on the spatial risk to drift to the outside of the lagoon, for particles exposed for 31 days to constant NW winds with speeds of 6 m s^{-1}. The left column shows the results for each numerical scheme. The right column gives the variability (boxplots) and absolute differences (maps) of results at each grid point. By default the Heun-Scheme is used in other numerical experiments.

Table 4: Percentage of removed particles of several sub-areas in dependency on the applied numerical scheme. Example shows the results for constant NW winds with speeds of 6 m s^{-1}. Extent of defined sub-areas are shown in figure 9. By default, the Heun-Scheme is used in other numerical experiments.

Scheme	GWB & Strelasund	total	GWB < 6 m	< 3 m	Strelasund
Milstein	54.6	55.3	55.5	46.3	50.6
Heun	53.0	53.9	54.3	45.4	48.6
Platen	55.7	56.2	56.1	46.6	52.9

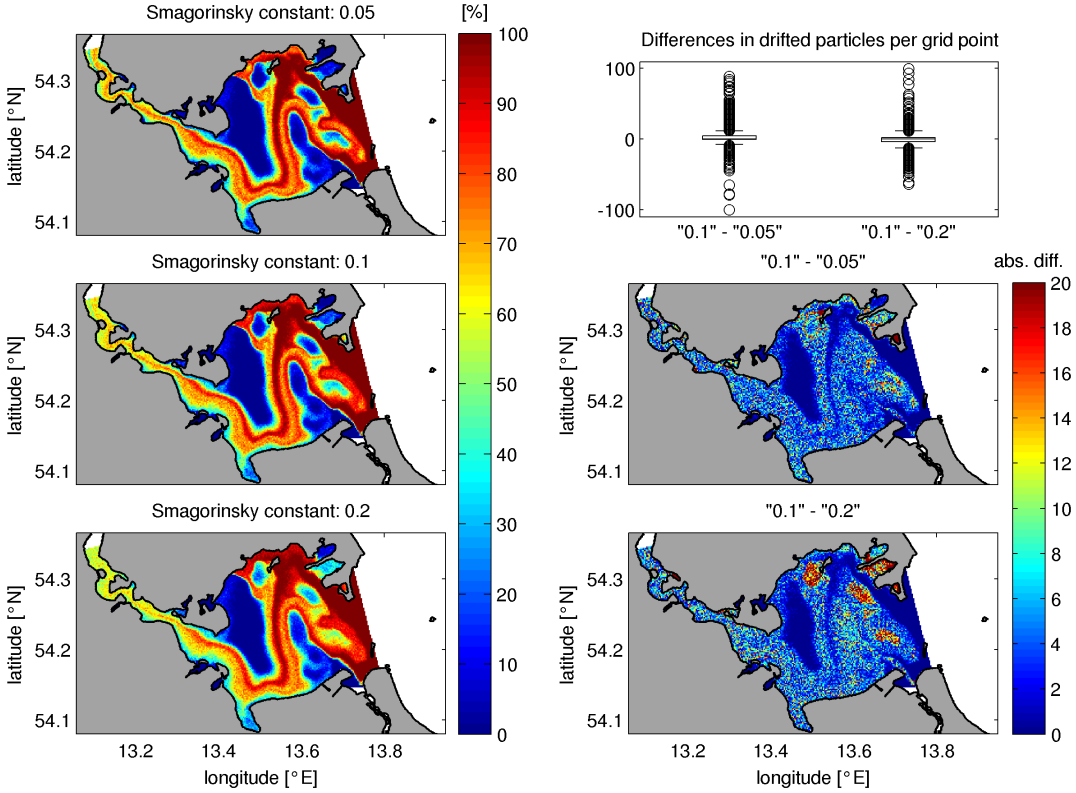

Figure 18: Influence of the applied *Smagorinski constant* (c_s) on the spatial risk to drift to the outside of the lagoon, for particles exposed for 31 days to constant NW winds with speeds of 6 m s^{-1}. The left column shows the results for each numerical scheme. The right column gives the variability (boxplots) and absolute differences (maps) of results at each grid point. The default value of c_s used in other experiments is 0.1.

Table 5: Percentage of removed particles of several sub-areas in dependency on the applied *Smagorinski constant* (c_s). The default value of c_s used in other experiments is 0.1. Example shows the results for constant NW winds with speeds of 6 m s^{-1}. Extent of defined sub-areas are shown in figure 9.

Smagorinsky Constant	GWB & Strelasund	total	GWB < 6 m	< 3 m	Strelasund
0.05	51.3	52.1	52.0	42.5	47.2
0.1	53.0	53.9	54.3	45.4	48.6
0.2	54.6	55.8	56.6	47.7	48.2

3.2 Experiments at Real Wind Conditions

Model Validation

The correlation between observed and simulated depth averaged temperature for both model years is shown in figure 19. Simulated and observed data are shown to be highly correlated with correlation coefficients being 0.962 and 0.978 for 2008 and 2009, respectively. However, temperature in 2009 was mostly underestimated, with a mean deviation of -0.9 K and a maximum deviation of -2.5 K. The same applies for low and high temperatures in 2008 (mean deviation: -0.3 K; maximum deviation: -3.7 K).
The 2008 and 2009 time series of simulated and observed sea level deviation for the three investigated stations are shown in figure 20 and 21, respectively. Sea level is shown to be variable during the selected timeframe, while strongest fluctuations occurred during March of 2008. The total range of SLD, comprising all stations and both years was between -0.8 and 1 m. Generally, the three stations exhibit an almost similar temporal development of SLD. Simulated SLD data coincide well with measurements, regardless the investigated station. This applies even for simulated data from Kosereow which is located outside the GWBM domain. Simulated SLD data of this station was provided by the coarse WBCM as mentioned above. Simulated and measured SLD data are highly correlated as shown by the results of the regression analyses. The maximum deviation between all measured and simulated pairs of values was 0.495 m but was on average below 1e-06 m and thus negligible. In general, correlation coefficients were above 0.75. Interestingly, strongest correlations were found at Koserow, for simulated data of the coarse scaled WBCM (r^2= 0.886).

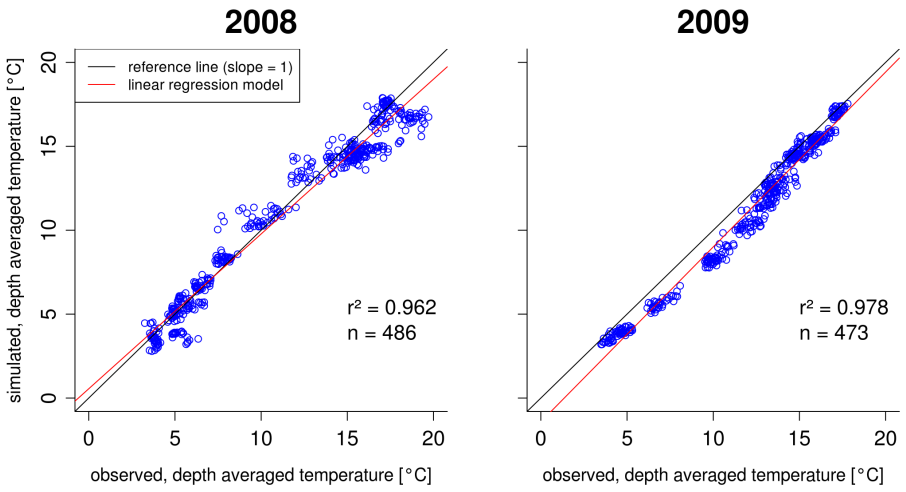

Figure 19: Scatter plot of the comparison between observed and simulated depth averaged temperature data. Reference and regression lines are drawn, coefficients of determination (r^2) are specified. Calculations were performed using the statistical package R (`http://www.r-project.org/`).

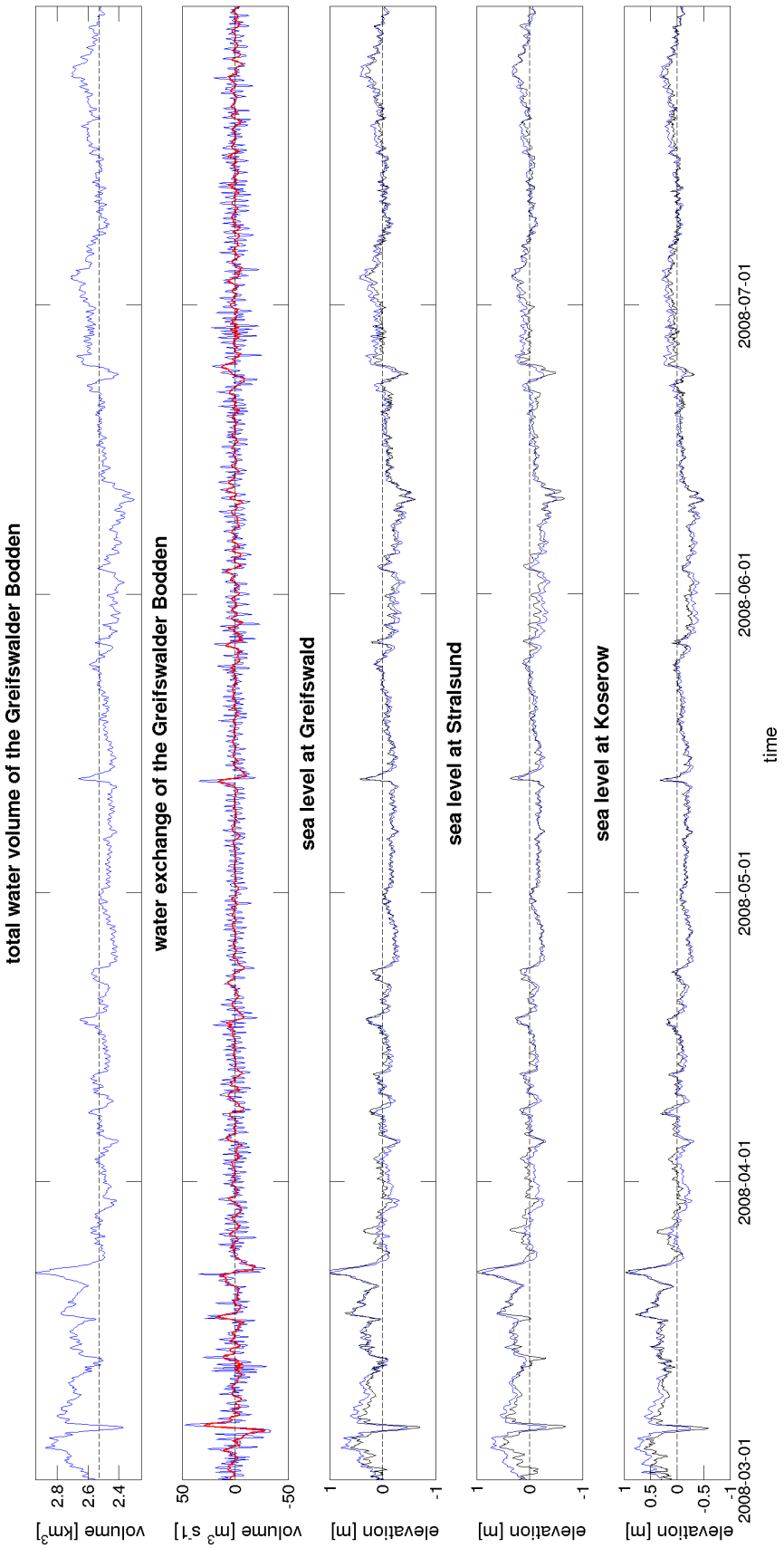

Figure 20: 2008 time series of total water volume and volume exchange of the GWB as well as simulated (blue) and observed (black) sea level deviations at selected stations (Stralsund, Greifswald and Koserow). Red line gives the 6-hour running mean of the water exchange.

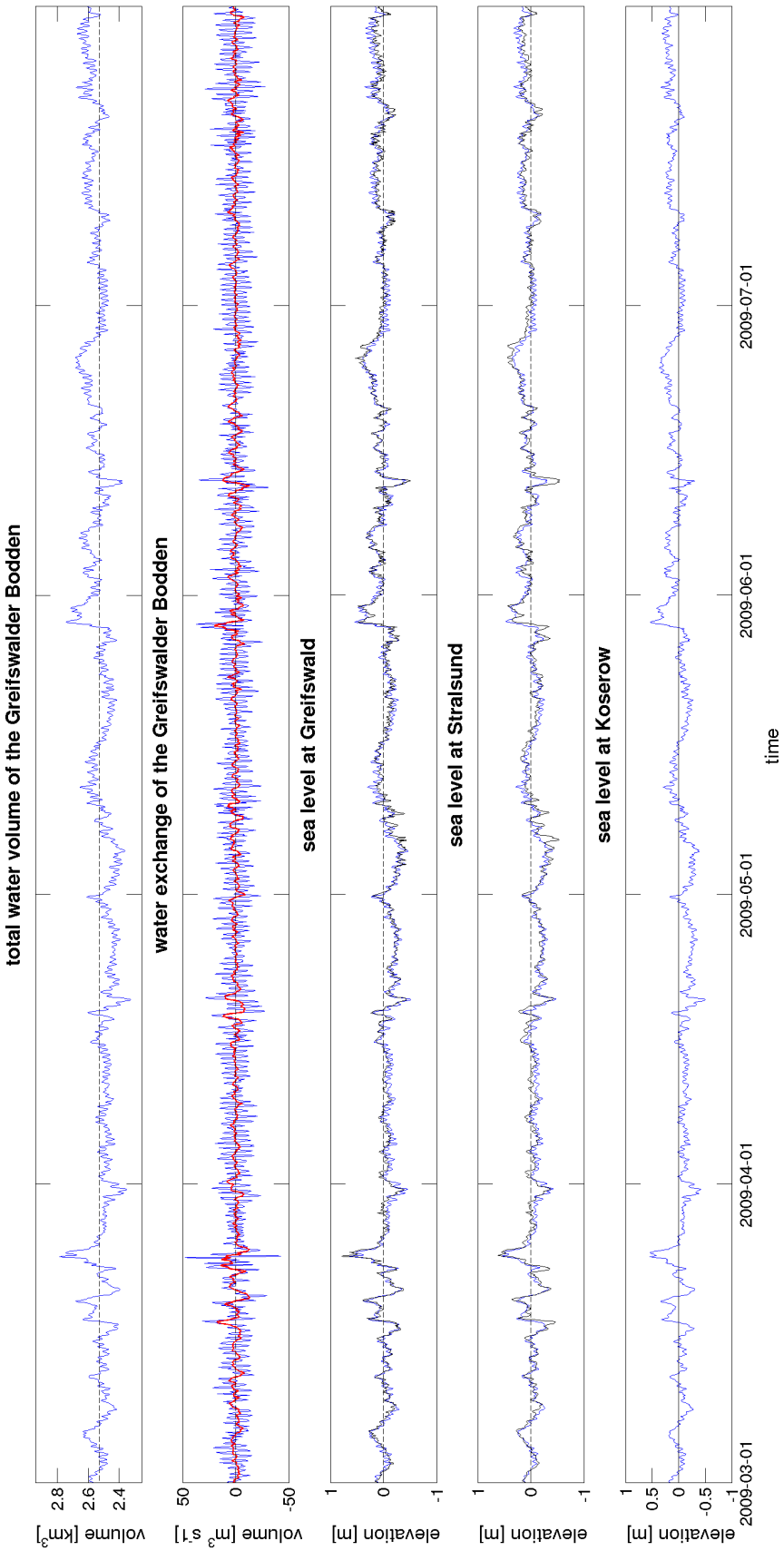

Figure 21: 2009 time series of total water volume and volume exchange of the GWB as well as simulated (blue) and observed (black) sea level deviations at selected stations (Stralsund, Greifswald and Koserow). Red line gives the 6-hour running mean of the water exchange. Observed sea levels at Koserow were not available for 2009.

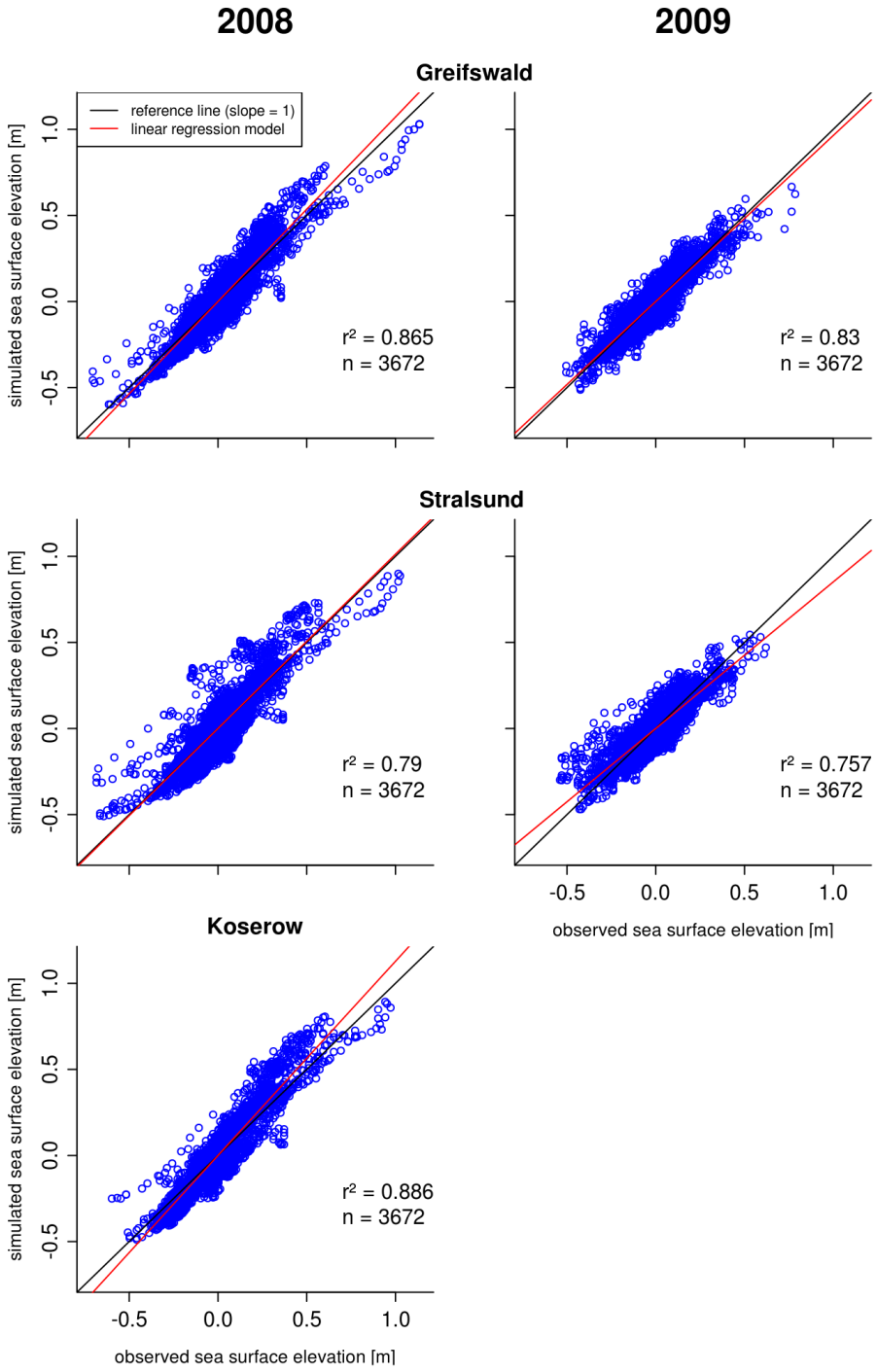

Figure 22: Scatter plot of the comparison between observed and simulated, hourly sea surface elevations during March - July 2008 and 2009, at Greifswald, Strelasund and Koserow. Observed sea levels at Koserow were not available for 2009. Reference and regression lines are drawn, coefficients of determination (r^2) are specified. Calculations were performed using the statistical package R (`http://www.r-project.org/`).

Water Exchange

Time series plots of the total water volume of the GWB as well as hourly volume differences during March-July 2008 and 2009 are given in figure 20 and 21, respectively. Within this timeframe, the total water volume of the GWB was not constant, but varied over time. Especially striking is the fact that temporal changes of the total water volume resemble those of presented sea levels which are highly correlated with each other. However, the inter-annual comparison shows no uniform pattern. Although, strong fluctuations appeared during March in 2008 and 2009. Afterwards, drastic fluctuations occurred less frequent, especially during 2008. The evaluation of related hourly volume differences reveal the high inconstancy of in- and outflow events, which alternated within few hours. The 6-hourly running mean shows much less oscillations and volume changes are much weaker. It is interesting to note that hourly fluctuations were much stronger in 2009 throughout almost the entire investigated period.
The calculated total and relative water exchange are presented in tables 6 and 7. Exchange rates were relatively high during both years, being at least 75% of the longterm mean volume. During March 2008 and 2009 exchange rates were almost similar. Rates remained relatively high and constant in 2009, not dropping to less than 106%. In contrast, exchange rates fell from March to April in 2008 by nearly 40%, with no noticeable rebound until August. Despite the high values and rates, the rapid succession of in- and outflow events make it unlikely that the entire water body of the GWB is included within and thus gets replaced by the water exchange.

Table 6: Total water exchange per month [km^3] between the GWB and the surrounding waters of the Strelasund and the Baltic Sea.

Year	Mar	Apr	May	Jun	Jul	Aug	$\bar{x}$
2008	2.986	2.012	1.954	2.168	2.019	2.696	2.306
2009	2.949	2.931	3.063	2.692	3.016	2.928	2.930

Table 7: Relative water exchange per month between the GWB and the surrounding waters of the Strelasund and the Baltic Sea.

Year	Mar	Apr	May	Jun	Jul	Aug	$\bar{x}$
2008	118.22	79.68	77.38	85.85	79.94	106.76	91.31
2009	116.75	116.05	121.30	106.60	119.40	115.95	116.01

Wind and Water Flow Patterns

Figure 23 and 24 display the 2008 and 2009 time series of wind fields based on 3 hourly, simulated data. As shown, wind conditions were not consistent throughout the investigated timeframe (March-July) in 2008 and 2009. Considerable changes in wind direction and speeds occurred within hours. However, almost uniform wind fields could last for several days, but seldom longer than a week. Despite the pronounced variability, wind rose plots prove that easterly and south-westerly winds were quite frequent (Figure 25). Thereby, wind was mainly from the southwest during April and May in 2008 and from the east during July 2009. In general, wind speeds did not exceed 20 m s^{-1}, with the average wind speed being usually less than 6 m s^{-1}. At the beginning of May 2008 (CW 18 & 19), winds were particularly weak. March 2008 and June 2009 were notable for extended periods of strong winds.

Monthly frequencies of different current directions in 2008 and 2009 at both boundaries are given in figures 29 and 26. Flow at both boundaries was mainly either from the west or the east. Moreover, both directions occurred usually with almost similar frequency. This applies especially for the western boundary where current directions were very uniform. By contrast, currents at the eastern opening were far less well defined. Westward flow at this location was more frequent in 2009 than in 2008.

The time series of zonal (west-east) current speeds demonstrate frequent changes in current directions at the eastern opening (Figures 30 and 31). The current directions changed often during subsequent time steps (6 hours), particularly in 2009. At the outlet to the Strelasund flow directions were more constant, lasting commonly for more than 1 week (Figures 27 and 28). In July 2008, westward flow was nearly absent, occurring only for 1 day.

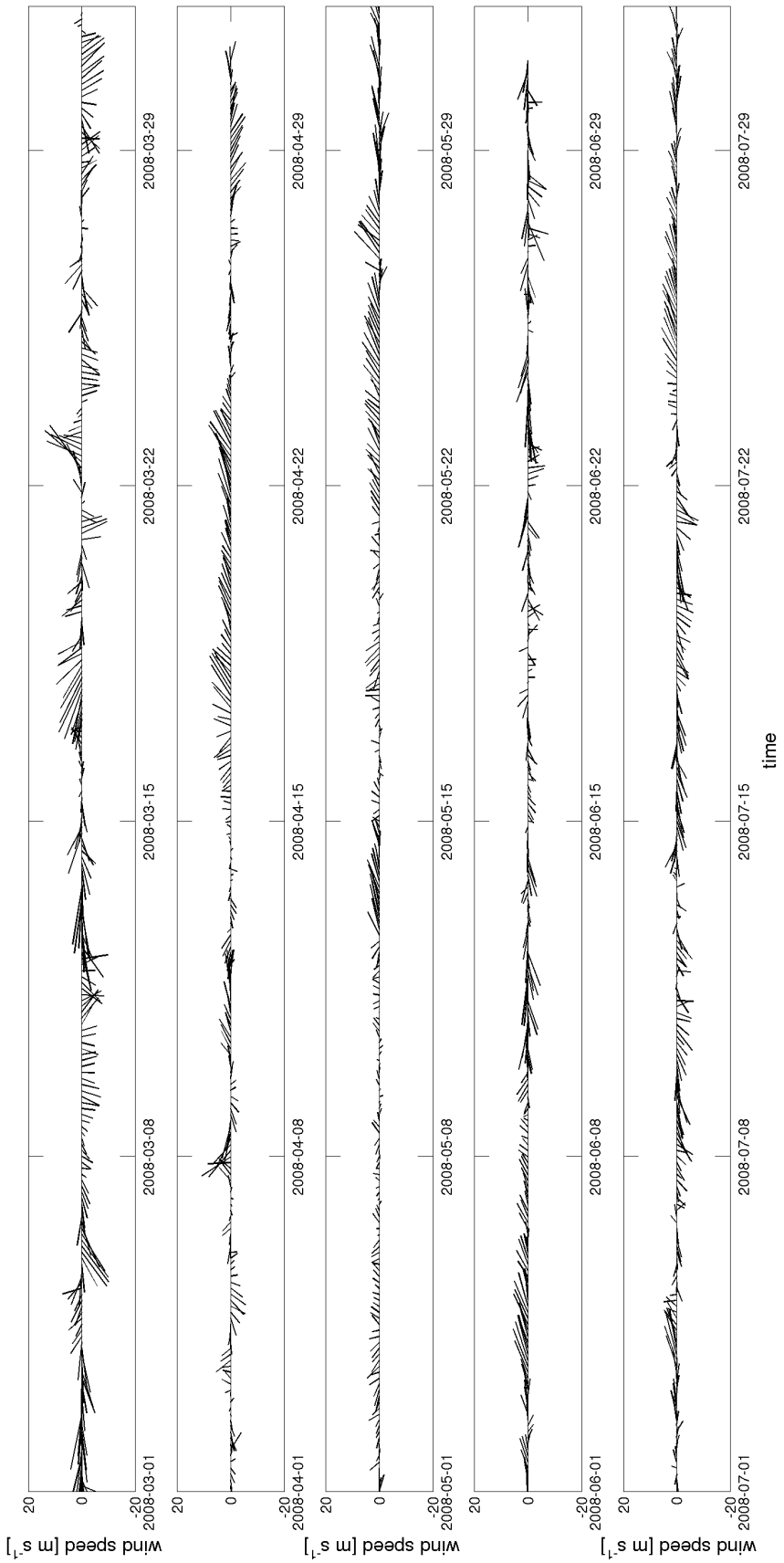

Figure 23: 2008 time series of wind direction and wind speed. The angle and length of plotted lines determine the direction to which the wind is blowing and speed. The location of the wind station is shown in figure 10.

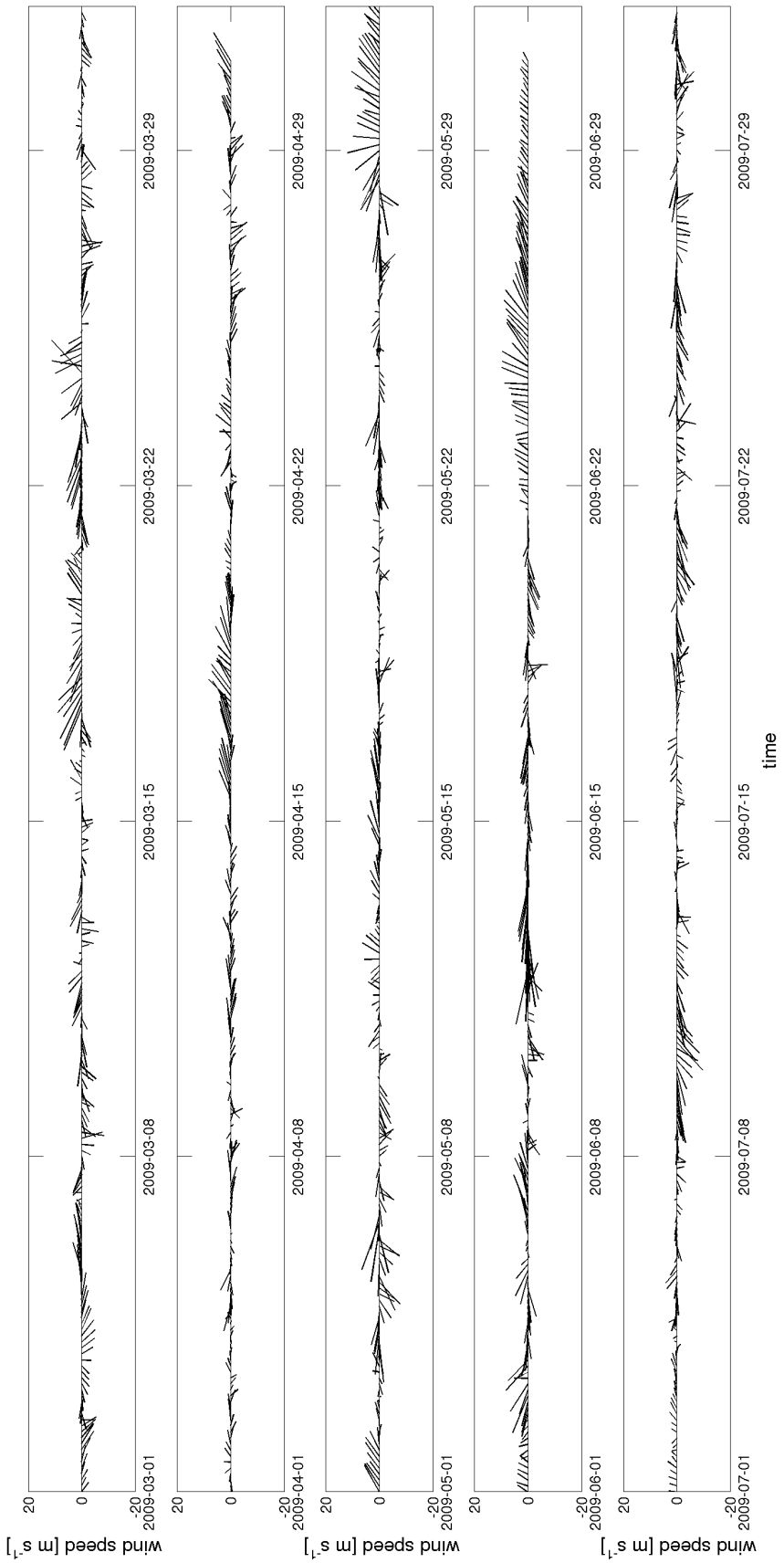

Figure 24: 2009 time series of wind direction and wind speed. The angle and length of plotted lines determine the direction to which the wind is blowing and speed. The location of the wind station is shown in figure 10.

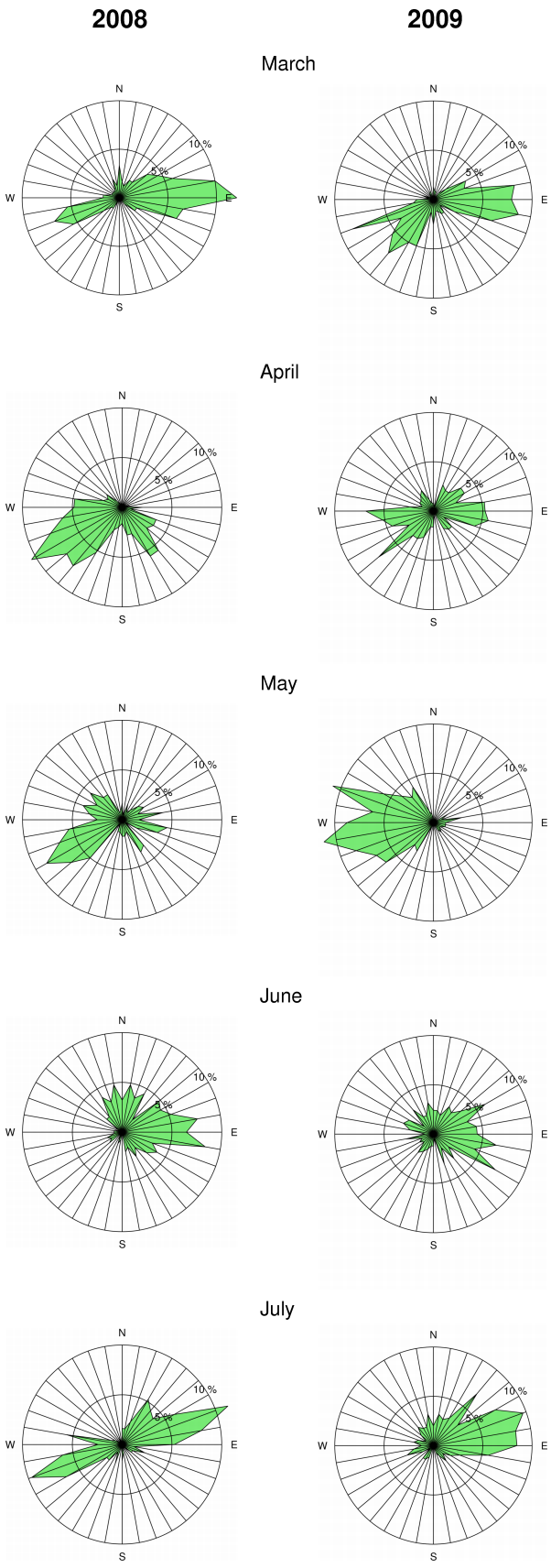

Figure 25: Monthly wind roses for WBSS spawning season in 2008 and 2009 showing the frequency of different wind directions at the center of the GWB. The location of the wind station is shown in figure 10.

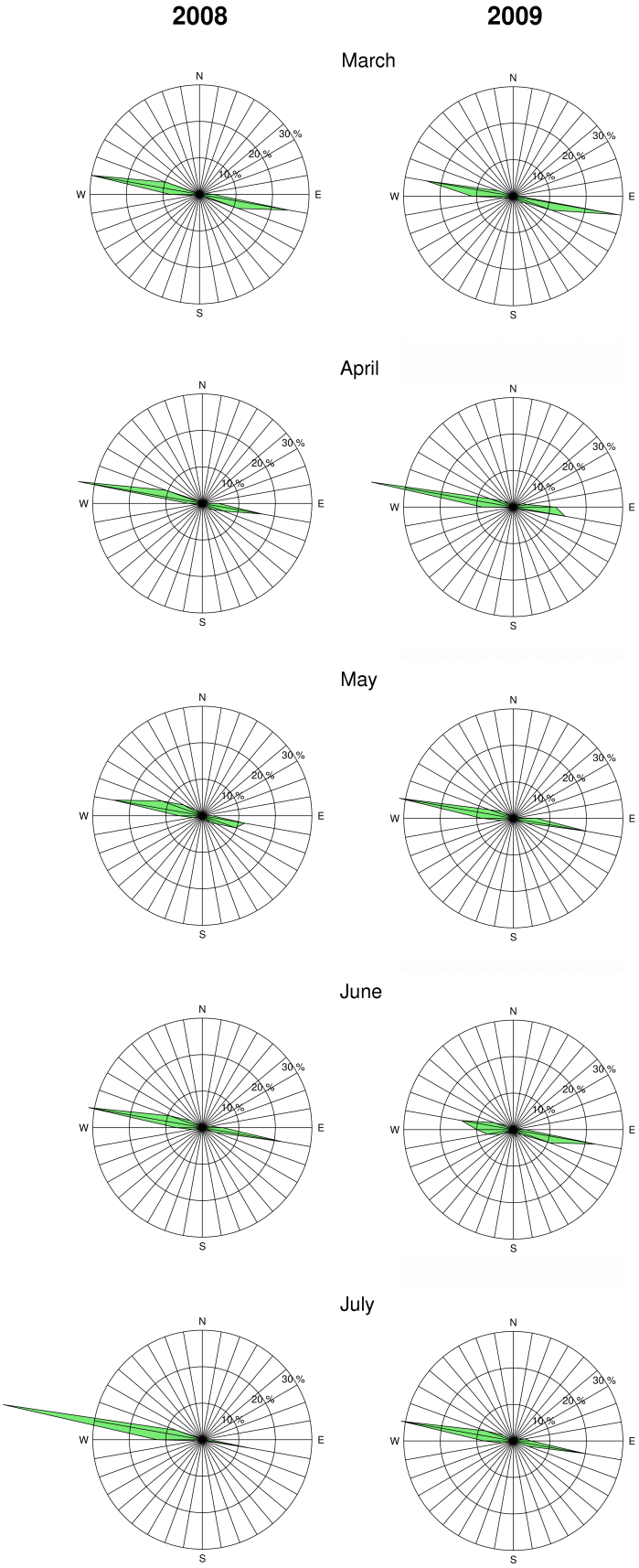

Figure 26: Monthly current roses for WBSS spawning season in 2008 and 2009 showing the frequency of different current directions at the western opening of the GWB (station 2). Station location is shown in figure 10.

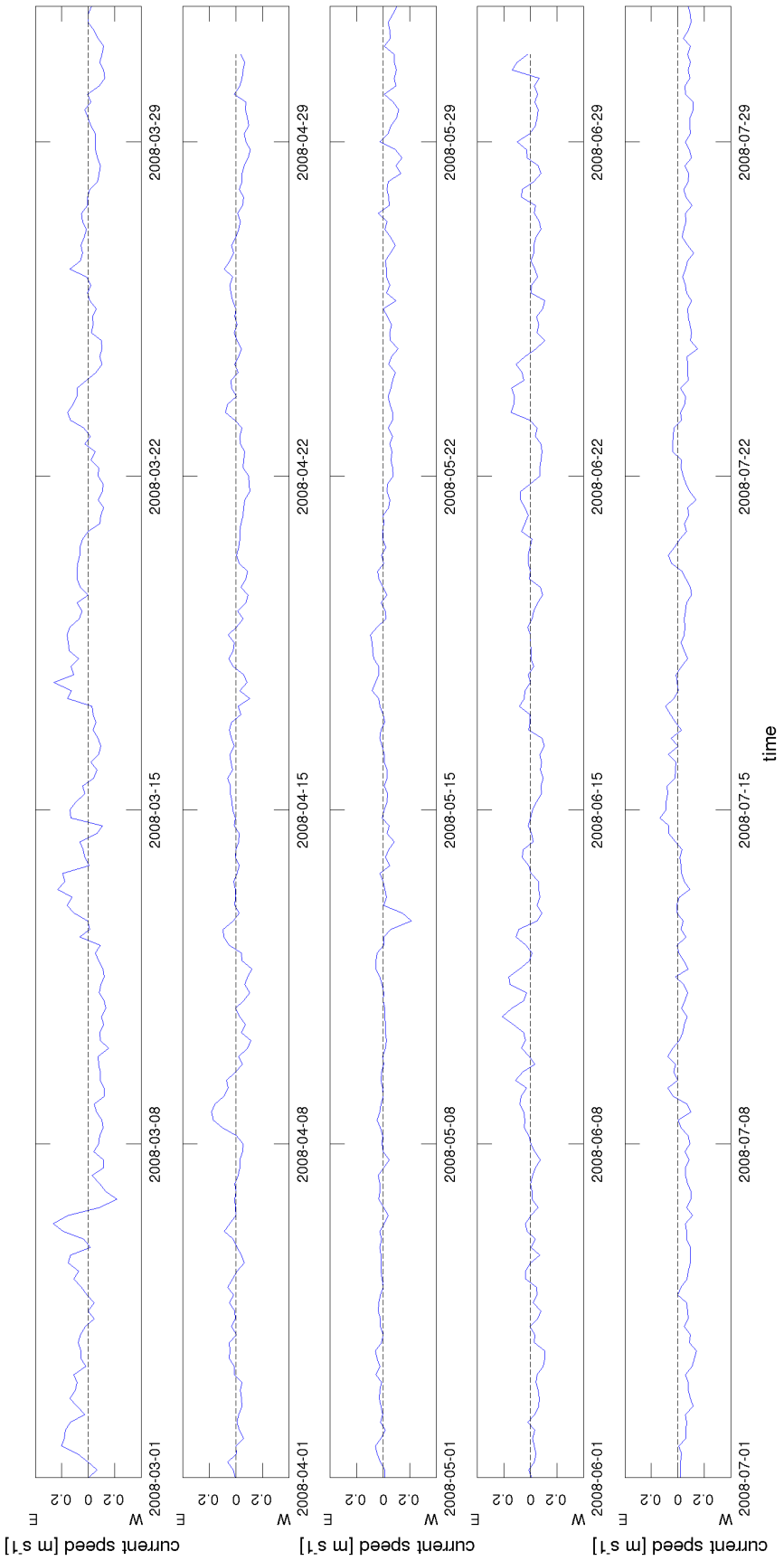

Figure 27: 2008 time series of zonal (west-east) current speeds at the western opening of the GWB (station 2). Station location is shown in figure 10.

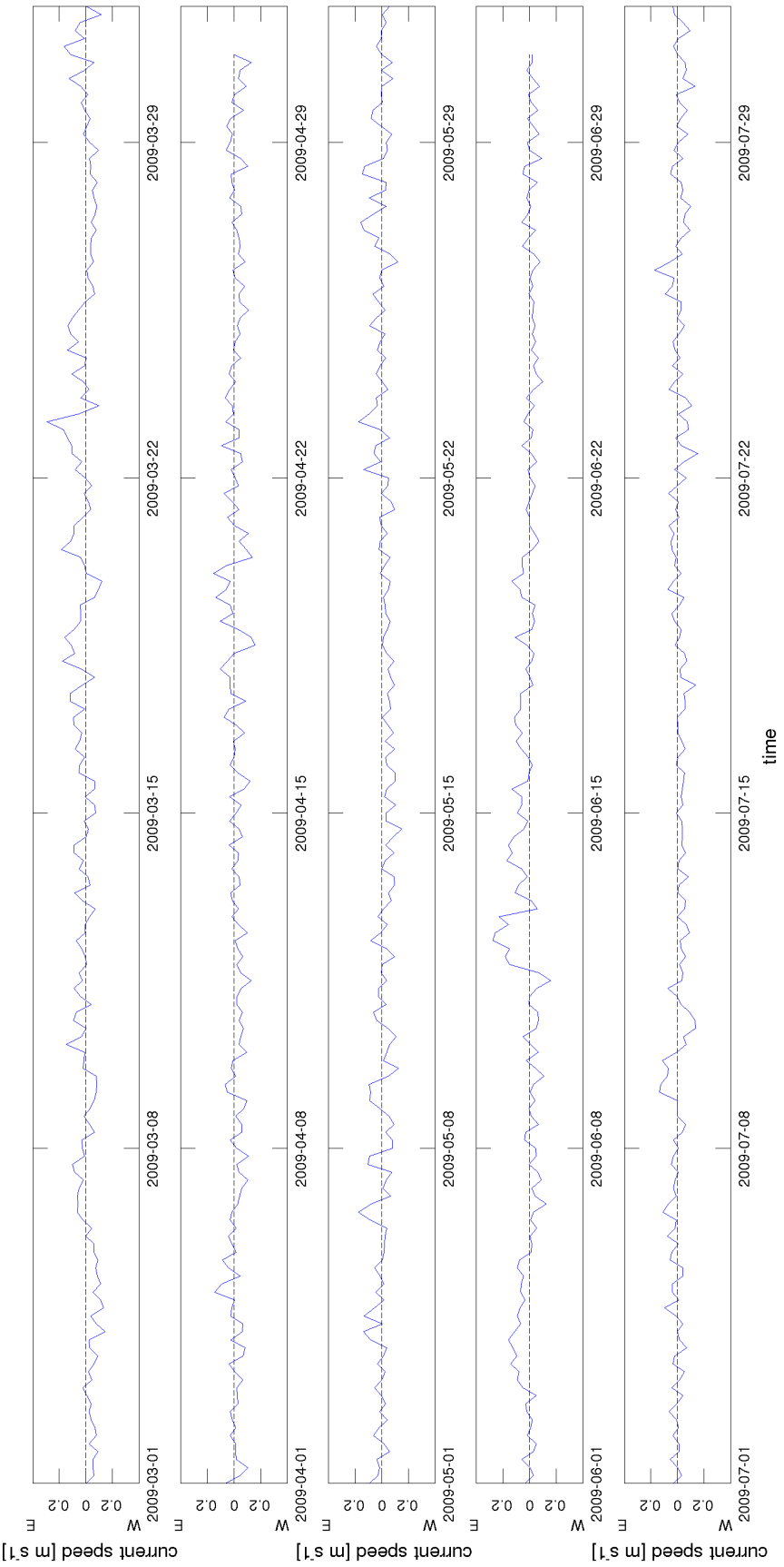

Figure 28: 2009 time series of zonal (west-east) current speeds at the western opening of the GWB (station 2). Station location is shown in figure 10.

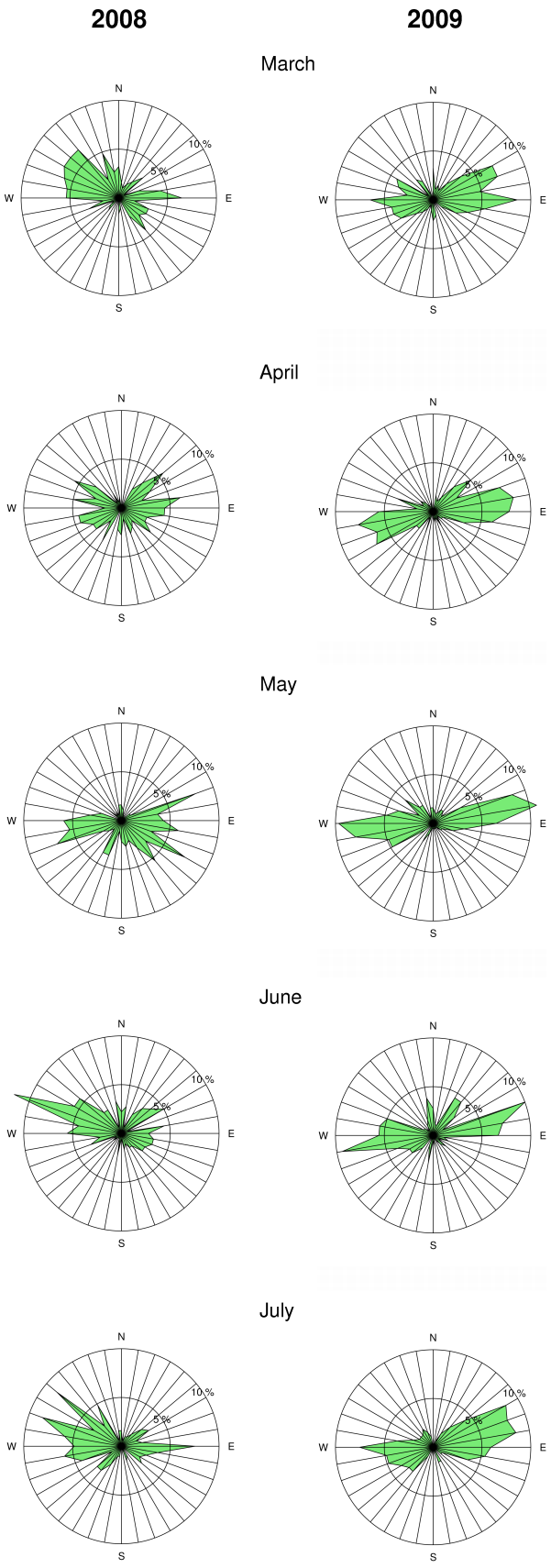

Figure 29: Monthly current roses for WBSS spawning season in 2008 and 2009 showing the frequency of different current directions at the eastern opening of the GWB (station 7). Station location is shown in figure 10.

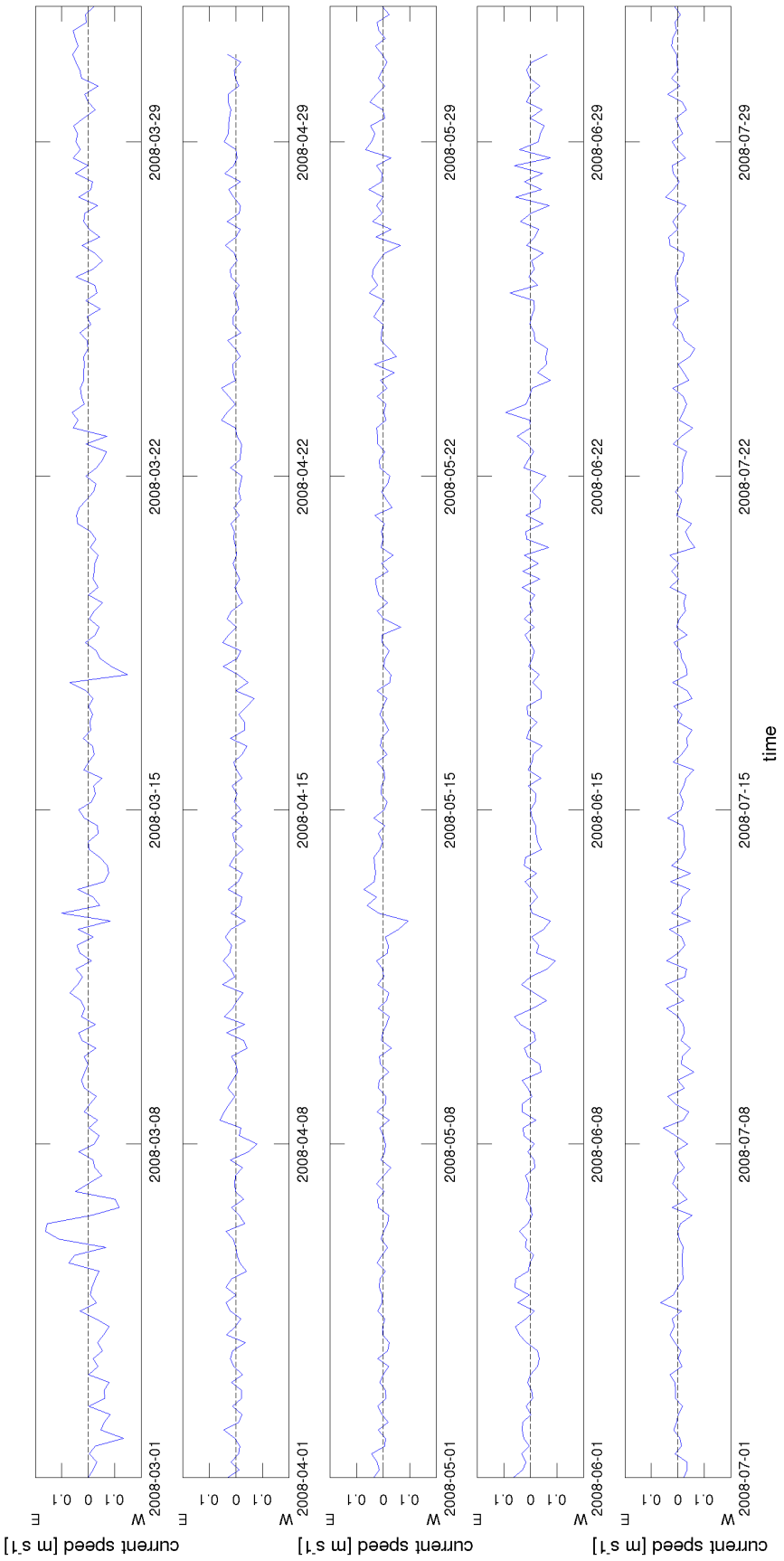

Figure 30: 2008 time series of zonal (west-east) current speeds at the eastern opening of the GWB (station 7). Station location is shown in figure 10.

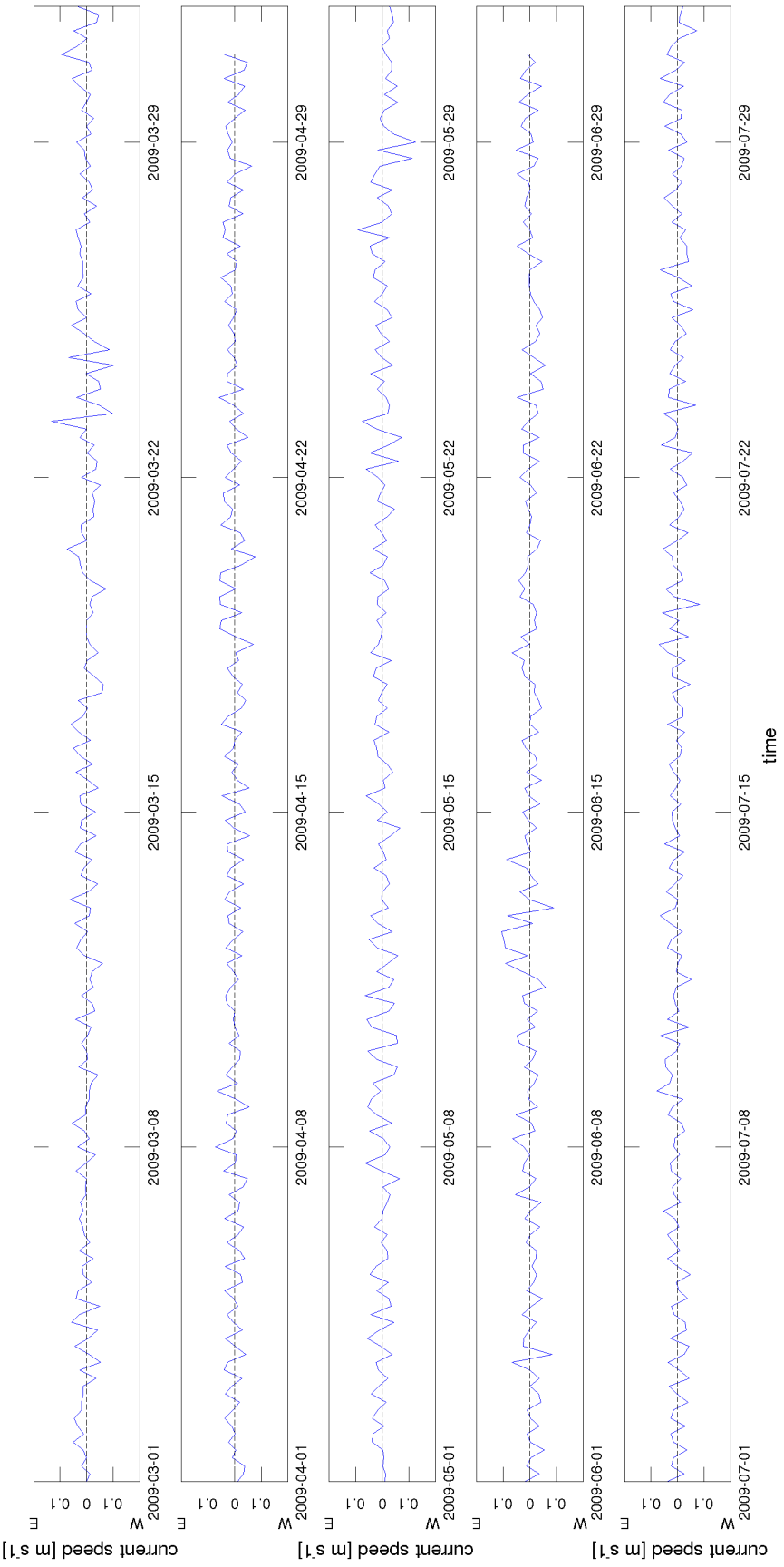

Figure 31: 2009 time series of zonal (west-east) current speeds at the eastern opening of the GWB (station 7). Station location is shown in figure 10.

Spatio-Temporal Variability of Vertical Salinity, Temperature and Velocity Profiles

As shown in figure 33, water temperature increased with time at every investigated station during May-July 2008 and 2009. Stratification occurred after heating periods when surface water and bottom temperature can differ by more than 5 K. However, temperature dependent stratification did not last longer than a week. Generally, stratification is shown to be strongest at station 3 to 7. These stations are located within the central GWB (Figure 10). By contrast no stratification could be observed throughout the entire timeframe at station 1 which is situated in the Strelasund. Generally, water warmed up faster in 2008 than in 2009. However, water temperatures were higher at the end of July in 2008 than one year earlier.
Spatial and inter-annual differences are much more pronounced for salinity profiles (Figure 34). While in 2008 salinity decreased at several stations in the GWB from March to July by approx. 2 PSU, this declining trend can not be seen for 2009. Instead, salinity remained largely constant at these stations. Although, a decline in salinity can be shown for stations located in the surrounding Pomeranian Bay. As shown already for the temperature profile, the water column at station 1 is generally well mixed, with no vertical salinity gradient being apparent at any time. By contrast, salinity stratification is frequent at stations that are located close to or beyond the eastern outlet of the GWB (stations 8 to 10). However, also salinity stratification did not last for longer time periods. By comparing salinity profiles of several stations inflow events can be examined. A strong inflow through the Strelasund at the end of June 2009, marked by a high salinity, can be traced towards station 5 which is situated in the central GWB. Though, these inflow events are extremely rare.
Vertical profiles of current speeds at the selected stations are given in figure 35. Current velocities are very low in the central GWB (stations 3 to 5). Highest current speeds can be found in the Strelasund. Strong flow throughout the water column occurs also at station 6. By contrast, vertical differences in water velocities are frequent in the Pomeranian Bay, at stations 8 to 10.

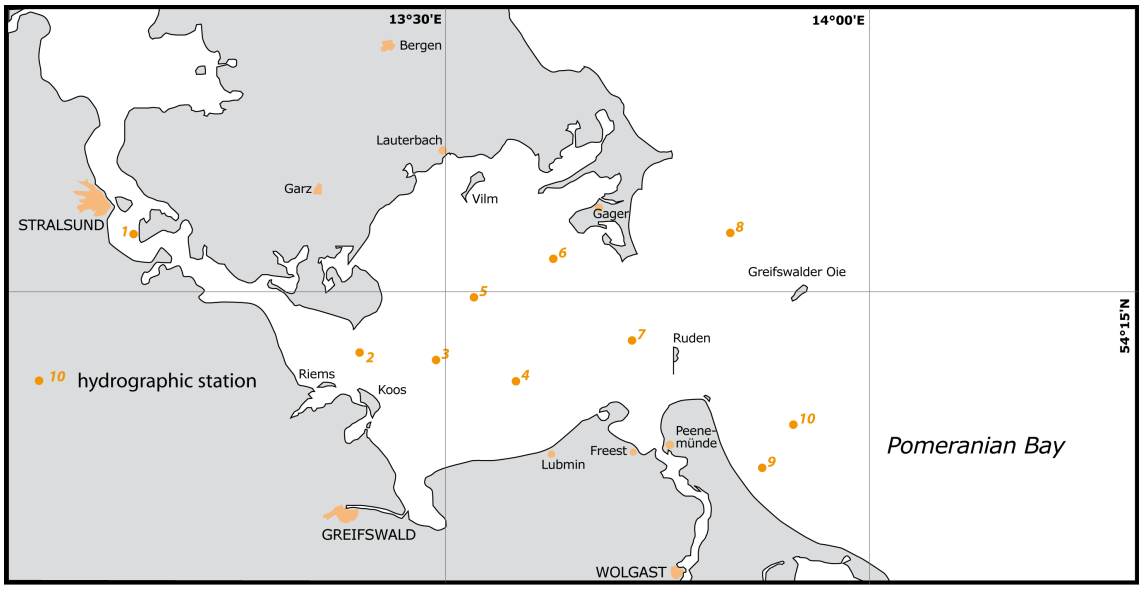

Figure 32: Overview of stations used in hydrographic analysis. Figure adopted from Zimmermann.

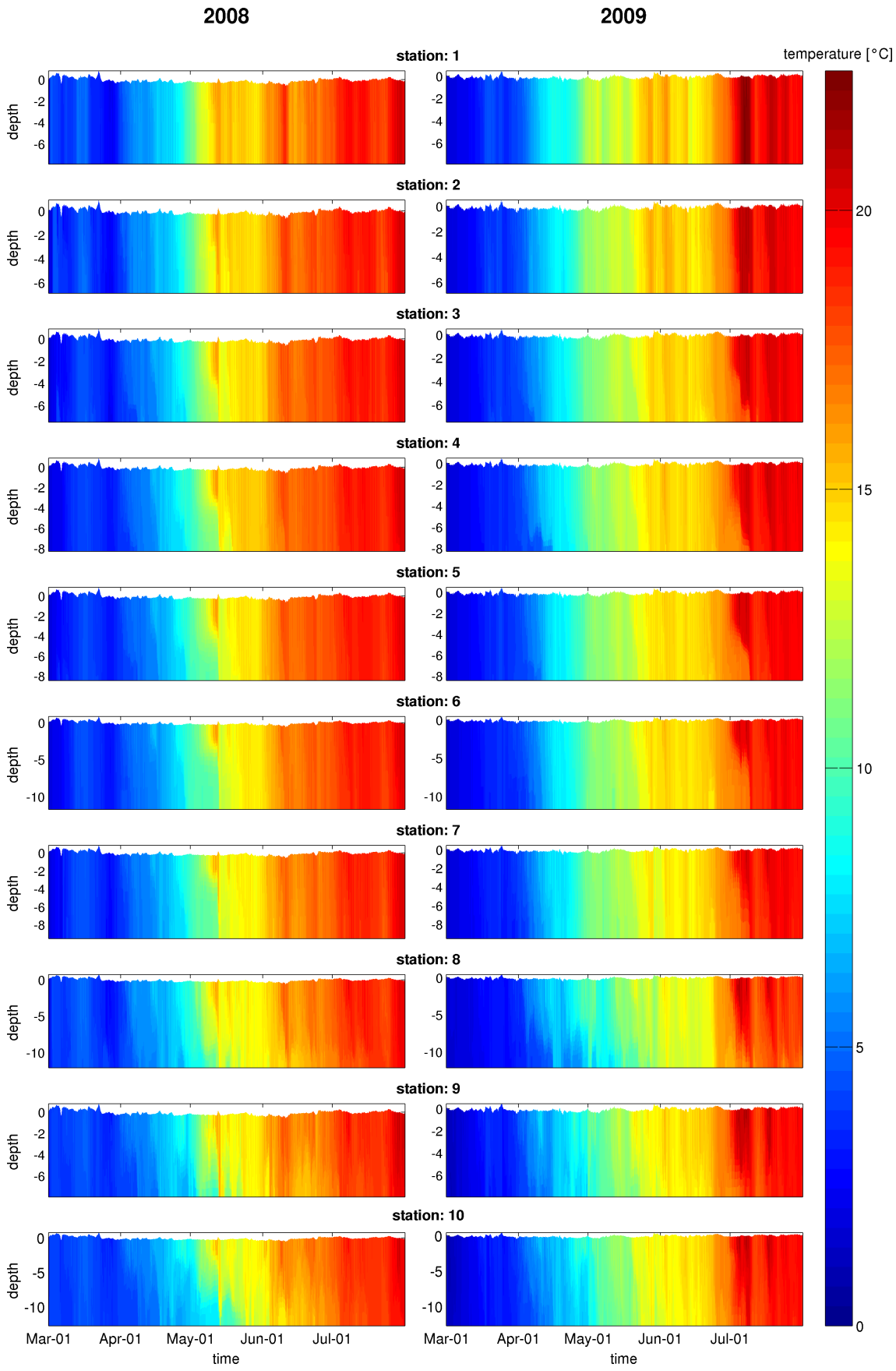

Figure 33: Temperature profiles at several stations of the study area during March-July in 2008 and 2009. Related station locations are given in figure 32.

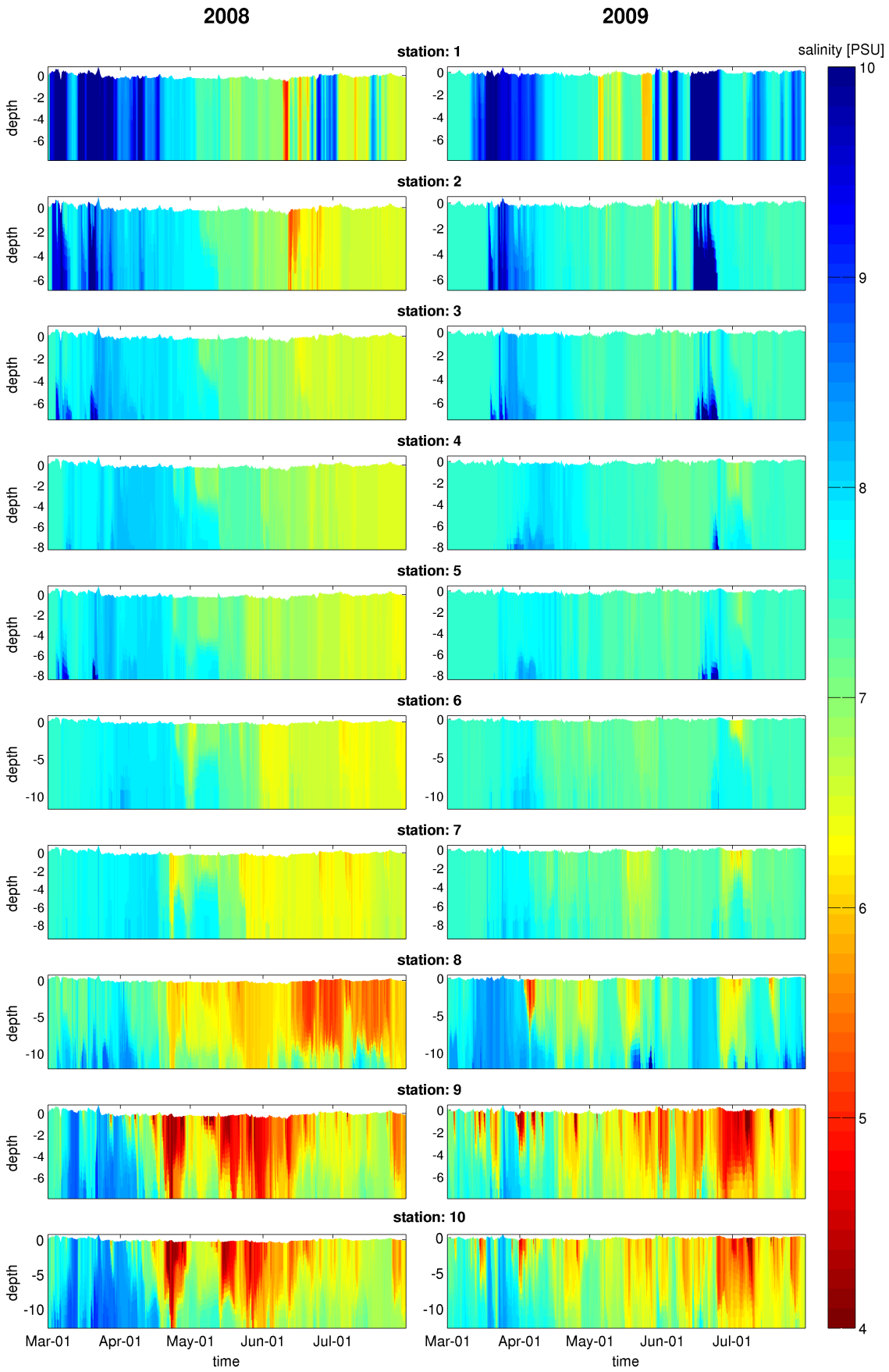

Figure 34: Salinity profiles at several stations of the study area during March-July in 2008 and 2009. Related station locations are given in figure 32.

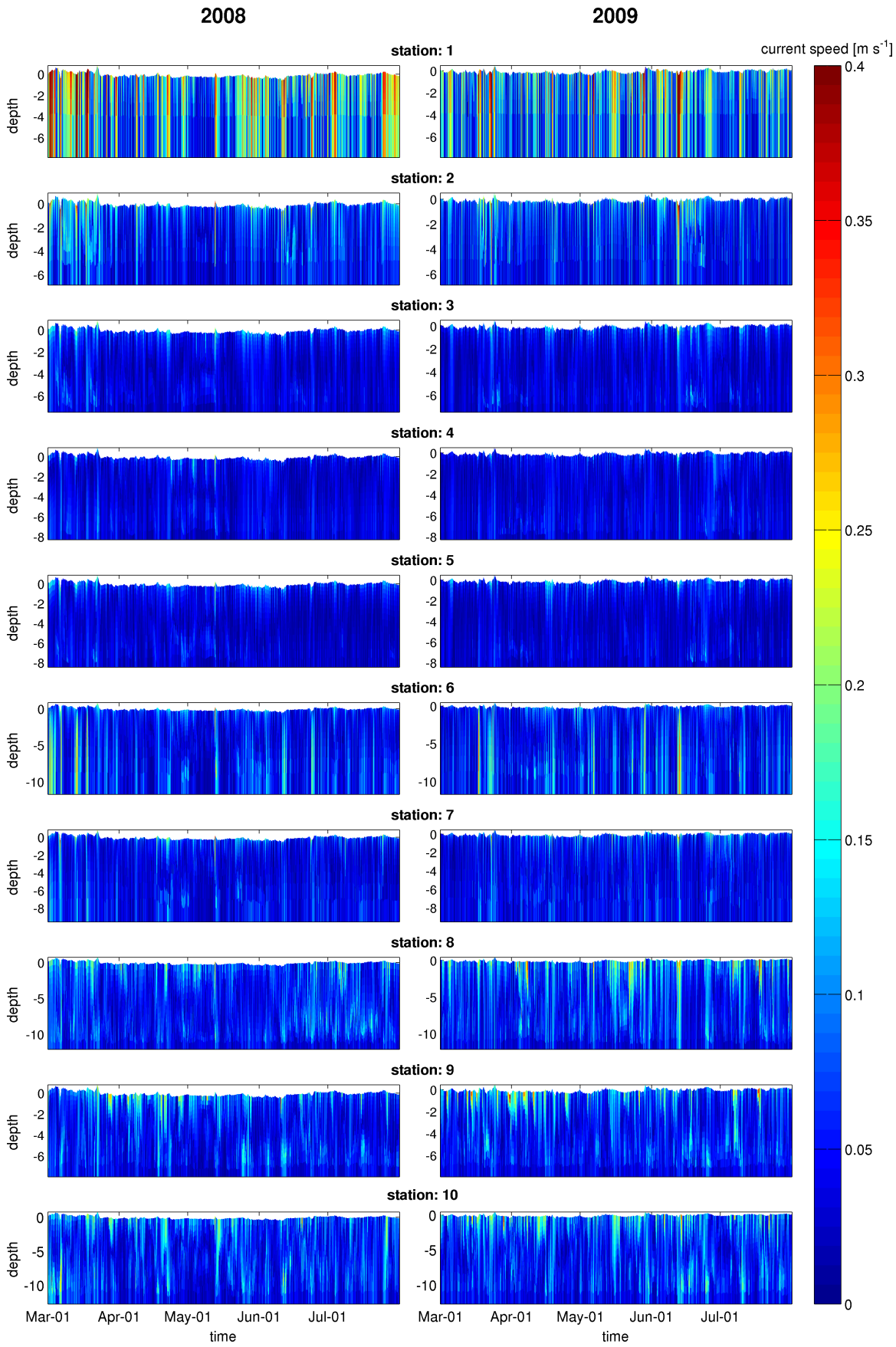

Figure 35: Velocity profiles for absolute current speeds at several stations of the study area during March-July in 2008 and 2009. Related station locations are given in figure 32.

Directed and Turbulent Flow

Spatially resolved advective and turbulent flow fields during 2008 and 2009 are shown in figure 36. Directed flow due to advection could cause displacement of more than 150 m during one hour in 2008 and 2009. By contrast, turbulences were considerably weaker, with possible horizontal transport rates of less than 100 m during one hour. Thus advection accounted for greater transport ranges. However, both processes were not constant in space and time. Directed flow in the Strelasund was much stronger in 2008 than in 2009. By contrast, turbulences were much stronger throughout the GWB in 2009 than in 2008, particularly in the Strelasund and around the eastern outlet of the GWB.

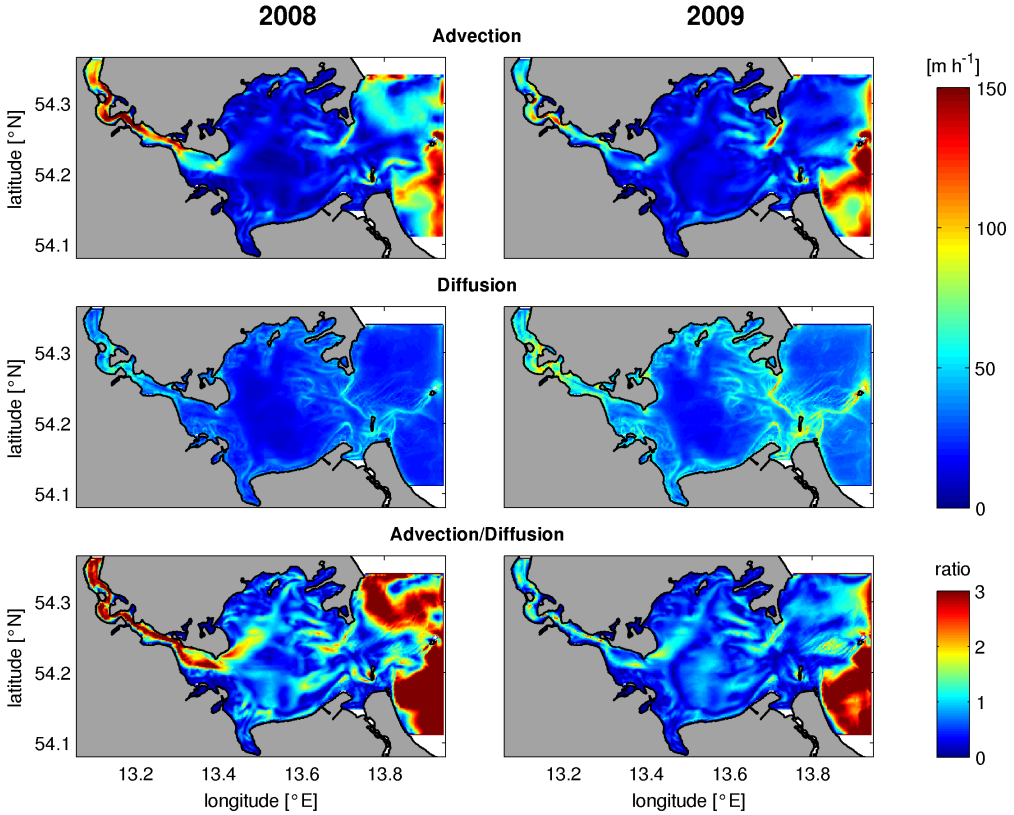

Figure 36: Average spatially resolved, hourly drifted distance by advection and diffusion and the corresponding ratio of both processes during 2008 and 2009.

Larval Drift

The results of the particle tracking experiments, conducted under real forcing conditions, are presented below. During the investigated timeframe (March - June of 2008 and 2009, CW 10-27) on average around 20%, but never more than one third of all "larvae", seeded in the GSA, were drifted out of this area (Table 8).

The time series of removed/remained larvae for weekly cohorts in 2008 and 2009 as long as cohort specific shares on annual abundances of larvae $\leqq$6 and larvae $\leqq$ 7 mm are given in figure 37. Tracking time decreased strongly from more than 60 days for CW 10 to less than 20 days for CW 27 (Figure 37 and 38; Table 9). Although there is a trend towards a reduced larval removal, the percentage of removed larvae remained variable during the investigated time frame of both model years. This particularly applies for weekly cohorts of 2008: Peaks of strong larval removal are shown for cohorts seeded in CW 20-21, both accounting for almost one third of all seeded larvae. Remarkably, these peaks match the abundance peaks of small larvae. Even in 2009, high abundances of small larvae were found in CW 20. However, these larvae were less threatened to be removed from the GSA. The time series reveals further that larvae were not continuously drifted out of the GSA. Instead larval removal occurred in batches. Moreover, return transports of larvae are evident.

Larval removal to the Baltic Sea occurred via the Strelasund and the eastern sill of the lagoon, with varying dominance over time (Table 8). However, on average loss of particles through the Strelasund accounted for the greater part during both years. This was particularly evident for cohorts released during CW 13-22 in 2008, of which around 80% of all removed larvae passed the Strelasund. Interestingly, almost the same applies for cohorts which were released one year later, during CW 13-20. In this context it has to be noted, that a reverse flow of larvae that have crossed the northern opening of the Strelasund was largely impeded, as already mentioned above. Most of these larvae have subsequently left the model domain of the GWBM and were thus lost from further analyses. Hence, the larval drift through the Strelasund and therefore estimated percentages of removed larvae can be assumed to be overestimated. As a consequence, particles that were seeded in the Strelasund were particularly at risk to drift outside the GSA. The average percentage of removed larvae was about 69% in 2008 and 51% in 2009, respectively. Although, this percentage showed strong fluctuations, ranging from 0.1% to 87.7% in 2008 and from 7.3% to 87.3% in 2009. Thereby, almost none of those particles were transported across the eastern sill of the GWB (Table 10). By contrast, if only the area of the GWB is considered the average percentage of removed larvae accounts only for 12-15% (Table 11). This is even less than that observed for the total area (GSA). In addition, larval drift to the open Baltic Sea is now found to be dominated through the eastern sill, especially in 2009 (Table 11). Flow through this outlet prevails in 2008 during CW 10-12 and 23-27 in 2008 and CW 18-27 during 2009, respectively. By restricting the area of investigation to shallower waters of 0-6 m and 0-3 m depth, the eastern sill becomes even more important for the relative particle outflow (Tables 12 and 13). In 2009, on average more than 70% of all removed larvae that originate from these areas have crossed this boundary. However, it is important to mention that the average percentage of removed larvae remains low, accounting approx. 14% in 2008 and 19% in 2009, regardless which sub-area is considered (Table 14).

Calculated proportions of removed larvae for several spawning sites of WBSS reported by Scabell (1988) are given in table 15 and 16. Larvae, seeded in the western and eastern spawning sites of the GSA, are constantly at high risk of getting drifted to the outside of the GSA. Up to 100% of those larvae were removed. By contrast, larvae originating from spawning sites of the northern, central and southern GWB are generally less threatened to be removed. Though, even from these areas, high proportions of larvae were occasionally drifted to the outside of the GSA.

Detailed maps showing the spatially resolved risk of larval removal for investigated weekly cohorts in 2008 and 2009 are presented in figures 40 to 42. Thereof, the probability to drift through the Strelasund is given in figures 62 to 64 whereas the risk to drift through the eastern opening is shown in figures 59 to 61.

Table 8: Percentage of removed particles seeded in the GSA (Total %) and related proportions that were drifted through the Strelasund or the eastern outlet (Sill).

	2008			**2009**		
CW	Total %	Strelasund	Sill	Total %	Strelasund	Sill
10	32.9	45.6	54.4	29.6	59.4	40.6
11	28.3	54.6	45.4	25.9	39.1	60.9
12	27.3	56.9	43.1	25.3	45.2	54.8
13	25.0	82.5	17.5	25.2	82.3	17.7
14	20.5	82.5	17.5	24.0	90.6	9.4
15	22.1	79.7	20.3	24.4	93.1	6.9
16	21.4	88.6	11.4	24.6	91.6	8.4
17	18.4	87.0	13.0	20.2	89.7	10.3
18	15.0	86.9	13.1	18.3	75.8	24.2
19	22.8	92.7	7.3	19.4	51.6	48.4
20	28.3	97.5	2.5	20.0	71.2	28.8
21	28.3	92.9	7.1	17.7	15.2	84.8
22	24.0	88.8	11.2	19.5	5.0	95.0
23	13.7	64.1	35.9	17.6	7.7	92.3
24	9.4	0.1	99.9	18.8	25.2	74.8
25	14.9	57.5	42.5	14.5	59.5	40.5
26	16.3	67.5	32.5	18.2	68.3	31.7
27	16.8	80.7	19.3	7.0	29.3	70.7
$\bar{x}$	21.4	72.6	27.4	20.6	55.5	44.5
σ	6.3	23.7	23.7	5.2	29.8	29.8

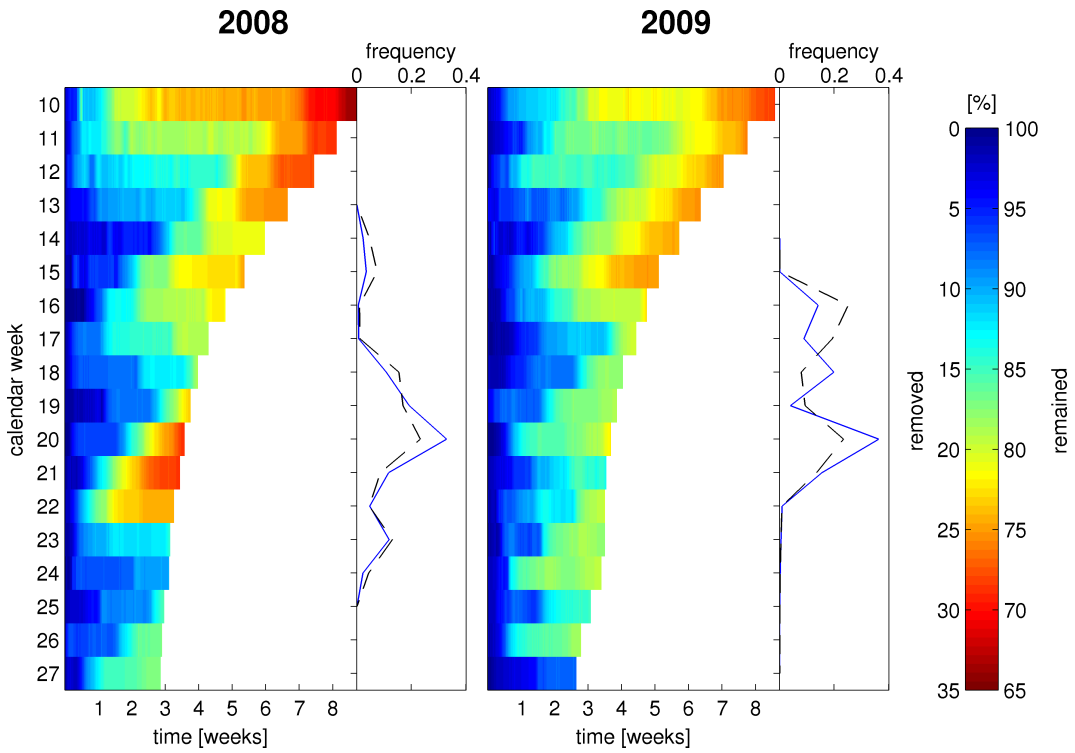

Figure 37: Time series of remained and removed particles for weekly cohorts in 2008 and 2009 and cohort specific shares on yearly amounts of larvae $\leqq 6$ (blue lines) and larvae $\leqq 7$ mm (black dashed lines). Note that the time series for the given cohort is stopped at the average tracking time of particles based on temperature dependent growth. Absolute values of removed particles are given in table 8.

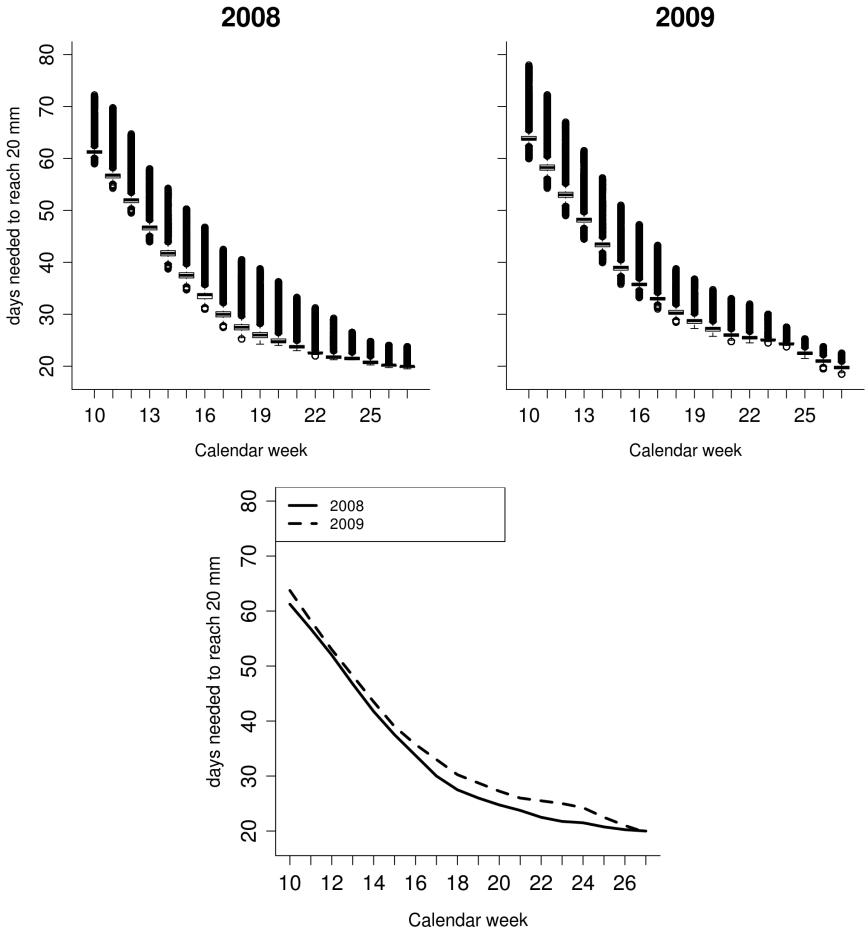

Figure 38: Tracking time, time needed to grow up to 20 mm of larvae that were seeded at the beginning of CW 10-27 in 2008 and 2009 (upper plots). Medians of cohort specific tracking time (lower plot).

Table 9: Minimum (min), average ($\bar{x}$) and maximum (max) tracking time [days], time needed to grow up to 20 mm for particles that were seeded at the beginning of CW 10-27 in 2008 and 2009

	2008			2009		
CW	min	$\bar{x}$	max	min	$\bar{x}$	max
10	59	61	72	60	64	78
11	54	57	70	54	58	72
12	50	52	65	49	53	67
13	44	47	58	45	48	62
14	39	42	54	40	43	56
15	35	37	50	36	39	51
16	31	34	47	33	36	47
17	28	30	42	31	33	43
18	25	28	41	28	30	39
19	24	26	39	27	29	37
20	24	25	36	26	27	35
21	23	24	33	25	26	33
22	22	23	31	25	26	32
23	21	22	29	25	25	30
24	21	22	27	24	24	28
25	20	21	25	22	23	25
26	20	20	24	20	21	24
27	20	20	24	19	20	23

Table 10: Percentage of removed particles seeded in the Strelasund (Total %) and related proportions that were drifted through the Strelasund or the eastern outlet (Sill). Average ($\bar{x}$) and standard deviation (σ) are also given.

	2008			2009		
CW	Total %	Strelasund	Sill	Total %	Strelasund	Sill
10	52.0	99.6	0.4	60.5	99.9	0.1
11	59.1	100.0	0.0	14.5	97.3	2.7
12	57.3	100.0	0.0	24.8	98.1	1.9
13	85.1	100.0	0.0	78.4	99.9	0.1
14	79.2	100.0	0.0	87.1	100.0	0.0
15	82.3	100.0	0.0	87.3	100.0	0.0
16	83.2	100.0	0.0	87.2	100.0	0.0
17	82.4	100.0	0.0	82.8	100.0	0.0
18	75.7	100.0	0.0	71.2	100.0	0.0
19	86.4	100.0	0.0	55.1	100.0	0.0
20	87.4	100.0	0.0	76.4	100.0	0.0
21	87.7	100.0	0.0	17.1	99.9	0.1
22	86.2	100.0	0.0	7.3	84.7	15.3
23	55.7	100.0	0.0	8.7	100.0	0.0
24	0.1	99.6	0.4	23.3	100.0	0.0
25	46.7	100.0	0.0	46.4	100.0	0.0
26	56.8	100.0	0.0	71.0	100.0	0.0
27	72.9	100.0	0.0	13.0	100.0	0.0
$\bar{x}$	68.7	100.0	0.0	50.7	98.9	1.1
σ	22.2	0.1	0.1	31.0	3.6	3.6

Table 11: Percentage of removed particles seeded in the GWB (Total %) and related proportions that were drifted through the Strelasund or the eastern outlet (Sill). Average ($\bar{x}$) and standard deviation (σ) are also given.

	2008			2009		
CW	Total %	Strelasund	Sill	Total %	Strelasund	Sill
10	29.3	27.8	72.2	23.8	40.2	59.8
11	22.6	32.5	67.5	28.0	33.5	66.5
12	21.7	35.8	64.2	25.3	35.5	64.5
13	13.9	62.5	37.5	15.3	65.4	34.6
14	9.5	55.5	44.5	12.2	78.1	21.9
15	11.0	51.2	48.8	12.6	84.3	15.7
16	9.9	70.9	29.1	12.9	81.1	18.9
17	6.5	56.3	43.7	8.6	71.3	28.7
18	3.7	36.8	63.2	8.5	37.8	62.2
19	11.0	82.1	17.9	12.7	12.5	87.5
20	17.4	95.2	4.8	9.6	28.4	71.6
21	17.2	86.2	13.8	17.8	0.0	100.0
22	12.4	74.3	25.7	21.7	0.0	100.0
23	5.9	0.7	99.3	19.3	0.0	100.0
24	11.1	0.0	100.0	17.9	7.1	92.9
25	9.0	16.5	83.5	8.6	18.9	81.1
26	8.8	28.4	71.6	8.4	18.6	81.4
27	6.4	39.6	60.4	5.8	0.0	100.0
$\bar{x}$	12.6	47.4	52.7	14.9	34.0	66.0
σ	6.7	28.0	28.0	6.6	30.1	30.1

Table 12: Percentage of removed particles seeded in the GWB in areas with a lower depth than 6 m (Total %) and related proportions that were drifted through the Strelasund or the eastern outlet (Sill). Average ($\bar{x}$) and standard deviation (σ) are also given.

	2008			2009		
CW	Total %	Strelasund	Sill	Total %	Strelasund	Sill
10	37.8	19.9	80.1	24.7	26.3	73.7
11	26.5	20.6	79.4	33.8	18.2	81.8
12	27.7	25.4	74.6	27.9	14.0	86.0
13	15.4	55.3	44.7	15.0	41.7	58.3
14	10.1	39.9	60.1	12.0	66.3	33.7
15	12.9	41.5	58.5	15.3	81.2	18.8
16	9.9	63.3	36.7	17.3	79.7	20.3
17	8.1	64.7	35.3	9.5	66.7	33.3
18	4.1	46.9	53.1	10.6	31.6	68.4
19	9.3	70.4	29.6	19.0	5.1	94.9
20	12.2	89.9	10.1	12.0	23.3	76.7
21	12.0	74.8	25.2	26.1	0.0	100.0
22	11.7	73.2	26.8	30.8	0.0	100.0
23	7.2	0.0	100.0	29.0	0.0	100.0
24	18.4	0.0	100.0	26.0	3.6	96.4
25	14.9	15.7	84.3	14.1	8.7	91.3
26	14.1	21.8	78.2	12.1	17.5	82.5
27	8.2	35.7	64.3	8.4	0.0	100.0
$\bar{x}$	14.5	42.2	57.8	19.1	26.9	73.1
σ	8.4	26.8	26.8	8.2	28.4	28.4

Table 13: Percentage of removed particles seeded in the GWB in areas with a lower depth than 3 m (Total %) and related proportions that were drifted through the Strelasund or the eastern outlet (Sill). Average ($\bar{x}$) and standard deviation (σ) are also given.

	2008			2009		
CW	Total %	Strelasund	Sill	Total %	Strelasund	Sill
10	37.7	16.6	83.4	24.3	22.1	77.9
11	27.1	15.3	84.7	34.5	11.4	88.6
12	27.9	27.1	72.9	27.4	13.5	86.5
13	15.2	51.1	48.9	15.0	36.8	63.2
14	10.9	40.5	59.5	11.5	70.0	30.0
15	12.7	49.7	50.3	13.4	79.3	20.7
16	9.0	64.0	36.0	16.7	79.2	20.8
17	6.4	61.9	38.1	8.4	59.9	40.1
18	2.4	38.6	61.4	11.0	25.0	75.0
19	8.5	86.3	13.7	19.9	3.1	96.9
20	11.0	87.1	12.9	9.8	9.3	90.7
21	10.7	78.2	21.8	29.3	0.0	100.0
22	10.6	72.4	27.6	30.7	0.0	100.0
23	7.7	0.0	100.0	30.6	0.0	100.0
24	19.3	0.0	100.0	29.4	2.8	97.2
25	17.8	10.4	89.6	18.0	5.6	94.4
26	12.8	4.5	95.5	9.9	19.5	80.5
27	6.3	6.7	93.3	9.0	0.0	100.0
$\bar{x}$	14.1	39.5	60.5	19.4	24.3	75.7
σ	8.9	30.6	30.6	9.0	28.4	28.4

Table 14: Percentage of removed particles in relation to seeding time (year, CW) and location (sub area). Extent of defined sub-areas are shown in figure 9. Average ($\bar{x}$) and standard deviation (σ) are also given.

	2008					2009				
		GWB					GWB			
CW	GSA	total	< 6 m	< 3 m	Strelasund	GSA	total	< 6 m	< 3 m	Strelasund
10	32.9	29.3	37.8	37.7	52.0	29.6	23.8	24.7	24.3	60.5
11	28.3	22.6	26.5	27.1	59.1	25.9	28.0	33.8	34.5	14.5
12	27.3	21.7	27.7	27.9	57.3	25.3	25.3	27.9	27.4	24.8
13	25.0	13.9	15.4	15.2	85.1	25.2	15.3	15.0	15.0	78.4
14	20.5	9.5	10.1	10.9	79.2	24.0	12.2	12.0	11.5	87.1
15	22.1	11.0	12.9	12.7	82.3	24.4	12.6	15.3	13.4	87.3
16	21.4	9.9	9.9	9.0	83.2	24.6	12.9	17.3	16.7	87.2
17	18.4	6.5	8.1	6.4	82.4	20.2	8.6	9.5	8.4	82.8
18	15.0	3.7	4.1	2.4	75.7	18.3	8.5	10.6	11.0	71.2
19	22.8	11.0	9.3	8.5	86.4	19.4	12.7	19.0	19.9	55.1
20	28.3	17.4	12.2	11.0	87.4	20.0	9.6	12.0	9.8	76.4
21	28.3	17.2	12.0	10.7	87.7	17.7	17.8	26.1	29.3	17.1
22	24.0	12.4	11.7	10.6	86.2	19.5	21.7	30.8	30.7	7.3
23	13.7	5.9	7.2	7.7	55.7	17.6	19.3	29.0	30.6	8.7
24	9.4	11.1	18.4	19.3	0.1	18.8	17.9	26.0	29.4	23.3
25	14.9	9.0	14.9	17.8	46.7	14.5	8.6	14.1	18.0	46.4
26	16.3	8.8	14.1	12.8	56.8	18.2	8.4	12.1	9.9	71.0
27	16.8	6.4	8.2	6.3	72.9	7.0	5.8	8.4	9.0	13.0
$\bar{x}$	21.4	12.6	14.5	14.1	68.7	20.6	14.9	19.1	19.4	50.7
σ	6.3	6.7	8.4	9.0	22.2	5.2	6.6	8.2	9.0	31.0

Table 15: Percentage of removed larvae for weekly cohorts and spawning sites in 2008. Bold numbers indicate important spawning sites reported by Scabell (1988). Average ($\bar{x}$) and standard deviation (σ) are also given. Location and extent of spawning sites are shown in figure 11 and 39.

CW	spawning site																							
	all	**1**	**2**	**3**	**4**	5	6	7	8	9	10	11	**12**	13	14	15	**16**	**17**	**18**	19	20	**21**	22	**23**	**24**
10	32.2	19.5	13.1	58.3	98.6	21.7	23.9	36.0	37.9	24.1	26.3	18.6	85.9	45.5	61.1	29.6	13.8	19.6	18.5	1.5	2.0	19.7	20.8	18.4	23.9
11	25.7	29.6	34.7	29.0	58.3	9.2	0.1	19.1	31.6	7.2	17.3	0.6	88.4	43.6	29.4	26.3	70.3	0.6	4.7	14.3	12.2	23.9	23.3	23.4	27.7
12	21.0	28.1	17.6	56.8	46.4	17.5	5.9	14.7	80.3	11.9	10.8	0.0	47.5	34.1	15.1	0.3	0.1	0.3	1.4	1.1	5.0	77.6	61.8	8.1	5.6
13	15.8	0.1	0.4	0.9	4.3	3.5	1.6	9.3	11.1	20.0	20.3	0.6	73.5	4.5	12.7	8.8	7.0	0.1	6.1	57.3	53.3	49.4	9.5	0.2	0.0
14	9.2	0.1	0.7	3.8	35.1	0.0	1.9	0.4	4.6	0.9	2.9	1.0	58.8	3.4	6.2	1.1	0.0	0.0	0.0	0.0	0.5	91.9	21.2	0.0	0.0
15	13.1	0.0	0.7	9.3	89.4	2.0	0.0	1.1	4.8	1.2	0.3	2.3	38.1	1.2	0.4	0.1	0.1	0.0	0.0	0.7	53.1	95.6	82.2	0.0	0.0
16	9.9	0.0	0.1	6.4	14.9	6.2	11.2	0.0	8.4	0.0	0.6	1.5	18.9	0.7	0.0	0.1	0.1	0.0	0.0	0.0	18.2	98.0	95.3	0.0	0.0
17	12.7	0.0	0.0	0.0	0.0	0.0	0.0	0.0	0.4	20.4	4.5	0.0	49.9	10.4	0.7	0.0	0.0	0.0	0.0	59.0	68.9	52.2	15.9	0.0	0.0
18	2.5	0.0	0.0	0.0	0.5	0.0	0.0	0.0	0.0	1.3	2.9	0.0	0.3	9.4	9.3	0.1	0.0	0.0	0.0	1.2	3.8	4.3	1.8	0.0	0.0
19	12.9	0.0	0.0	0.6	0.1	0.0	0.0	0.0	0.1	0.0	0.0	0.0	28.8	3.1	0.0	0.0	0.0	0.0	0.0	0.2	94.8	97.3	88.4	0.0	0.0
20	14.9	0.1	0.0	0.0	2.2	0.0	0.4	8.6	0.3	1.6	11.9	0.4	27.2	0.3	0.1	0.0	0.0	0.0	0.0	13.5	96.0	99.1	93.6	0.1	0.0
21	14.9	0.3	1.8	6.2	1.0	0.2	0.1	5.5	8.4	0.0	0.0	3.2	46.1	2.3	0.1	0.1	0.1	0.0	0.0	0.0	95.5	99.4	95.2	0.3	0.2
22	16.6	0.0	0.1	0.0	2.0	1.7	0.0	1.3	3.3	0.8	1.6	0.0	26.5	5.5	0.5	0.0	0.1	0.1	0.1	95.1	98.2	95.0	30.7	0.0	0.0
23	5.5	0.0	2.6	4.8	49.3	4.8	0.0	3.5	2.2	1.8	2.2	0.9	55.5	7.2	6.5	2.3	0.6	0.4	0.4	0.0	0.0	0.0	0.0	0.0	0.0
24	10.0	0.7	17.8	36.5	61.6	0.7	1.5	6.6	12.2	1.4	4.6	0.9	22.7	17.9	25.4	5.1	7.2	6.6	5.5	0.2	0.0	0.0	0.0	1.0	0.5
25	7.7	0.1	1.4	1.4	37.6	0.0	0.0	0.7	38.6	0.0	0.2	0.0	21.5	6.7	20.2	8.5	2.3	0.8	0.0	28.4	18.4	0.0	0.0	0.1	0.0
26	6.0	0.0	0.7	7.1	8.2	0.0	0.0	0.1	60.8	0.2	0.1	0.0	63.2	5.1	6.0	9.9	1.6	0.2	0.0	4.5	0.0	0.0	0.0	0.0	0.0
27	3.4	0.0	0.0	1.9	41.5	1.6	0.0	7.0	1.1	0.4	1.4	0.3	15.3	0.7	1.7	1.7	4.1	6.2	0.1	0.0	3.2	0.3	0.0	0.0	0.0
$\bar{x}$	12.3	4.1	4.8	11.7	29.0	3.6	2.4	6.0	16.1	4.9	5.7	1.6	40.4	10.6	10.3	5.0	5.6	1.8	1.9	14.6	32.8	47.6	33.7	2.7	3.1
σ	7.4	9.7	9.3	18.7	31.0	6.1	5.9	9.0	22.8	7.9	7.8	4.2	24.2	14.1	15.1	8.7	16.0	4.7	4.5	26.6	38.5	42.3	37.5	6.7	8.1

Table 16: Percentage of removed larvae for weekly cohorts and spawning sites in 2009. Bold numbers indicate important spawning sites reported by Scabell (1988). Average ($\bar{x}$) and standard deviation (σ) are also given. Location and extent of spawning sites are shown in figure 11 and 39.

CW	spawning site																							
	all	**1**	**2**	**3**	**4**	5	6	7	8	9	10	11	**12**	13	14	15	**16**	**17**	**18**	19	20	**21**	22	**23**	**24**
10	23.5	11.9	22.4	36.0	49.0	0.3	0.9	23.9	38.1	15.9	23.7	2.3	30.9	30.4	43.2	71.3	7.4	0.4	0.6	1.2	3.1	43.1	39.7	11.6	19.1
11	31.5	15.6	45.6	48.2	88.6	4.4	3.6	17.1	16.4	8.6	29.8	0.7	100.0	46.3	72.8	40.6	0.7	0.4	0.9	2.2	1.1	52.0	45.8	39.7	40.9
12	20.7	29.0	18.9	73.2	55.8	4.2	0.5	6.4	58.9	7.9	13.2	5.8	93.4	46.4	18.2	0.1	0.8	1.5	1.3	0.9	1.2	36.1	29.0	8.8	9.0
13	15.0	37.0	0.0	45.6	8.7	0.1	1.2	1.8	3.4	1.6	2.4	7.1	48.3	13.4	5.5	0.3	1.5	2.3	1.2	3.1	3.7	98.8	98.8	1.1	0.7
14	14.4	0.1	0.0	0.2	1.0	0.0	6.5	0.4	1.0	0.6	4.0	1.9	18.1	11.0	7.0	1.9	0.3	3.1	0.7	15.9	95.1	97.3	50.8	1.1	0.6
15	17.1	0.2	0.0	0.0	0.1	0.0	0.0	0.1	1.4	2.0	1.5	0.0	1.0	9.7	5.5	1.6	1.9	4.6	0.6	98.7	98.4	91.2	39.5	0.2	0.0
16	21.7	24.1	0.0	0.0	1.2	0.5	0.8	0.9	1.9	6.0	3.0	0.1	28.6	13.9	11.3	1.0	0.9	1.2	0.5	98.7	99.1	90.1	82.3	13.2	6.1
17	13.7	0.0	0.0	0.0	0.1	0.0	0.0	0.4	0.0	0.0	0.1	0.0	29.4	18.0	1.9	0.0	0.0	0.0	0.0	29.9	72.5	78.7	58.6	0.0	0.1
18	13.0	0.1	0.0	0.2	14.9	0.0	0.0	0.1	0.4	0.3	9.1	0.3	80.0	29.4	17.1	3.8	0.1	0.1	0.0	29.8	11.3	37.0	11.0	0.0	0.0
19	12.1	5.1	7.8	11.6	26.6	0.5	0.2	4.1	55.4	1.6	0.8	1.9	93.7	25.2	16.2	7.4	5.1	1.1	0.0	0.1	0.2	6.5	4.0	5.6	3.9
20	7.4	0.5	20.3	19.7	12.6	19.6	0.0	0.0	9.6	0.0	1.8	5.4	62.5	3.9	1.0	1.3	0.3	0.4	0.1	0.0	7.5	37.6	12.7	0.3	0.5
21	23.0	32.9	36.9	34.3	63.4	0.1	1.5	11.4	24.0	12.8	13.5	0.6	97.7	57.0	38.7	16.1	1.2	1.1	0.1	0.0	0.2	0.0	0.0	41.8	20.2
22	25.0	10.4	55.4	78.9	38.5	8.6	3.7	23.4	20.3	17.1	19.6	14.2	97.8	43.9	38.7	20.6	4.0	5.9	13.9	2.7	0.1	0.0	0.0	29.3	27.1
23	28.0	0.6	13.1	57.1	64.9	1.9	0.1	22.4	28.8	25.6	42.9	28.8	98.5	72.7	18.5	31.1	13.5	37.6	8.4	0.4	0.0	0.1	0.0	1.0	0.9
24	31.2	4.8	5.0	31.4	35.5	1.5	0.0	2.1	47.8	46.6	21.4	42.6	98.9	56.2	71.9	91.1	85.5	9.9	0.0	0.0	0.0	44.6	19.6	4.4	3.0
25	12.4	0.3	3.8	10.3	27.4	0.0	0.0	0.2	0.8	0.0	0.1	0.0	75.9	24.3	14.6	0.4	0.1	0.1	0.0	0.0	0.0	55.1	58.5	0.7	0.8
26	10.1	0.0	0.2	61.1	22.0	8.8	6.9	3.8	1.7	0.3	0.0	1.3	45.6	0.2	0.1	0.1	0.0	0.0	0.0	0.0	66.9	50.5	12.9	0.0	0.0
27	5.8	0.0	0.0	0.0	25.8	0.0	0.0	0.0	0.0	0.3	1.8	0.2	97.6	10.6	0.0	0.2	0.0	0.0	0.0	0.0	0.0	0.0	0.0	0.0	0.0
$\bar{x}$	17.1	9.1	12.1	26.7	28.2	2.6	1.4	6.2	16.3	7.7	9.9	6.0	63.0	27.0	20.1	15.2	6.5	3.7	1.5	14.9	24.2	43.1	29.6	8.4	7.0
σ	7.6	12.4	16.9	26.6	25.2	4.9	2.2	8.6	19.9	11.8	12.1	11.2	32.8	20.2	22.3	26.0	19.4	8.6	3.5	30.8	38.5	34.1	29.1	13.4	11.4

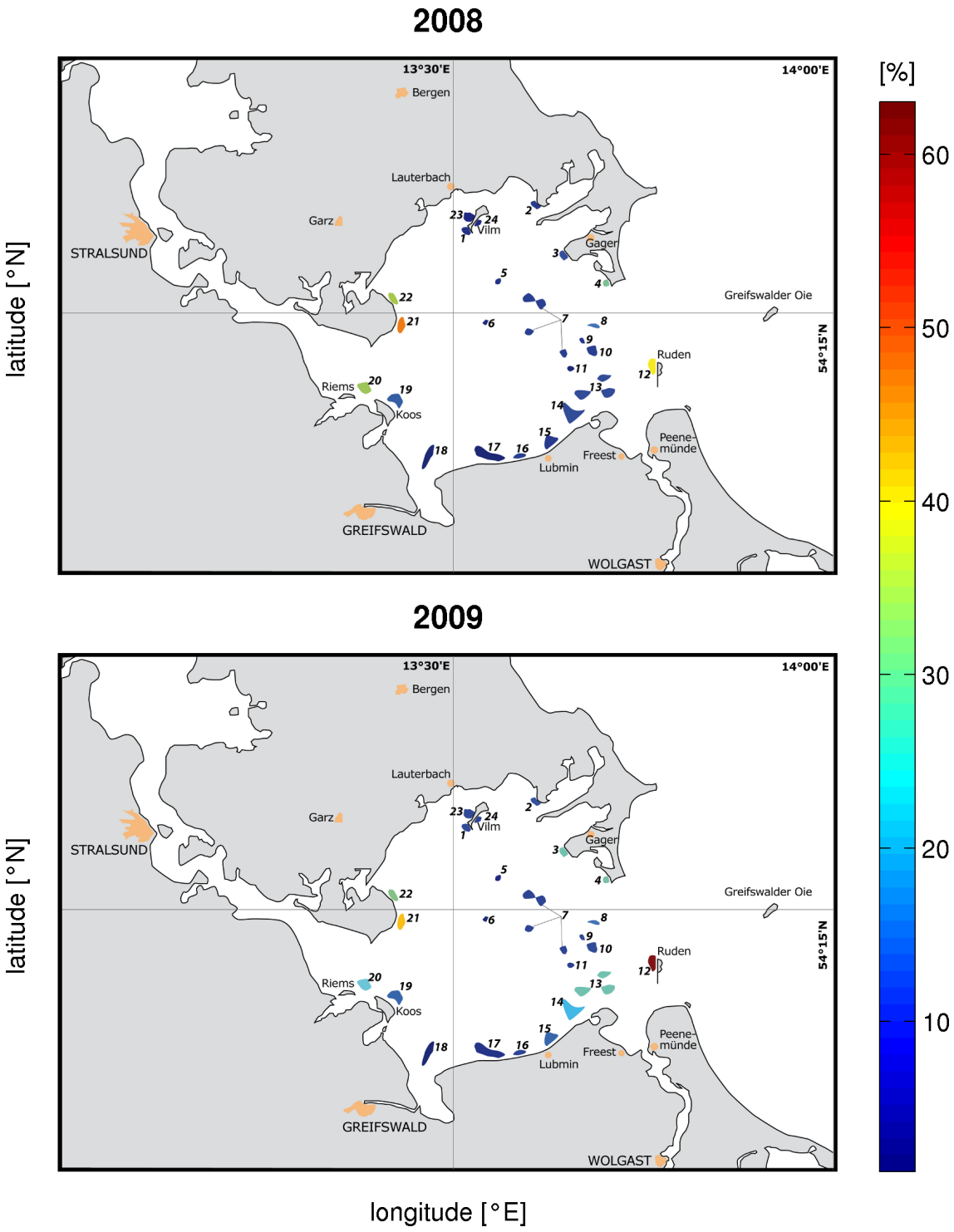

Figure 39: Average percentage of removed larvae per spawning site in 2008 and 2009. Figure adopted from Zimmermann.

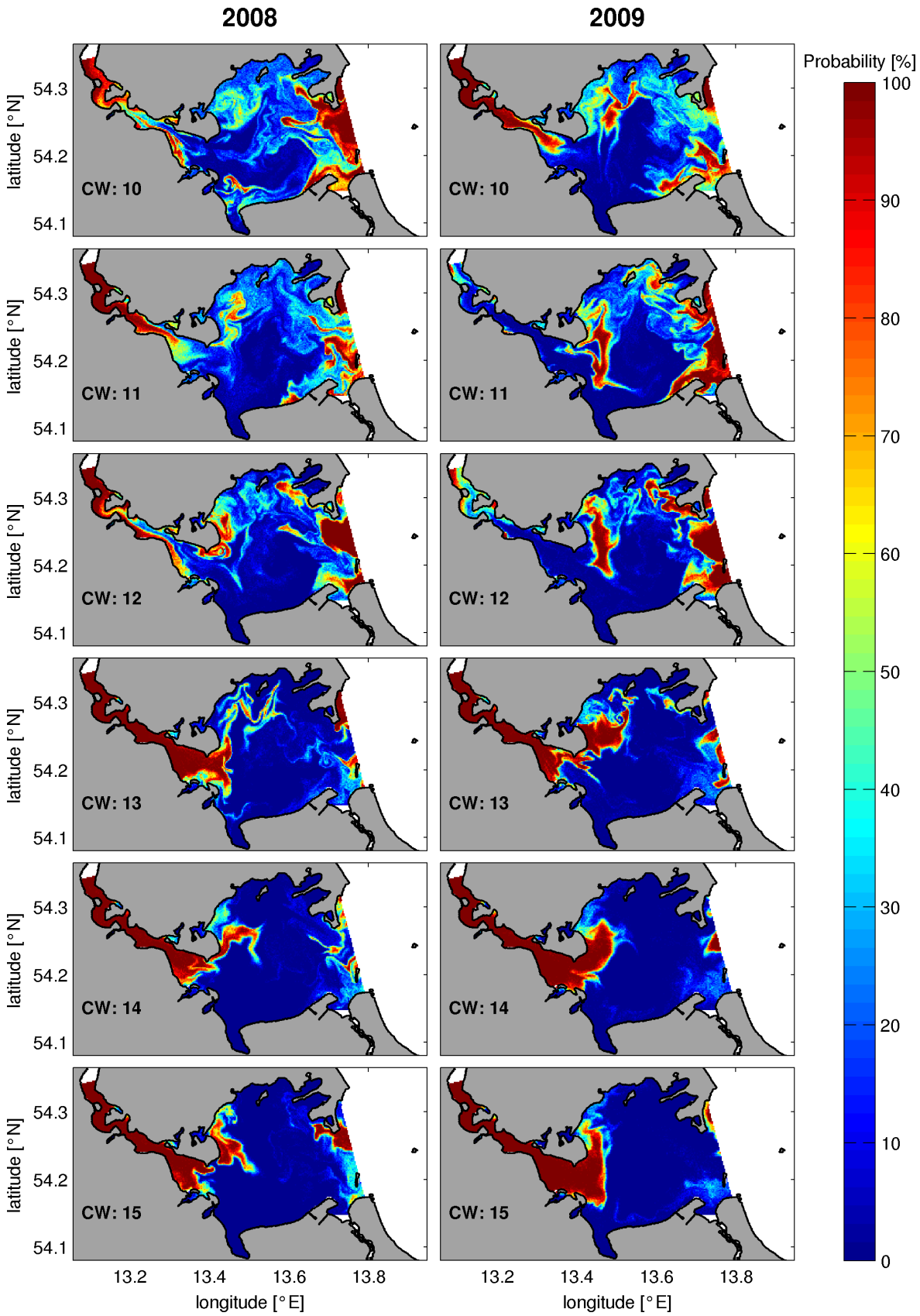

Figure 40: Spatially resolved probability to drift outside the lagoon, for particles which were seeded at the beginning of CW 10-15, given in percent.

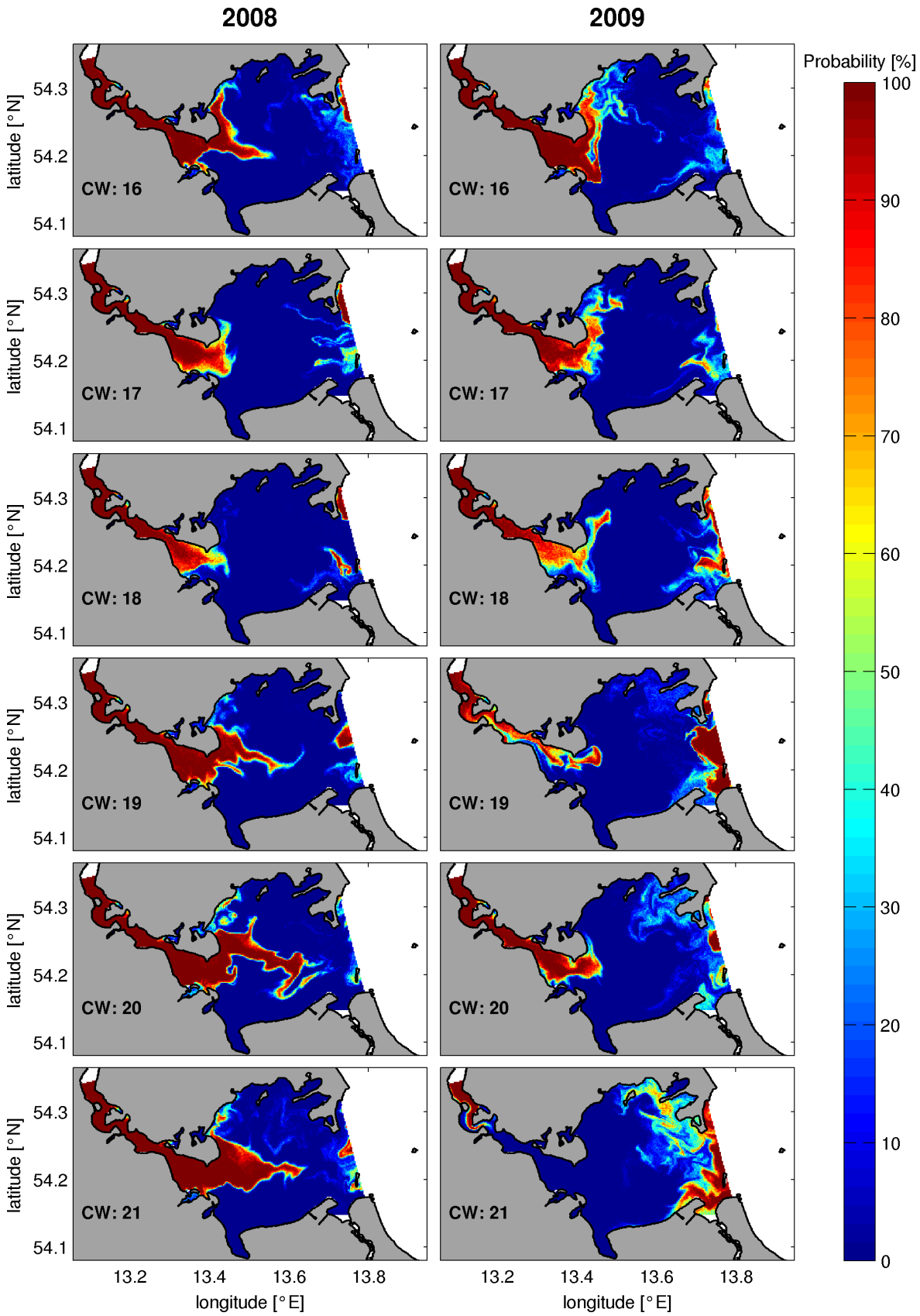

Figure 41: Spatially resolved probability to drift outside the lagoon, for particles which were seeded at the beginning of CW 16-21, given in percent.

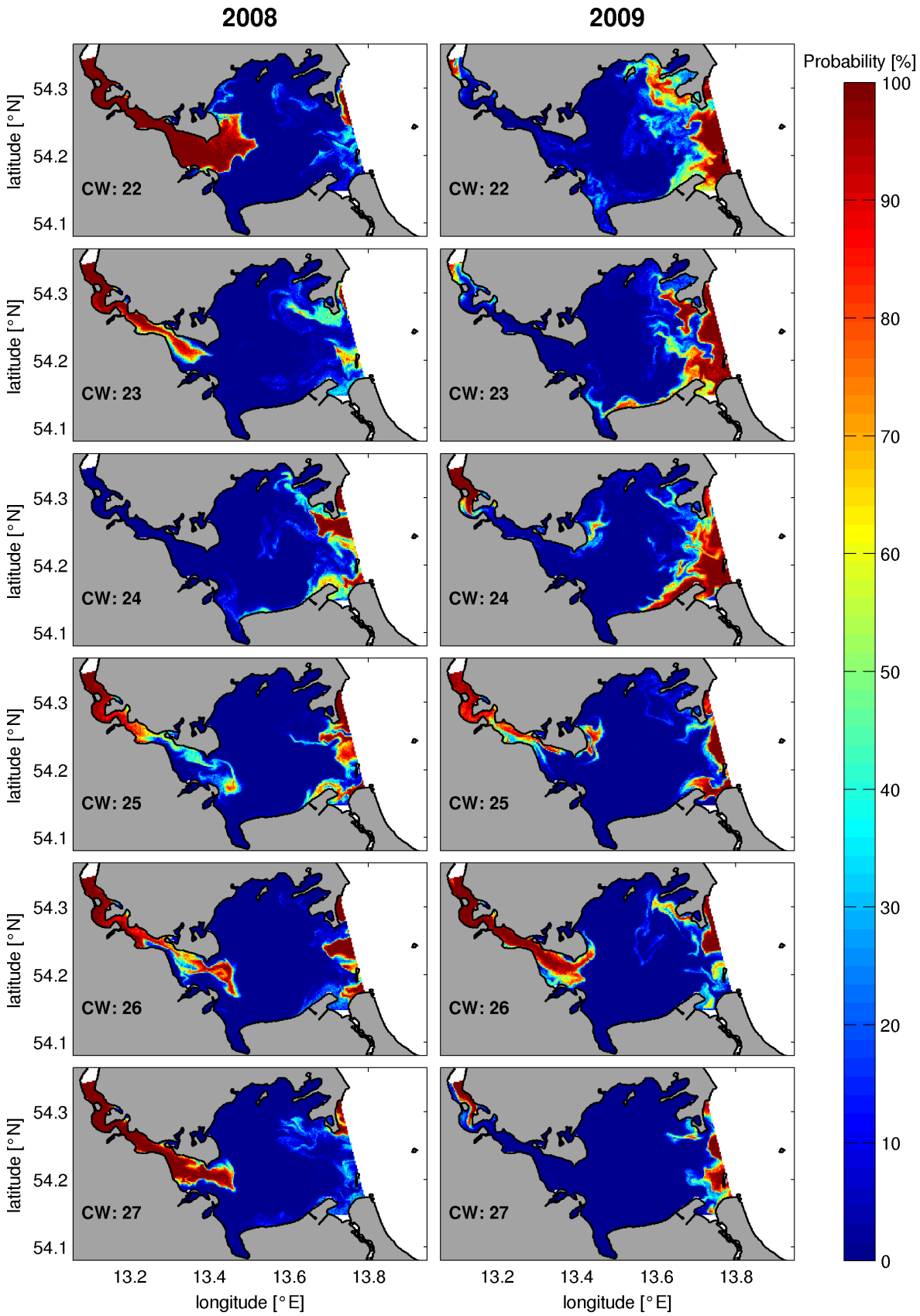

Figure 42: Spatially resolved probability to drift outside the lagoon, for particles which were seeded at the beginning of CW 22-27, given in percent.

3.3 Retention Index

Calculated retention indices for larval abundances found in 2008 and 2009 are given in table 17. The obtained estimates indicate that more than 75% of all larvae, hatched in 2008 and 2009 remained in the GSA until they have reached a size of 20 mm.

Table 17: Retention index (R_a) for WBSS larvae of 2008 and 2009.

length group [mm]	R_{2008}	R_{2009}
$\leqq$6	77.0	80.1
$\leqq$7	78.6	79.3

4 Discussion

Individual based biophysical models have become a powerful tool for studying larval biology (Miller, 2007). These models are capable to simulate larval drift based on the particle-tracking scheme of its physical component. By now, they have been used to model larval drift and biology of various marine species including herring (Miller, 2007). However, larval drift of WBSS and its potential influences on recruitment have not been studied yet. Within this study a Lagrangian Particle Tracking model has been applied to analyze larval drift and its implications on WBSS recruitment success. This model was forced with depth integrated 2-D flow fields obtained from a high resolution circulation model. As a first step, the accuracy of the applied model approach shall be discussed. Afterwards focus is set on the evaluation of presented presented results.

4.1 Circulation Model

Within the present approach, simulated flow fields at real wind conditions were validated with observed temperature and sea level data. Observed and simulated temperature data were shown to be highly correlated. Correlations for sea surface elevation data were less accurate but still significant. Thereof, the station at the Strelasund exhibits the lowest fits. Generally, one reason for the slightly lower agreement between modeled and measured sea level data could be seen in the resolution of the GWBM. Especially, effects of small bathymetric features as well as local circulation patterns in some areas may not be sufficiently resolved. This certainly applies for the narrow Strelasund which measures less than 1 km at its narrowest point. Another reason can be seen in the location of the GWBM boundaries which cut the Strelasund at its northern opening. Unlike the eastern opening of the GWB, the northern opening of the Strelasund is not directly linked to the Baltic Sea. In between there are some other lagoons which possess only narrow connections to the Baltic Sea. Thus, water exchange between the Strelasund and the Baltic Sea is greatly hampered causing water masses to remain in the neighboring lagoons. These processes are certainly not sufficiently resolved by the coarse grid resolution (600 m) of the adjacent WBSM. As a consequence, simulated sea-surface elevations in the Strelasund are less accurate. However, the mentioned deviations between the observed and simulated sea level elevations were generally low throughout the investigated time series.

Previous studies have demonstrated that the circulation patterns in lagoons are strongly affected by wind fields (Miller et al., 1990). This applies also for flow patterns of the GWB (Hackert, 1969; Correns, 1977; Lampe, 1994). The obtained circulation patterns at constant wind conditions highlight this dependency. Opposite wind directions produced inverse circulation patterns which is in agreement with results reported by (Hackert, 1969). Strongest currents were found at NW and SE winds, especially within the Strelasund, which has also been described by Birr (1988). Increasing wind speeds cause an amplification of the water flow. Generally, areas of weak and strong flow can be distinguished. Thereby, the location and extent of these areas strongly depend on the bathymetry of the lagoon, being almost the same for the different wind fields. Strong flow occurs along the shorelines and the shoals in the eastern part of the GWB. Particularly strong flow is found in the Strelasund due to a pronounced funnel effect. By

contrast, currents in the deeper central area of the GWB are weak. The different exposure to currents coincide with the sediment distribution shown by Katzung (2004) (Figure 4). Coarser sediments dominate in areas of strong currents.
Taken together, the results of the model validation as well as information gained from earlier studies suggest that flow fields of the Strelasund and the GWB are sufficiently reproduced.

4.2 Particle Tracking Model

In this study, a particle tracking model has been applied to simulate drift and growth of WBSS larvae. Thereby, model runs were performed on 2-D depth integrated flow fields. Analyses demonstrated that model results are largely unaffected by the numerical setup (Figure 17 and 18). Moreover, the simplified 2-D approach seems justified. It was shown that water masses in the GSA are vertically mixed over long periods throughout the investigated timeframe. Temperature and salinity stratification did not last long. As a consequence of the unimpeded vertical mixing, particles do experience a current regime that is comparable to the depth-integrated flow. Though, the underlying assumption that WBSS larvae behave like physical drifters has to be questioned. Certainly, swimming abilities of larvae are generally low (s.a.). However, many larvae are known to perform diel or semi-diel vertical migrations (VM) (Stephenson & Power, 1988; Haslob et al., 2009). Vertical migrations are often related to feeding and/or predator avoidance strategies (Zaret & Suffern, 1976; Munk et al., 1989). Furthermore, vertical migration has also been identified as a mechanism capable to affect larval dispersal (Grioche et al., 2000). This was also shown for herring larvae (Graham, 1972; Stephenson & Power, 1988). Current speeds are generally low close to the sea ground due to the bottom friction. Thus, larvae that are located at the bottom layer are far less exposed to the currents and hence threatened by larval drift than those in the upper water column. In addition, currents are deflected by bathymetric features and the Coriolis effect (Ekman, 1905). As a result, current speed and direction can significantly vary with depth. In fact, vertical changes in current speed and direction were apparent in the GWB as shown by the differences in surface and depth-integrated circulation patterns for constant wind fields as well as by the vertical velocity profiles at real wind conditions. However, *in situ* VM patterns of WBSS are currently unknown. Hence, in view of the current state of knowledge, neglecting VM seems reasonable.
Within the current approach a temperature dependent growth model described by Oeberst et al. (2009a) has been applied to simulate individual larval growth and to calculate the associated tracking period up to a larval length of 20 mm. This model does not account for length dependent changes in growth rates. In this context, Oeberst et al. (2009a) stated that "growth rate was not length-dependent over the size range studied (5-20 mm)". This seems unlikely from a physiological point of view and from the experience gained in rearing experiments (Kanstinger, personal discussion). Certainly, growth rates are strongly affected by the temperature dependent metabolism. However, larval growth also depends on the foraging behavior of larvae as well as on the prey density and quality. More advanced individual based models (IBM) which incorporate some of these dependencies (Hauss & Peck, 2009) could be applied in further studies. Though, the benefits of more accurate estimates are accompanied by higher computational effort. In this respect, the used simplified growth model is assumed to

provide sufficiently accurate results.

4.3 Larval Retention

The amount and origin of particles/larvae that were removed from the GSA differed with wind-driven circulation patterns. 3.9 to 76.4% of all seeded larvae were drifted to the open Baltic Sea after one month of steady wind forcing, depending on wind direction and strength. The retention of larvae in the GSA is especially favored at NE and SW winds. By contrast, larval drift to the open Baltic Sea was strongest at NW and SE winds. Even at strong, long lasting winds and associated relatively strong water flows through the whole GWB a significant proportion of larvae remains in the GWB.This proves the hypothesis that the Greifswalder Bodden area is a pronounced retention area. Nevertheless, the intensity of retention is strongly affected by prevailing wind conditions.
However, wind conditions were not constant but changed frequently during the investigated spawning season of WBSS in 2008 and 2009 (March - July). As a result, current directions and intensities were shown highly variable at the eastern and western opening of the GWB. This variability in flow fields cause water masses to oscillate at the openings of the GWB, forming a transition zone between the lagoon and the Baltic Sea. Such an effect has been discussed earlier (Lampe, 1994) for the GWB and was already described for adjacent lagoons (Brosin, 1970) . The oscillation of water masses along the boundaries of the GWB helps to explain the calculated water exchange rates in terms of the retention properties of the GWB. Presented monthly water exchange rates of 2008 and 2009 are relatively high and stable but within the range of previous results reported by Stigge (1989) and Jönsson et al. (1998). Generally, high water exchange rates can indicate a strong water replacement which contradicts the hypothesis that the GWB serves as retention area for WBSS larvae. However, as a consequence of the mentioned water oscillation, mostly the same water is involved in the water exchange. Based on salinity profiles it was demonstrated that inflow events rarely reach the center of the GWB. Thus, real water replacement on a lagoon scale can be expected to be much lower. This hypothesis is also supported by the conducted particle tracking experiments at real forcing conditions. On the one hand, the percentage of particles that were drifted out of the GWB was extremely low in both model years. On the other hand, those removed particles originated most often from areas close to the GWB's boundaries. These findings are not in agreement with the hypothesis of a residual eastern flow through the GWB as postulated by Lampe (1994). A steady eastward flow would result in a stronger particle drift across the eastern sill. Moreover, more particles originating from the central GWB were drifted to the Baltic Sea, especially with increasing tracking time, as shown by particle tracking experiments for flow patterns at constant westerly winds. Instead, the wind-driven oscillation of water masses also prevents particles from being drifted outside the GSA, enhancing the retention capacity of the GWB. This illustrates that, apart from wind directions and wind speeds, the duration and temporal variability of wind fields, driving the water oscillation, is of major importance for the retention of WBSS larvae.
As another consequence of the frequent changes in wind fields, larval removal was not constant during the investigated timeframe. Nor was the amount of removed larvae generally decreasing with the progressing season as could be expected due to the decreasing tracking time. Instead,

the percentage of removed larvae differed by cohort. Moreover, it was shown that the risk to drift outside the GSA highly depends on the seeding position of larvae and thus the hatching location of larvae. Larvae that were seeded close to the openings of the GWB were at highest risk to be removed from the GSA. Although, calculated larval drift through the Strelasund is assumed to be strongly overestimated due to an impeded reverse flow of larvae from nearby areas, caused by the model setup (s.a.). By contrast, larvae originating from the southern, central and northern part of the GWB were far less affected. Though, temporarily even from these areas high proportions of larvae could be transported out of the GSA.

Taken together, these results demonstrate that the risk for larvae of being drifted outside the GSA is subject to temporal and spatial variability. However, despite the high temporal variability and regardless which seeding location/spawning site is considered, a significant proportion of larvae remained in the GSA during the spawning season of WBSS in 2008 and 2009. In fact, apart from border areas, the percentage of removed larvae accounts on average for less than 25%. Moreover, inter-annual differences in the percentage of removed larvae are very low for both investigated years. This impressively proves the hypothesis that the GWB serves as retention area for WBSS larvae also at real wind conditions.

Strong larval removal occurred in 2008 at the same time as peak abundances of small WBSS larvae. Though, results of the newly defined retention index indicate that in both years more than 75% of all larvae, hatched in the GSA, remained in this area until they have reached a size of 20 mm. Hence, it is unlikely that larval removal accounted for the observed recruitment failure of WBSS in 2008. Furthermore, the analysis on larval abundances has revealed that already the abundances of small larvae were significantly lower in 2008 than in 2009. One could argue, that spawning in 2008 occurred mainly in areas close to the openings of the GSA, resulting in a rapid larval removal and hence low larval survival/abundances found in the field. Spawning sites at the eastern sill of the GWB were generally less affected in 2008 than in 2009, especially at times of the observed abundance peaks. By contrast, larval drift occurred mainly through the Strelasund. Thereby, affected larvae do not directly flow into the supposed desert, the open Baltic Sea. Instead, they are transported into a system of lagoons which possesses a much more restricted water exchange to the open Baltic Sea than the GWB (Schiewer, 2008a). In addition, these lagoons were reported to exhibit an even higher productivity than the GWB, making food limitation unlikely (Schiewer, 2008a). Indeed, field studies have shown high abundances of WBSS larvae in the Strelasund (Hesse, 2010). Thus, the results presented in this study contradict the hypothesis that larval drift out of the supposed main spawning area of WBSS is responsible for the recruitment failure observed in 2008.

Instead, results have demonstrated that the GWB serves as stable retention area for WBSS larvae, leading back to the Iles & Sinclair (1982) "herring hypothesis". According to this hypothesis, "The number of herring stocks and the geographic location of their respective spawning sites are determined by the number, location, and extent of geographically stable larval retention areas" (Iles & Sinclair, 1982). Though, the associated definition of a retention area given by Iles & Sinclair (1982) is misleading. In fact, every circulation system that in conjunction with an active larval behavior allows larvae to maintain an aggregated distribution, is considered as a retention area. Thereby, larval drift over huge distances is not denied by this

hypothesis. The results presented in this study have shown that larval retention in the GWB does not require any larval behavior. Moreover, it is the magnitude of larval retention in this extremely localized area which is striking. The annual spawning runs of WBSS to this retention area further suggests that the highly localized larval retention is a crucial and stable feature of the life strategy of WBSS.

Although inter- and intra-annual variability in larval retention was not found to be responsible for the drastic changes in the recent stock development of WBSS, results might help to explain significant changes in the development of Baltic herring stocks within the larger historical context: Anthropogenic eutrophication starting in the 1950s has been related to the registered decline of Baltic Autumn-Spawning herring (BAS) in the 1960s (Aneer, 1985; Rechlin, 1991). According to Rechlin (1991), eutrophication has led to improved feeding conditions for adult herring but also to a dramatic decrease of dissolved oxygen in the deeper bottom layers in the late summer and autumn months. Thereby, the latter could have reduced egg and larval survival of BAS which spawn on gravel in the deeper waters of the Baltic Sea (Rechlin, 1991). Furthermore, eutrophication has significantly increased the productivity of the lagoons in the Western Baltic Sea. As shown in this study for the GWB, these lagoons can be considered as strong retention areas and are known to act as spawning areas for WBSS. Thus, locally hatched larvae of WBSS could and can benefit from improved feeding conditions of the surrounding waters leading to an enhanced recruitment success of WBSS. By contrast, Western Baltic Autumn-Spawner (WBAS) recruitment could have become even more disadvantaged due to an associated increased predation pressure of adult WBSS on WBAS larvae (Rechlin, 1991).

5 Conclusions

1. The GWB acts as pronounced retention area for WBSS larvae. Most of the larvae hatched in the GWB remain in this area until they have passed the critical period of development.

2. Larval retention mainly depends on spawning ground locations and prevailing wind fields (direction, speed & duration).

3. Larval drift out of the GWB is subject to intra-annual variations

4. The temporal variability of retention can not sufficiently explain the observed recruitment failure of WBSS in 2008. Nevertheless, a retention index was established which can be used to investigate the inter-annual variability of retention and its impact on the recruitment of WBSS.

6 Further Thoughts and Recommendations

While it was shown that larval drift can not sufficiently explain the recent decline of WBSS recruitment, many other factors could have contributed to the observed development. Hammer et al. (2009) hypothesized a) a reduced productivity of adult herring, b) a reduction of macrophytes and therefore suitable spawning substrates, c) changes in egg and larval development and d) an increased predation on early life stages as potential causes. Although the assessment of these factors was beyond the scope of this study, they should be discussed below.

Generally, a reduced productivity of adults can be caused by physiological and hormonal changes, an increased parasite infestation or changes in the spawning behavior (Hammer et al., 2009). Of those factors listed, hormonal changes have received greater attention in the recent years. Related potential effects include inter-sexuality, feminization of males, malformed reproductive organs, changes in sex ratios and reduced fertility (Hammer et al., 2009). Furthermore, egg and larval development are potentially also affected. These crucial effects can be induced by endocrine-active compounds such as persistent organic pollutants (POP), pesticides and pharmaceuticals (Hinck et al., 2009; Tetreault et al., 2011). While loads of POP have decreased in the Baltic Sea (Bignert et al., 1998), the degree of pharmaceutical pollution and associated effects of drugs remain largely unclear. However, assuming that contaminants are retained in important spawning regions like the GWB as shown for larvae and nutrient loads, early life stages could be more influenced by the pollution.

Egg development rates are strongly affected by temperature. Optimum incubation temperature for Baltic herring was reported to be 12-13 °C (Saat & Veersalu, 1996). Remarkably, preliminary analysis on climate related effects in recruitment revealed no dependencies for WBSS, although such effects were evident for other pelagic fish stocks in the Baltic Sea (ICES, 2007). This is surprising since the GWB warms up rapidly especially in shallow areas. On the other side, at temperatures higher than 17 °C malformation of larvae can occur (Ojaveer, 1981). This threshold was exceeded at the end of May in 2008 and thus nearly one month earlier than in 2009. Apart from excessive temperatures, egg development is further impaired by reduced oxygen supply. Generally, ventilation of eggs is significantly hampered by sedimentation, thick egg layers and epiphytes (Aneer, 1985; Messieh & Rosenthal, 1989). Sedimentation occurs mainly in sheltered areas of weak-flow such as areas that are covered by macrophytes (Schulz et al., 2003; Schernewski & Dolch, 2004). High sedimentation rates are a consequence of the resuspension of particulate matter. Thereby, resuspension can be caused by induced turbulences from winds and shipping traffic (Munkes, 2005). Resuspension also increases turbidity and nutrient concentrations which may also affect the macrophyte community. Though, crucial temporal changes in the macrophyte distribution and community in the GWB are not obvious. Recent coverage estimates and depth limits are comparable with those of the 1990s (Hammer et al., 2009). Also, the overall trophic state of the GWB has not changed during the last two decades (Westphal & Lenk, 1998; Bachor, 2005a). However, relevant changes for herring recruitment might be less apparent. In general, opportunistic fast-growing macroalgae such as *Pilayella littoralis* and *Enteromorpha* spp. are advantaged at higher nutrient concentrations (Lotze et al., 1999; Mertens & Selig, 2007). These algae often occur as epiphytes on important spawning substrates for WBSS, like *Fucus vesiculosus* and *Zostera marina* (Lotze et al., 1999).

In this context, high mortality rates were reported for eggs attached to *Pilayella littoralis* (Aneer, 1987, 1991).
Predation pressure can also account for high mortality rates of eggs and larvae (Palsson, 1984; Scabell, 1988). Thereby, spatial differences in mortality rates are likely. Sticklebacks for example, known as important predators of herring larvae and eggs (Hammer et al., 2009), spawn in the littoral zone during spring and summer months. High abundances of the jellyfish *Aurelia aurita,* which also preys on herring larvae (Gamble & Hay, 1989), occur primarily in the summer months throughout the GWB (Seifert, 1938). Hence, predation pressure might be increased for eggs and nearshore larvae but reduced for herring larvae that are dispersed into the open water. In summary, more rapid warming and resuspension of sediments may have led to a decrease of suitable spawning substrates and impaired the egg development in the GWB. Negative effects on the egg and larval survival related to pollution and predation are also possible. Thus, further field and laboratory experiments are required to assess the impact of the potential factors on the recruitment success of WBSS.
Most likely, the recruitment decline of WBSS was not caused by a single factor. Instead, it can be assumed that the decline is based on the interaction of several factors. Moreover, the relative importance of these factors is likely to vary in space and time. A great advantage of biophysical models is that they can simulate the complex interaction of diverse processes at a very high spatial and temporal resolution. Besides, the applied experimental design can be easily adjusted and it is possible to repeat conducted experiments. Whereas it was shown that the recruitment failure of WBSS can not be explained by drift modeling alone, the current modeling approach offers a great potential for further individual based analyses, especially regarding the investigation of other potential causes of the recruitment failure. Some suggestions are given below:

- Based on the results of this study, opportunities arise to improve the stock assessment of WBSS. The amount of removed larvae is currently not considered in the stock assessment. The N-20 recruitment index accounts only for larvae that have reached 20 mm while being located in the GSA (Oeberst et al., 2009b). Although this index has been stated to correlate well with the abundance of recruits at age 1 and 2, some deviations remain. Within this study, removed larvae are assumed to be faced with starvation and are thus likely to die. However, this assumption has to be questioned. In case that a significant number of removed larvae survives, as has been suggested for larvae that are transported through the Strelasund, this number could help to explain parts of the mentioned deviations between the N-20 recruitment index and age 1 recruitment estimates. This in turn could help to improve the current stock assessment of WBSS.

- In this context, the hypothesis whether removed larvae out of the GSA facing starvation needs further to be addressed. For this purpose, in depth studies of the temporal and spatial variability of zooplankton abundances, composition and quality found in the GSA and in the adjacent Pomeranian Bay are required. In this context, simulation runs could be conducted to quantify prey and predator encounter rates in the GSA and the surrounding Baltic Sea.

- Future analyses should focus on egg and larval mortality rates caused by temperature, predation and starvation. These mortality rates are assumed to show a high spatial and temporal variability. Here, too, field studies are required to provide mortality estimates and to identify spawning sites of WBSS. Mortality rates can be implemented in several ways. Multiple-species approaches are perhaps the most accurate method to simulate related effects. However, mortality rates could also be linked to abiotic factors of the environment. E.g., predator encounter rates could be related to the current speed. In addition, predation by stickleback could be defined as a function of depth and surrounding temperature, assuming that sticklebacks seek shallow waters for spawning with increasing spawning season.

- The particle/larvae transport to the Baltic Sea via the Strelasund is currently largely overestimated and thus needs to be revised. Reasons for this are the nearby northern boundary of the GWBM model domain and the restricted but insufficiently resolved water exchange between these lagoons and the surrounding Baltic Sea. To compensate for these insufficiencies the model resolution and the domain have to be increased. Thereby, adjacent lagoons to the north of the Strelasund should be included. In addition, by extending the model domain exchange rates between the GSA and the adjacent lagoons could be estimates, particular with regard to effects on the larval distribution. Larval abundances in the adjacent lagoons are currently not recorded by the RHLS.

- The influence of VM on the dispersal of herring larvae should be investigated. Appropriate analyses could help to identify whether VM affect position of larvae in the Strelasund and thus contributing to the high abundances of herring larvae frequently found at this site during the RHLS. Hence, field studies are necessary to provide the required information about VM patterns.

- Current spawning sites need to be examined. Supplementary analyses have shown that the larval distribution becomes more uniform with increasing tracking time. However, small larvae may be found close to the spawning sites. Thus, backtracking of small larvae could help to identify spawning sites. Results can help to determine spatially dependent effects on larval survival and to reduce potential anthropogenic impacts (e.g. shipping traffic). Furthermore, results could be used for further analyses on the patchiness of larger larval stages which are important for the WBSS stock assessment.

- Further studies are needed to investigate the reliability of model simulations. Besides validating modeled data, model simulations can also be calibrated. Therefore, hydrographic data, such as current speeds, salinity and temperature data are needed to validate/calibrate the circulation model. Besides, tracer experiments could be performed to assess the accuracy of results obtained from the particle tracking model. Appropriate measurements and experiments could be conducted during the annual RHLS.

7 References

Aneer, G., 1985. Some Speculations about the Baltic Herring (*Clupea harengus membras*) in Connection with the Eutrophication of the Baltic Sea. Canadian Journal of Fisheries and Aquatic Sciences **42**:83–90.

Aneer, G., 1987. High natural mortality of Baltic herring (*Clupea harengus*) eggs caused by algal exudates? Marine Biology **94**:163–169.

Aneer, G., 1991. Mortality of Baltic herring (*Clupea harengus* L.) eggs caused by spawning substratum algae. Acta Ichthyologica et Piscatoria **21(S)**:327–344.

Anwand, K., 1962. Die Fruchtbarkeit des Frühjahrs- und Herbstheringe aus den Gewässern um Rügen. Zeitschrift für Fischerei und deren Hilfswissenschaften **11 NF**:463–473.

Arnold, L., 1974. Stochastic differential equations: Theory and applications. Wiley, London.

Bachor, A., 2005a. Nährstoff- und Schwermetallbilanzen der Küstengewässer Mecklenburg-Vorpommerns unter besonderer Berücksichtigung ihrer Sedimente. Schriftenreihe des Landesamtes für Umwelt, Naturschutz und Geologie **2**:219.

Bachor, A., 2005b. Nährstoffeinträge in die Küstengewässer Mecklenburg-Vorpommerns – eine Belastungsanalyse. Rostocker Meeresbiologische Beitrage **14**:17–32.

Bartels, S. & U. Klüber, 1999. Determination of the Submerged Macrophyte Coverage of Greifswalder Bodden. Limnologica - Ecology and Management of Inland Waters **29**:311–313.

Biester, E., 1989. The distribution of spring spawning herring larvae in coastal waters of the German Democratic Republic. Rapports et Procès-Verbaux des Réunions du Conseil Permanent International pour l'Exploration de la Mer **190**:109–112.

Bignert, A., M. Olsson, W. Persson, S. Jensen, S. Zakrisson, K. Litzén, U. Eriksson, L. Häggberg, & T. Alsberg, 1998. Temporal trends of organochlorines in Northern Europe, 1967-1995. Relation to global fractionation, leakage from sediments and international measures. Environmental Pollution **99**:177–198.

Birr, H.-D., 1988. Zu den Strömungsverhältnissen des Strelasundes. Beiträge zur Meereskunde **58**:3–8.

Birr, H.-D., 1997. Hydrographische Charakteristik und Umweltprobleme der mecklenburg-vorpommerschen Boddengewässer. Greifswalder Geographische Arbeiten **14**:111–128.

Blaxter, J. H. S., J. A. B. Gray, & A. C. G. Best, 1983. Structure and development of the free neuromasts and lateral line system of the herring. Journal of the Marine Biological Association of the United Kingdom **63**:247–260.

Blaxter, J. H. S. & G. Hempel, 1961. Biologische Beobachtungen bei der Aufzucht von Heringsbrut. Helgoland Marine Research **7**:260–283.

Blaxter, J. H. S. & G. Hempel, 1963. The Influence of Egg Size on Herring Larvae (*Clupea harengus* L.). Journal du Conseil **28**:211–240.

Blümel, C., A. Domin, J. C. Krause, M. Schubert, U. Schiewer, & H. Schubert, 2002. Der historische Makrophytenbewuchs der inneren Gewässer der deutschen Ostseeküste. Rostocker Meeresbiologische Beitrage **10**:5–111.

Bonhommeau, S., B. Blanke, A.-M. Tréguier, N. Grima, E. Rivot, Y. Vermard, E. Greiner, & O. Le Pape, 2009. How fast can the European eel (*Anguilla anguilla*) larvae cross the Atlantic Ocean? Fisheries Oceanography **18**:371–385.

Bonhommeau, S., M. Castonguay, E. Rivot, R. Sabatié, & O. Le Pape, 2010. The duration of migration of Atlantic Anguilla larvae. Fish and Fisheries **11**:289–306.

Brosin, H. J., 1970. Die Wasserzirkulation in einigen Boddengewässern der DDR-Küste und ihre Beeinflussung durch meteorologische Faktoren. Veröffentlichungen des Geophysikalischen Instituts der Universität Leipzig **19**:435–445.

Buckmann, K., U. Gebhardt, A. Weidauer, K. D. Pfeiffer, K. Duwe, A. Fey, B. Hellmann, & J. Post, 1998. Simulation und Messung von Zirkulations- und Transportprozessen im Greifswalder Bodden, Oderästuar und den angrenzenden Küstengewässern. Greifswalder Geographische Arbeiten **16**:12–41.

Burchard, H. & K. Bolding, 2002. GETM, a General Estuarine Transport Model. European Commission Joint Research Centre.

Burchard, H., F. Janssen, K. Bolding, L. Umlauf, & H. Rennau, 2009. Model simulations of dense bottom currents in the Western Baltic Sea. Continental Shelf Research **29**:205–220.

Burchard, H., H. Lass, V. Mohrholz, L. Umlauf, J. Sellschopp, V. Fiekas, K. Bolding, & L. Arneborg, 2005. Dynamics of medium-intensity dense water plumes in the Arkona Basin, Western Baltic Sea. Ocean Dynamics **55**:391–402.

Burchard, H., G. Schernewski, O. Bittner, K. Bolding, M. Gerth, R. Hetland, R. Hofmeister, S. Maack, T. Neumann, H. Siegel, P. Springer, & I. Stottmeister, 2008. Physikalische und ökologische Auswirkungen einer Kühlwasserausbreitung im Greifswalder Bodden - Endbericht. Leibniz Institute for Baltic Sea Research Warnemünde, Rostock.

Busch, A., 1996. Transition from endogenous to exogenous nutrition: larval size parameters determining the start of external feeding and size of prey ingested by Ruegen spring herring *Clupea harengus*. Marine Ecology Progress Series **130**:39–46.

Bückmann, A., W. Mielck, & A. Kotthaus, 1950. Die Untersuchungen der Biologischen Anstalt über die Ökologie der Heringsbrut in der Südlichen Nordsee. Helgoland Marine Research **3**:1–57.

Correns, M., 1977. Grundzüge von Hydrographie und Wasserhaushalt der Boddengewässer an der Küste der Deutschen Demokratischen Republik. Acta Hydrochimica et Hydrobiologica **5**:517–526.

Correns, M., 1978. Water balance in the bodden waters along the G.D.R. coastline. Journal of Hydrological Sciences **5**:81–86.

Correns, M., 1979. Der Wasserhaushalt der Bodden- und Haffgewässer der DDR als Grundlage für die weitere Erforschung ihrer Nutzungsfähigkeit zu Trink- und Brauchwasserzwecken. Ph.D. thesis, Humboldt-Universiät Berlin.

Cushing, D. H., 1975. Marine Ecology and Fisheries. Cambridge University Press, Cambridge.

Cushing, D. H., 1986. The migration of larval and juvenile fish from spawning ground to nursery ground. Journal du Conseil **43**:43–49.

Ekman, V. W., 1905. On the Influence of the Earth's Rotation on Ocean-Currents. Arkiv för matematik, astronomi och fysik **11**:1–53.

Fennel, W., H. Radtke, M. Schmidt, & T. Neumann, 2010. Transient upwelling in the central Baltic Sea. Continental Shelf Research **30**:2015–2026.

Fuiman, L. & R. Batty, 1997. What a drag it is getting cold: partitioning the physical and physiological effects of temperature on fish swimming. Journal of Experimental Biology **200**:1745–1755.

Gamble, J. C. & S. J. Hay, 1989. Predation by the scyphomedusan *Aurelia aurita* on herring larvae in large enclosures: effects of predator size and prey starvation. Rapports et Procès-Verbaux des Réunions du Conseil Permanent International pour l'Exploration de la Mer **191**:366–375.

Gillis, G. B., 2003. Swimming with the larval fishes. Journal of Experimental Biology **206**:1768.

Graham, J. J., 1972. Retention of larval herring within the Sheepscot estuary of Maine. Fishery Bulletin **70**:299–304.

Griffies, S. M., M. J. Harrison, R. C. Pacanowski, & A. Rosati, 2004. A Technical Guide to MOM4. GFDL Ocean Group Technical Report No. 5, Princeton, NJ: NOAA/Geophysical Fluid Dynamics Laboratory.

Grioche, A., X. Harlay, P. Koubbi, & L. Lago, 2000. Vertical migrations of fish larvae: Eulerian and Lagrangian observations in the Eastern English Channel. Journal of Plankton Research **22**:1813–1828.

Gräwe, U., 2011. Implementation of high-order particle-tracking schemes in a water column model. Ocean Modelling **36**:80–89.

Gräwe, U. & J.-O. Wolff, 2010. Suspended particulate matter dynamics in a particle framework. Environmental Fluid Mechanics **10**:21–39.

Gröger, J. & T. Gröhsler, 2001. Comparative analysis of alternative statistical models for differentiation of herring stocks based on meristic characters. Journal of Applied Ichthyology **17**:207–219.

Hackert, K., 1969. Die Strömungsverhältnisse des Greifswalder Boddens bei Ost- und Westwinden. Wasserwirtschaft, Wassertechnik **19**:191–195.

Hammer, C., C. Zimmermann, C. von Dorrien, D. Stepputtis, & R. Oeberst, 2009. Begutachtung der Relevanz der Auswirkung des Kühlwassers des geplanten Steinkohlekraftwerks in Lubmin auf die fischereilich genutzten marinen Fischbestände der westlichen Ostsee (Hering, Dorsch, Flunder, Scholle, Hornhecht). Endbericht für das Ministerium für Landwirtschaft, Umwelt und Verbraucherschutz Mecklenburg-Vorpommern, vertreten durch das Staatliche Amt für Umwelt- und Naturschutz Stralsund (StAUN Stralsund). Johann-Heinrich von Thünen-Institut, Bundesforschungsinstitut für Ländliche Räume, Wald und Fischerei/Institut für Ostseefischerei Rostock.

Harden Jones, F. R., 1968. Fish migration. Edward Arnold, London.

Haslob, H., N. Rohlf, & D. Schnack, 2009. Small scale distribution patterns and vertical migration of North Sea herring larvae (*Clupea harengus*, Teleostei: Clupeidea) in relation to abiotic and biotic factors. Scientia Marina **73S1**:13–22.

Hauss, H. M. & M. A. Peck, 2009. Comparing observed and modeled growth of larval herring (*Clupea harengus*): Testing individual-based model (IBM) parameterizations. Scientia Marina **73S1**:37–45.

Hay, D. E. & P. B. McCarter, 1991. Proceedings of the International Herring Symposium, chapter Retention and dispersion of larval herring in British Columbia Canada and implications for stock structure, pages 107–114. Number 91-01 in Alaska Sea Grant College Program Report. Alaska Sea Grant College Program, University of Alaska, Fairbanks, Alaska, USA.

Hay, D. E. & P. B. McCarter, 1997. Larval distribution, abundance, and stock structure of British Columbia herring. Journal of Fish Biology **51**:155–175.

Heemink, A. W. & P. A. Blokland, 1995. On random walk models with space varying diffusivity. Journal of Computational Physics **119**:388–389.

Henri, M., J. J. Dodson, & H. Powles, 1985. Spatial Configurations of Young Herring (*Clupea harengus harengus*) larvae in the St. Lawrence Estuary: Importance of Biological and Physical Factors. Canadian Journal of Fisheries and Aquatic Sciences **42**:91–104.

Hesse, J., 2010. Quantitative and qualitative analyses of the food consumption of *Clupea harengus* L. larvae in the Greifswalder Bodden and Strelasund, Baltic Sea, Germany. Diploma thesis, Universität Rostock.

Hinck, J. E., V. S. Blazer, C. J. Schmitt, D. M. Papoulias, & D. E. Tillitt, 2009. Widespread occurrence of intersex in black basses (*Micropterus* spp.) from U.S. rivers, 1995-2004. Aquatic Toxicology **95**:60–70.

Hjort, J., 1914. Fluctuations in the great fisheries of Northern Europe viewed in the light of biological research. Rapports et Procès-Verbaux des Réunions du Conseil Permanent International pour l'Exploration de la Mer **20**:1–228.

Hofmeister, R., H. Burchard, & J.-M. Beckers, 2010. Non-uniform adaptive vertical grids for 3D numerical ocean models. Ocean Modelling **33**:70–86.

Hoss, D. & J. Blaxter, 1979. The effect of rapid changes of hydrostatic pressure on the Atlantic herring *Clupea harengus* L. I. Larval survival and behaviour. Journal of Experimental Marine Biology and Ecology **41**:75–85.

Hunt von Herbing, I., 2002. Effects of temperature on larval fish swimming performance: the importance of physics to physiology. Journal of Fish Biology **61**:865–876.

Hunt von Herbing, I. & K. Keating, 2003. The big fish bang, chapter Temperature-induced changes in viscosity and its effects on swimming speed in larval haddock, pages 22–34. Institute of Marine Research, Bergen.

Hunter, J., P. Craig, & H. Phillips, 1993. On the use of random walk models with spatially variable diffusivity. Journal of Computational Physics **106**:366–376.

Hübel, H.-J., U. Vietinghoff, M.-L. Hubert, S. Rambow-Bartels, B. Korth, H. Westphal, & B. Lenk, 1995. Ergebnisse des ökologischen Monitorings Greifswalder Bodden September 1993 bis März 1995. Rostocker Meeresbiologische Beiträge **3**:5–67.

ICES, 1998. Report of the Baltic Herring Age-Reading Study Group. ICES Council Meeting papers **H:2**:86.

ICES, 2007. Report of the Herring Assessment Working Group South Of 62 N (HAWG). 13 - 22 March 2007, ICES Headquarters. ICES CM 2007/ACFM:11. 538 pp.

ICES, 2011. Report of the ICES Advisory Committee 2011. ICES Advice, 2011. Book 6.

Iles, T. D. & M. Sinclair, 1982. Atlantic Herring: Stock Discreteness and Abundance. Science **215**:627–633.

Jönsson, N., A. Busch, T. Lorenz, & B. Korth, 1998. Struktur und Funktion von Boddenlebensgemeinschaften im Ergebnis von Austausch- und Vermischungsprozessen. Greifswalder Geographische Arbeiten **16**:250–285.

Jørgensen, H. B. H., M. M. Hansen, & V. Loeschcke, 2005. Spring-spawning herring (*Clupea harengus* L.) in the southwestern Baltic Sea: do they form genetically distinct spawning waves? ICES Journal of Marine Science **62**:1065–1075.

Katzung, G., 2004. Geologie von Mecklenburg-Vorpommern. E. Schweizerbart'sche Verlagsbuchhandlung (Nägele u. Obermiller).

Klenz, B., 2000. Abundance and distribution of larvae of commercially important fish species in the Western Baltic Sea during the period 1993-1998. ICES Council Meeting papers **N:15**.

Klinkhardt, M., 1996. Der Hering: *Clupea harengus harengus*. Westarp Wissenschaften.

Klinkhardt, M. & E. Biester, 1984. Erste Ergebnisse von experimentellen Felduntersuchungen am Laich von Rügenschen Frühjahrsheringen. Fischerei-Forschung **22**:76–78.

Klinkhardt, M. & E. Biester, 1985. Untersuchungen zum Ablauf der Frühjahrslaichsaison 1982 und 1983 der Rügenheringe (*Clupea harengus harengus* L.) auf einem ausgewählten Laichplatz des Greifswalder Boddens. Fischerei-Forschung **23**:41–48.

Kloeden, P. E. & E. Platen, 1999. Numerical Solution of Stochastic Differential Equations (Stochastic Modelling and Applied Probability), 3rd Edition. Springer, corrected edition.

Kändler, R., 1952. Über das Laichen des Frühjahrsherings bei Rügen und die Häufigkeit def Brut des Herbstherings in der Beltsee und südlichen Ostsee. Kieler Meeresforschungen **8**:145–163.

Lambert, T. C., 1987. Duration and intensity of spawning in herring *Clupea harengus* as related to the age structure of the mature population. Marine Ecology Progress Series **39**:209–220.

Lampe, R., 1994. Die vorpommerschen Boddengewässer - Hydrographie, Bodenablagerungen und Küstendynamik. Die Küste **56**:25–49.

Lasker, R., 1975. Field criteria for survival of anchovy larvae: the relation between inshore chlorophyll maximum layers and successful first feeding. Fishery Bulletin **73**:453–462.

Lasker, R., 1978. The relation between oceanographic conditions and larval anchovy food in the California Current: identification of factors contributing to recruitment failure. Rapports et Procès-Verbaux des Réunions du Conseil Permanent International pour l'Exploration de la Mer **173**:212–230.

Lasker, R., 1981. Marine fish larvae, morphology, ecology and relation to fisheries, chapter The role of a stable ocean in larval fish survival and subsequent recruitment, pages 80–87. University Washington Press.

Li, Y., A. Vodacek, N. Raqueño, R. Kremens, A. Garrett, I. Bosch, J. Makarewicz, & T. Lewis, 2008. Circulation and Stream Plume Modeling in Conesus Lake. Environmental Modeling and Assessment **13**:275–289.

Lotze, H. K., W. Schramm, D. Schories, & B. Worm, 1999. Control of macroalgal blooms at early developmental stages: *Pilayella littoralis* versus *Enteromorpha* spp. Oecologia **119**:46–54.

Mertens, M. & U. Selig, 2007. Vergleich von historischen und rezenten Makrophytenbeständen in den inneren Küstengewässern Schleswig – Holsteins. Rostocker Meeresbiologische Beitrage **17**:55–66.

Messieh, S. N. & H. Rosenthal, 1989. Mass mortality of herring eggs on spawning beds on and near Fisherman's Bank, Gulf of St. Lawrence, Canada. Aquatic Living Resources **2**:1–8.

Messner, U. & J.-A. Von Oertzen, 1990. Recent Changes in the Phytal Zone of Greifswald Bay. Limnologica - Ecology and Management of Inland Waters **20**:183–186.

Messner, U. & J.-A. Von Oertzen, 1991. Long-term Changes in the Vertical Distribution of Macrophytobenthic Communities in the Greifswalder Bodden. Acta Ichthyologica et Piscatoria **21(S)**:135–143.

Meyer, H., R. Lampe, P. Jonas, & K. Buckmann, 1998. Nährstoffe im Oderästuar – Transporte und Inventare. Greifswalder Geographische Arbeiten **16**:99–129.

Miller, J. M., L. J. Pietrafesa, & N. P. Smith, 1990. Principles of hydraulic management of coastal lagoons for aquaculture and fisheries. FAO Fisheries Technical Paper. No. 314. Rome, FAO.

Miller, T. J., 2007. Contribution of individual-based coupled physical-biological models to understanding recruitment in marine fish populations. Marine Ecology Progress Series **347**:127–138.

Munk, P., T. Kiørboe, & V. Christensen, 1989. Vertical migrations of herring, *Clupea harengus*, larvae in relation to light and prey distribution. Environmental Biology of Fishes **26**:87–96.

Munkes, B., 2005. Eutrophication, phase shift, the delay and the potential return in the Greifswalder Bodden, Baltic Sea. Aquatic Sciences - Research Across Boundaries **67**:372–381.

Nelson, J. S., 2006. Fishes of the world. John Wiley & Sons, Inc.

Nielsen, J. R., B. Lundgren, T. F. Jensen, & K.-J. Stæhr, 2001. Distribution, density and abundance of the western Baltic herring (*Clupea harengus*) in the Sound (ICES Subdivision 23) in relation to hydrographical features. Fisheries Research **50**:235–258.

North, E. W., A. Gallego, & P. Petitgas, 2009. Manual of recommended practices for modelling physical-biological interactions during fish early life. ICES Cooperative Research Report **5**:111.

Oeberst, R., M. Dickey-Collas, & R. D. M. Nash, 2009a. Mean daily growth of herring larvae in relation to temperature over a range of 5-20°C, based on weekly repeated cruises in the Greifswalder Bodden. ICES Journal of Marine Science: Journal du Conseil **66**:1696–1701.

Oeberst, R., B. Klenz, T. Gröhsler, M. Dickey-Collas, R. D. M. Nash, & C. Zimmermann, 2009b. When is year-class strength determined in western Baltic herring? ICES Journal of Marine Science: Journal du Conseil **66**:1667–1672.

Ojaveer, E., 1981. Influence of temperature, salinity, and reproductive mixing of Baltic herring groups on its embryonal development. Rapports et Procès-Verbaux des Réunions du Conseil Permanent International pour l'Exploration de la Mer **178**:409–415.

Palsson, W. A., 1984. Egg mortality upon natural and artificial substrata within Washington state spawning grounds of Pacific herring (*Clupea harengus pallasi*). Master's thesis, University of Washington, Seattle.

Purcell, J. E., T. D. Siferd, & J. B. Marliave, 1987. Vulnerability of larval herring (*Clupea harengus pallasi*) to capture by the jellyfish *Aequorea victoria*. Marine Biology **94**:157–162.

Puttler, G., 1972. Die Abhängigkeit der Eigröße von der Konstitution der Mutter beim Hering (*Clupea harengus* L.) der westlichen Ostsee. Ph.D. thesis.

Rajasilta, M., J. Eklund, J. Kääriä, & K. Ranta-Aho, 1989. The deposition and mortality of the eggs of the Baltic herring *Clupea harengus membras* L., on different substrates in the south-west archipelago of Finland. Journal of Fish Biology **34**:417–427.

Rajasilta, M., P. Laine, & J. Eklund, 2006. Mortality of herring eggs on different algal substrates (*Furcellaria* spp. and *Cladophora* spp.) in the Baltic Sea – An experimental study. Hydrobiologia **554**:127–130.

Rambow, S., 1994. Untersuchungen zur quantitativen Erfassung des Bedeckungsgrades von submersen Makrophyten im nordöstlichen Greifswalder Bodden mit Hilfe der Unterwasservideographie und der Luftbild-Auswertung. Diploma thesis.

Rechlin, O., 2000. Fischbestände der Ostsee, ihre Entwicklung seit 1970 und Schlussfolgerungen für ihre fischereiliche Nutzung - Teil 2: Hering. Informationen für die Fischwirtschaft aus der Fischereiforschung **47**:25–30.

Rechlin, O. & O. Bagge, 1996. Entwicklung der Nutzfischbestände. In: Lozan, J., Lampe, R., Matthäus, W., Rachor, E., Rumohr, H. & von Westernhagen, H. (eds.): Warnsignale aus der Ostsee. Parey Buchverlag, Berlin.

Rechlin, O. K. W., 1991. Tendencies in the Herring Population Development of the Baltic Sea. Internationale Revue der gesamten Hydrobiologie und Hydrographie **76**:405–412.

Saat, T. & A. Veersalu, 1996. Duration of synchronous cleavage cycles and rate of development at different temperatures in the Baltic herring. Journal of Fish Biology **48**:658–663.

Scabell, J., 1988. Der Rügensche Frühjahrshering - das Laichgeschehen. Ph.D. thesis, Universität Rostock.

Scabell, J. & N. Jönsson, 1984. Untersuchungen zum natürlichen Laichverhalten des Rügenschen Frühjahrsherings im Greifswalder Bodden. Fischerei-Forschung **22**:68–72.

Schernewski, G. & T. Dolch, editors, 2004. The Oder Estuary - against the background of the European Water Framework Directive. Marine Science Reports 57.

Schiewer, U., 2008a. Ecology of Baltic Coastal Waters, chapter Greifswalder Bodden, Wismar-Bucht and Salzhaff, pages 87–114. Springer Verlag, Berlin Heidelberg.

Schiewer, U., 2008b. Ecology of Baltic Coastal Waters. Springer Verlag, Berlin Heidelberg.

Schlitzer, R., 2010. Ocean Data View, http://odv.awi.de.

Schulz, J.-P., 2006. The new Lokal-Modell LME of the German Weather Service. COSMO Newsletter **No. 6**:210–212.

Schulz, M., H.-P. Kozerski, T. Pluntke, & K. Rinke, 2003. The influence of macrophytes on sedimentation and nutrient retention in the lower River Spree (Germany). Water Research **37**:569–578.

Seifert, R., 1938. Die Bodenfauna des Greifswalder Boddens. Ein Beitrag zur Ökologie der Brackwasserfauna. Zoomorphology **34**:221–271.

Sinclair, M., 1988. Marine Populations: An essay on population, regulation and speciation. University of Washington Press.

Smagorinsky, J., 1963. General circulation experiments with the primitive equations. Monthly Weather Review **91**:99–164.

Spagnol, S., E. Wolanski, E. Deleersnijder, R. Brinkman, F. McAllister, B. Cushman-Roisin, & E. Hanert, 2002. An error frequently made in the evaluation of advective transport in two-dimensional Lagrangian models of advection-diffusion in coral reef waters. Marine Ecology Progress Series **235**:299–302.

Spittler, P., U. Brenning, & G. Arlt, 1990. Protozoans—the first food of larval herring (*Clupea harengus* L.)? Internationale Revue der gesamten Hydrobiologie und Hydrographie **75**:597–603.

Stephenson, R. & M. J. Power, 1988. Semidiel vertical movements in Atlantic herring *Clupea harengus* larvae: a mechanism for larval retention? Marine Ecology Progress Series **50**:3–11.

Stigge, H.-J., 1989. Der Wasserkörper Bodden und seine Hydrodynamik. Meer und Museum **5**:10–14.

Sætre, R., R. Toresen, H. Søiland, & P. Fossum, 2002. The Norwegian spring-spawning herring - spawning, larval drift and larval retention. Sarsia **87**:167–178.

Tetreault, G. R., C. J. Bennett, K. Shires, B. Knight, M. R. Servos, & M. E. McMaster, 2011. Intersex and reproductive impairment of wild fish exposed to multiple municipal wastewater discharges. Aquatic Toxicology **104**:278–290.

Vietinghoff, U., M.-L. Hubert, & H. Westphal, 1994. Zustandsanalyse und Langzeitveränderungen des Ökosystems Greifswalder Bodden, Abschlußbericht. UBA-FB 95-003, Rostock.

Vietinghoff, U., H. J. Hübel, H. Westphal, B. Lenk, S. Rambow, & B. Korth, 1995. Die Forschung begleitendes Monitoring Greifswalder Bodden. - Abschlußbericht für das Ministerium für Bau, Landesentwicklung und Umwelt des Landes Mecklenburg-Vorpommern, Abteilung Wasserwirtschaft. Rostock.

Visser, A. W., 2008. Lagrangian modelling of plankton motion: From deceptively simple random walks to Fokker-Planck and back again. Journal of Marine Systems **70**:287–299.

von Westernhagen, H. & H. Rosenthal, 1979. Laboratory and in-situ studies on larval development and swimming performance of Pacific herring *Clupea harengus pallasi*. Helgoland Marine Research **32**:539–549.

Wasmund, N. & V. Kell, 1991. Characterization of Brackish Coastal Waters of Different Trophic Levels by Means of Phytoplankton Biomass and Primary Production. Internationale Revue der gesamten Hydrobiologie und Hydrographie **76**:361–370.

Westphal, H. & B. Lenk, 1998. Die räumlich-zeitliche Verteilung von Primärproduktion und Bakterienkeimzahlen. Greifswalder Geographische Arbeiten **16**:228–249.

Yin, M. & J. Blaxter, 1987. Feeding ability and survival during starvation of marine fish larvae reared in the laboratory. Journal of Experimental Marine Biology and Ecology **105**:73–83.

Zaret, T. M. & J. S. Suffern, 1976. Vertical migration in zooplankton as a predator avoidance mechanism. Limnology and Oceanography **21**:804–813.

Appendix

Particle Tracking Model Configuration File - LADOS.inp

```
! nx                 : number of grid points in x direction
! ny                 : number of grid points in y direction
! totalnumber        : number of particles
! time_step          : particle time step
! startstr           : start time (format = "yyyy-mm-dd hh:mm:ss)
! stopstr            : stop time  (format = "yyyy-mm-dd hh:mm:ss)
! outstep            : print output every time_step
! inputfile          : name of the velocity input file
! gridtype           :  1 - cartisian
!                       2 - spherical
! K_h_const          : diffusivity
!                       K_h_const < 0 using formulation of Smagorinsky
!                       K_h_const > 0 using constant horizontal diffusivity
! c_smag             : Smagorinsky constant
! particle_position  : .true. - output of all particle positions
!                      .false.- output as concentration field
! depth_averaged     : .true. - velocity file provides depth averaged currents
!                      .false.- velocity file provides surface currents
! interpolation_method: 1 - linear interpolation
!                       2 - cubic splines
! solver2d           :  1 - Milstein scheme (1.order - SDE)
!                       2 - Heun scheme (1.order - SDE)
!                       3 - Platen scheme (2.order - SDE)
!                       4 - Taylor scheme (3.order - ODE)
!                       5 - Runge-Kutta scheme (4.order - ODE)
&initlados
nx=318
ny=180
totalnumber=2,
time_step=300.,
startstr='yyyy-mm-dd hh:mm:ss',
stopstr='yyyy-mm-dd hh:mm:ss',
outstep=72,
inputfile='path_to_flow_field(netcdf_file)',
gridtype=2
K_h_const=-1.
c_smag=0.1
particle_position=.true.
depth_averaged=.true.
```

```
interpolation_method=1
solver2d=2
bulk_transport=.false.
packedinput=.false.
use_temp=.true.
save_temp=.true.
/
```

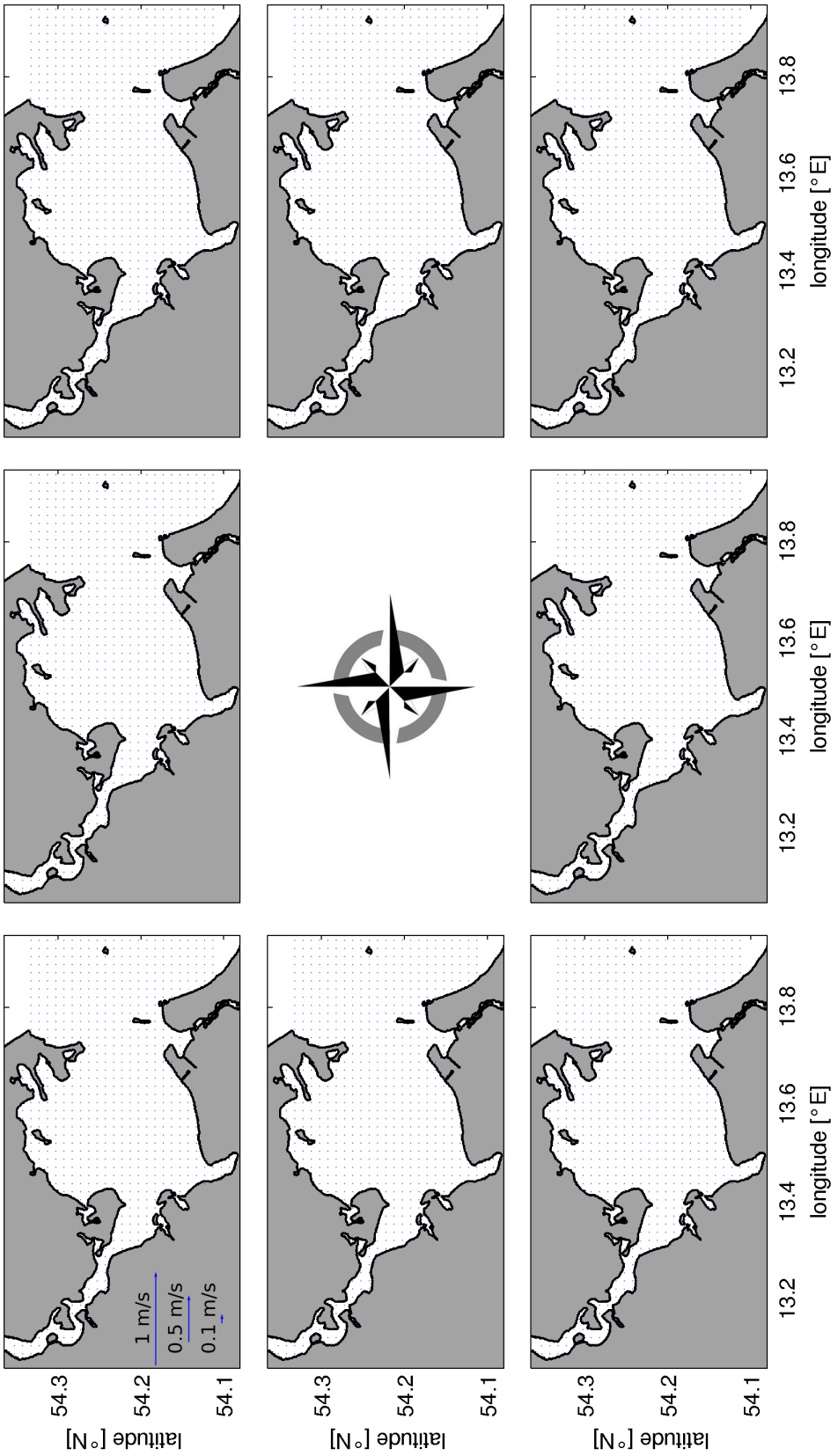

Figure 43: Simulated, surface flow fields for constant wind speed (1 m s^{-1}) and different wind directions. Plot orientation with respect to the compass rose corresponds to the forcing wind direction (e.g. upper left plot refers to north-westerly winds). The vector length gives the current speed, vector direction relates to the current direction.

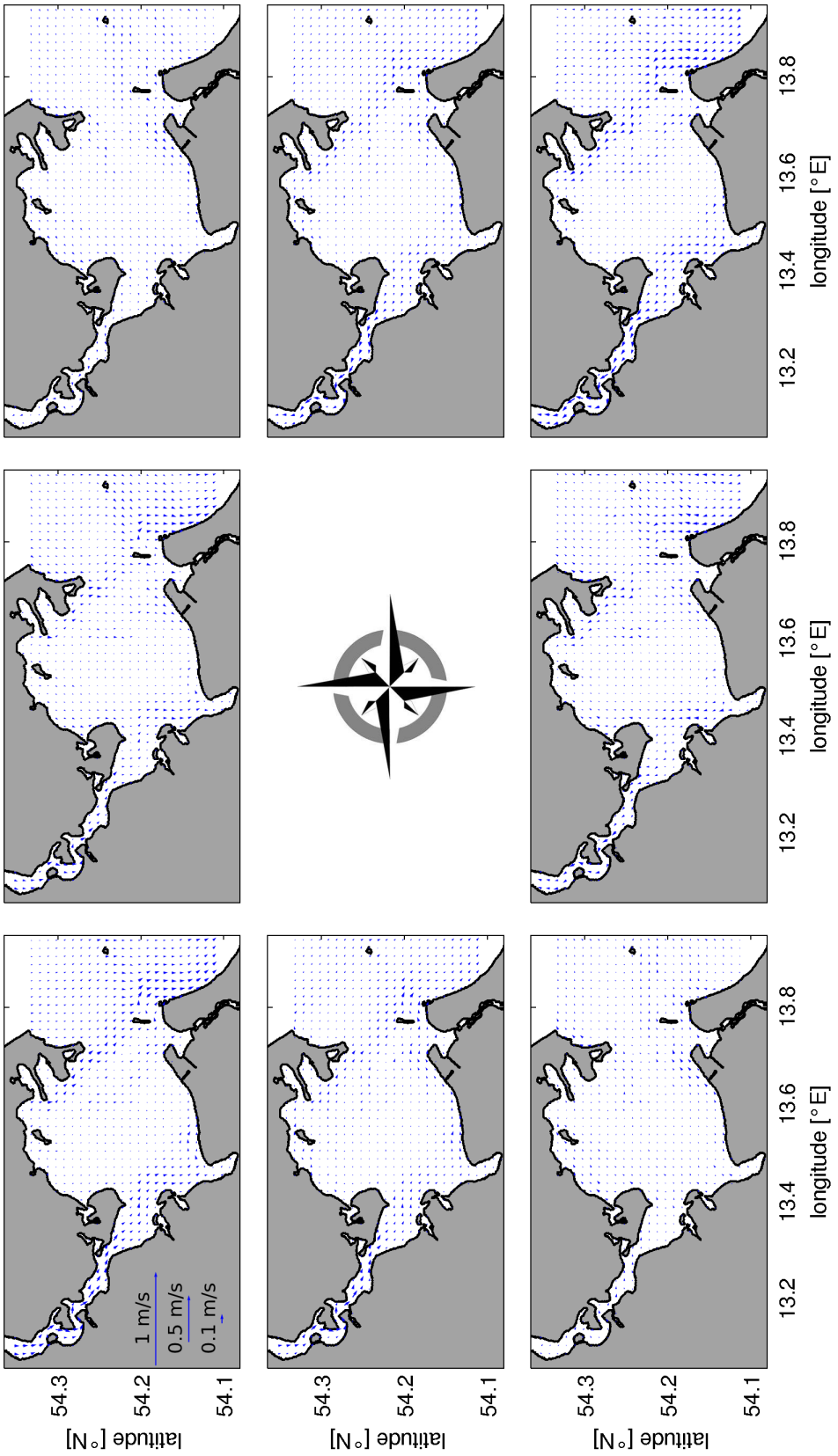

Figure 44: Simulated, surface flow fields for constant wind speed (3 m s^{-1}) and different wind directions. Plot orientation with respect to the compass rose corresponds to the forcing wind direction (e.g. upper left plot refers to north-westerly winds). The vector length gives the current speed, vector direction relates to the current direction.

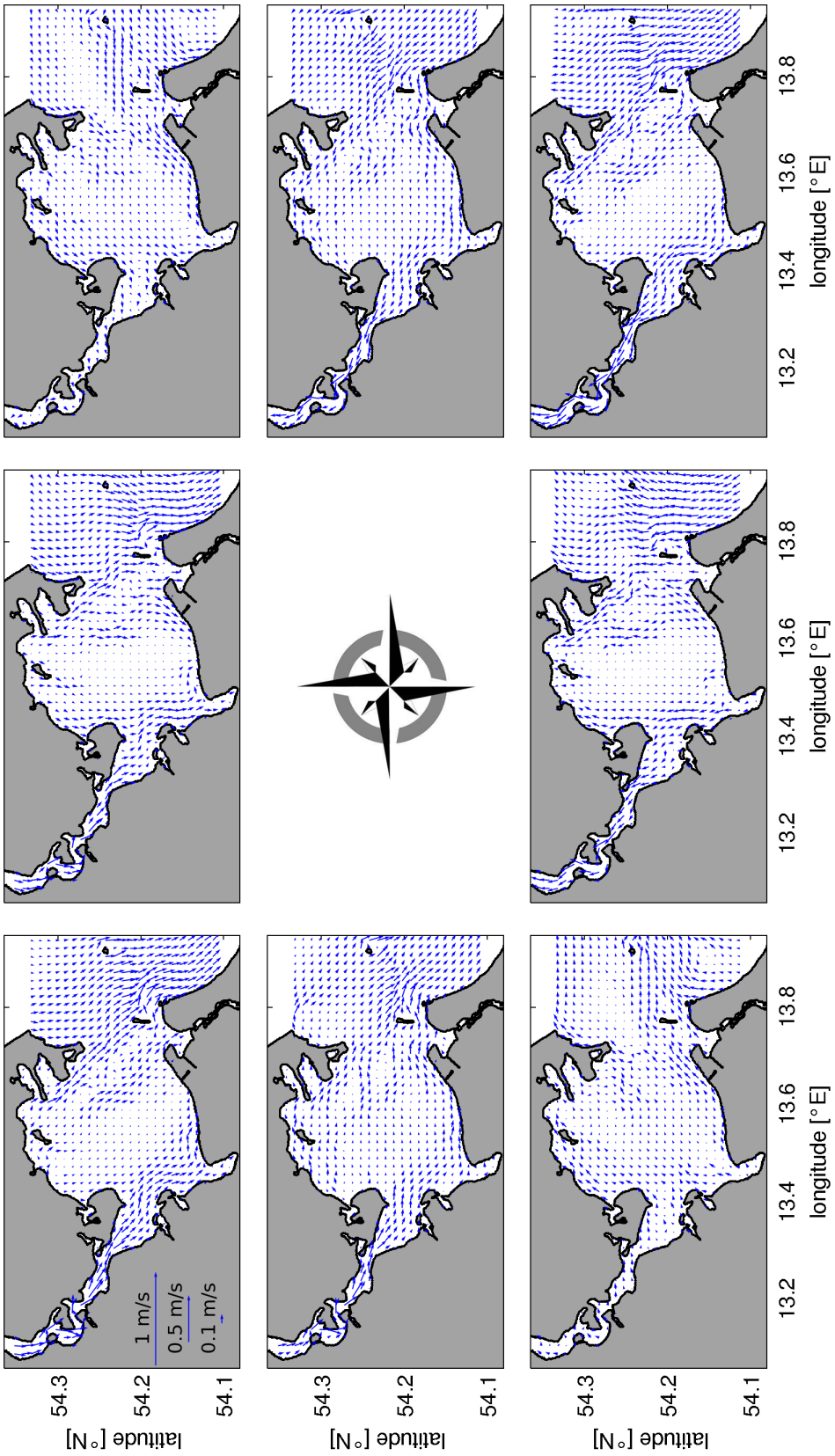

Figure 45: Simulated, surface flow fields for constant wind speeds (6m s^{-1}) and different wind directions. Plot orientation with respect to the compass rose corresponds to the forcing wind direction (e.g. upper left plot refers to north-westerly winds). The vector length gives the current speed, vector direction relates to the current direction.

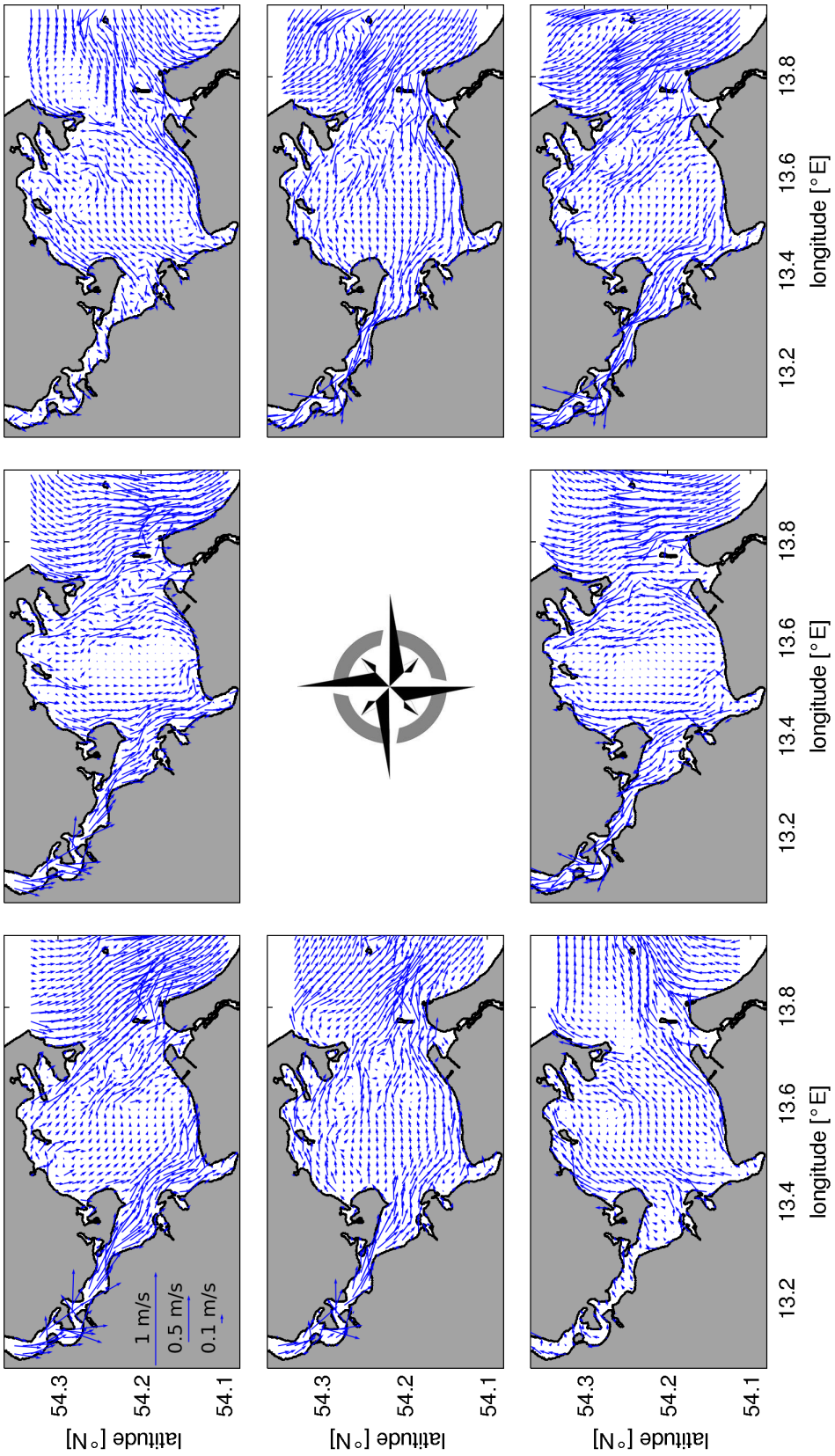

Figure 46: Simulated, surface flow fields for constant wind speeds (9 m s^{-1}) and different wind directions. Plot orientation with respect to the compass rose corresponds to the forcing wind direction (e.g. upper left plot refers to north-westerly winds). The vector length gives the current speed, vector direction relates to the current direction.

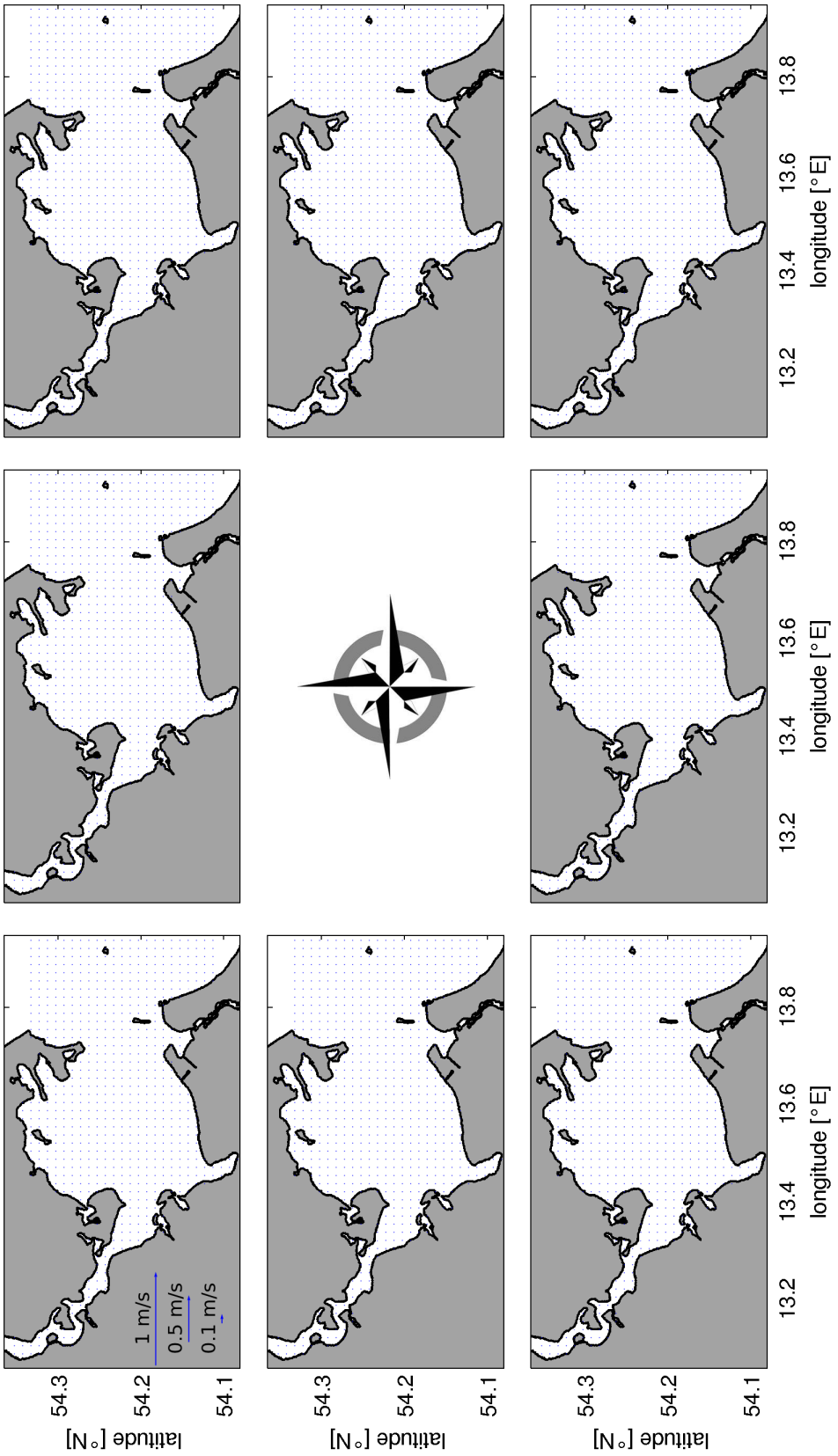

Figure 47: Simulated, depth averaged flow fields for constant wind speeds (1 m s^{-1}) and different wind directions. Plot orientation with respect to the compass rose corresponds to the forcing wind direction (e.g. upper left plot refers to north-westerly winds). The vector length gives the current speed, vector direction relates to the current direction.

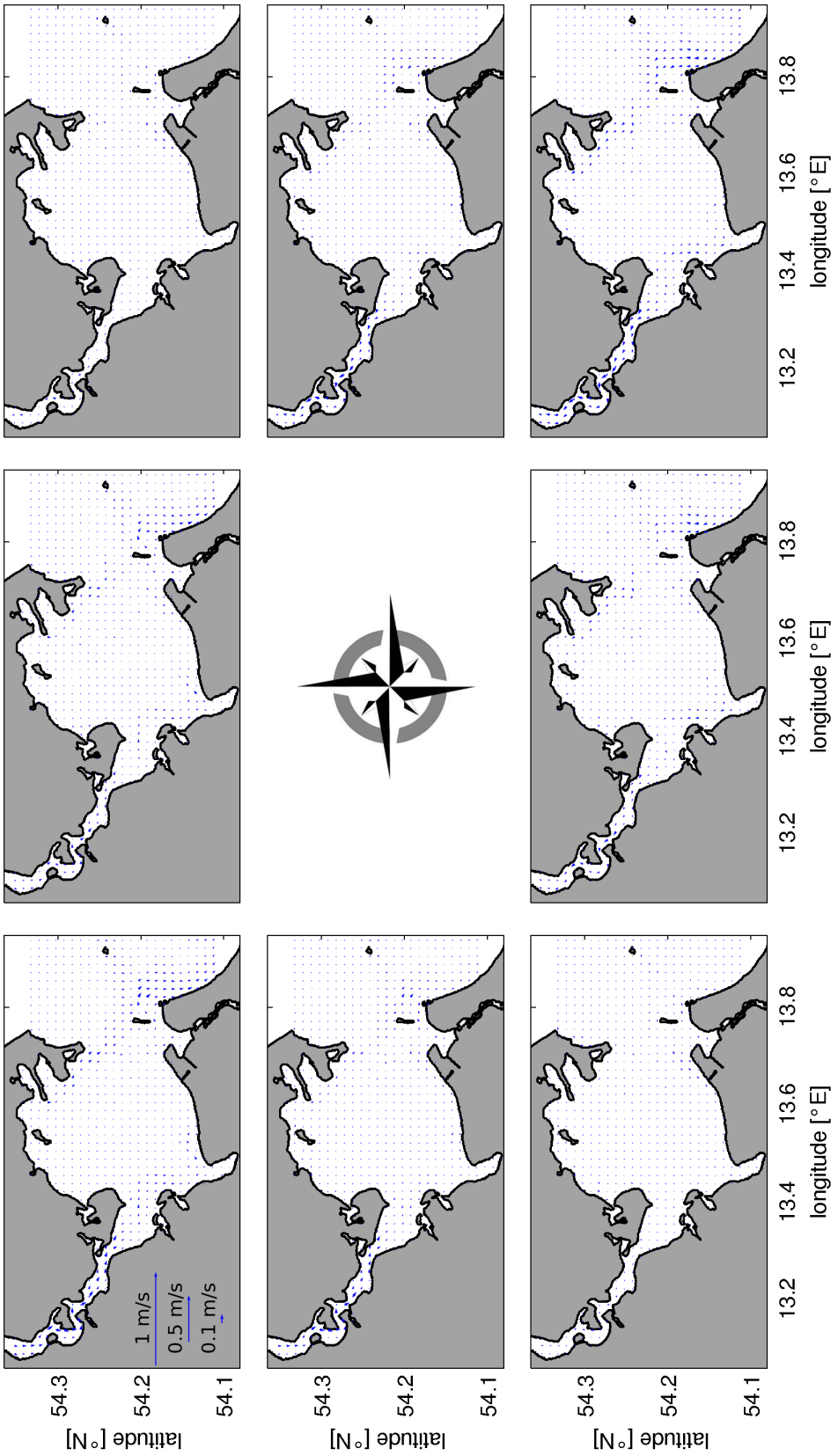

Figure 48: Simulated, depth averaged flow fields for constant wind speeds (3 m s^{-1}) and different wind directions. Plot orientation with respect to the compass rose corresponds to the forcing wind direction (e.g. upper left plot refers to north-westerly winds). The vector length gives the current speed, vector direction relates to the current direction.

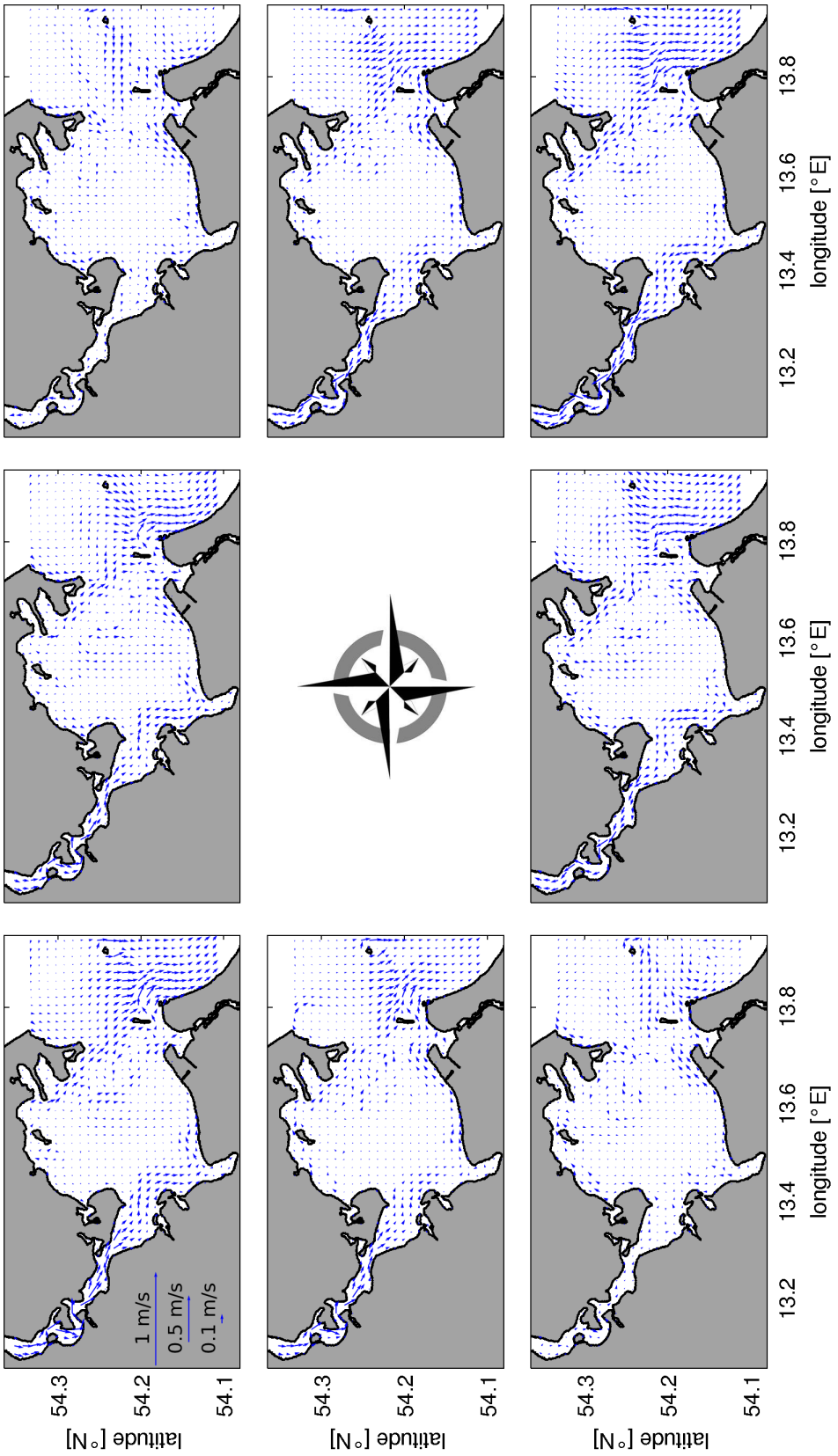

Figure 49: Simulated, depth averaged flow fields for constant wind speeds (6 m s^{-1}) and different wind directions. Plot orientation with respect to the compass rose corresponds to the forcing wind direction (e.g. upper left plot refers to north-westerly winds). The vector length gives the current speed, vector direction relates to the current direction.

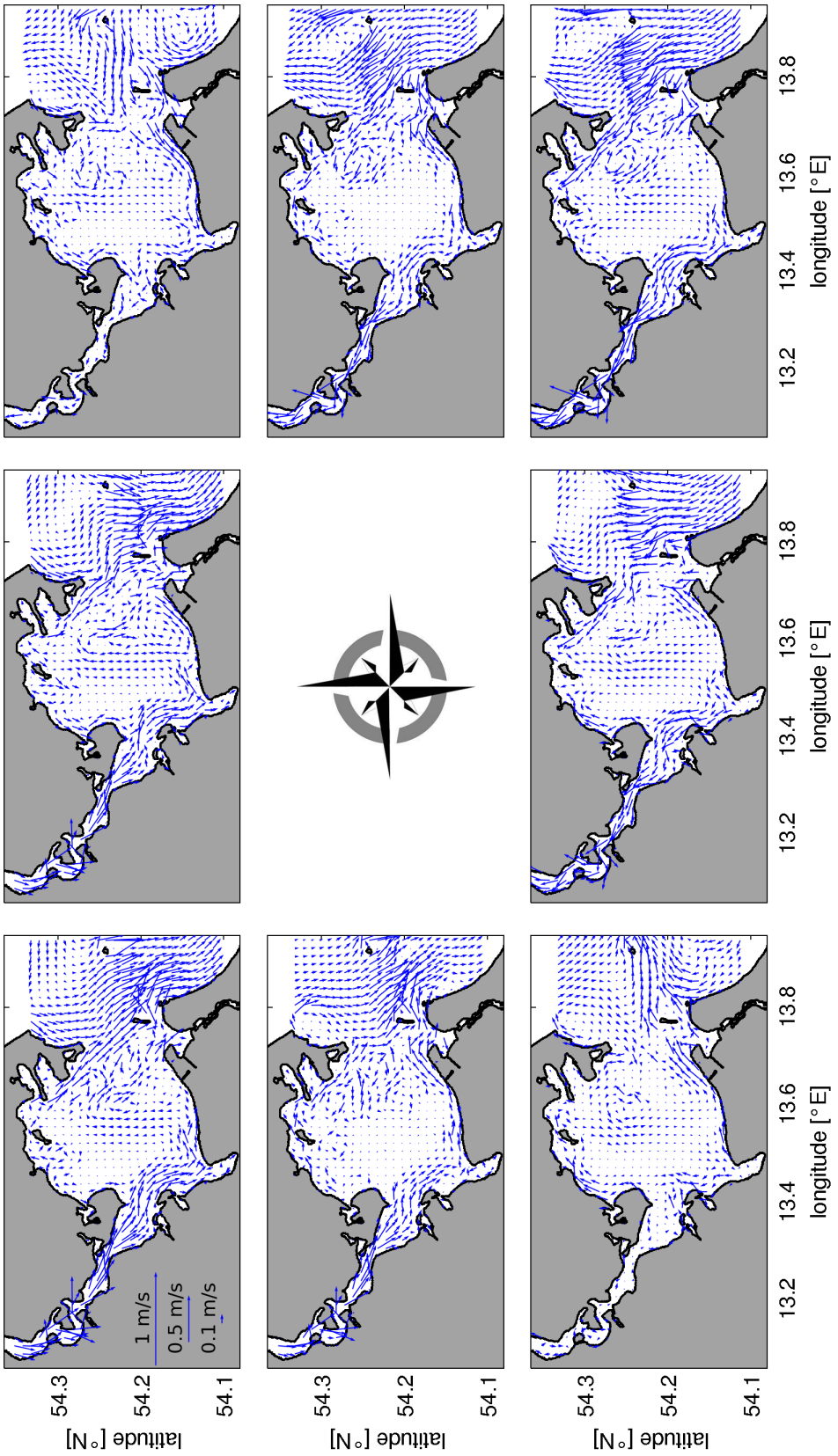

Figure 50: Simulated, depth averaged flow fields for constant wind speeds (9 m s^{-1}) and different wind directions. Plot orientation with respect to the compass rose corresponds to the forcing wind direction (e.g. upper left plot refers to north-westerly winds). The vector length gives the current speed, vector direction relates to the current direction.

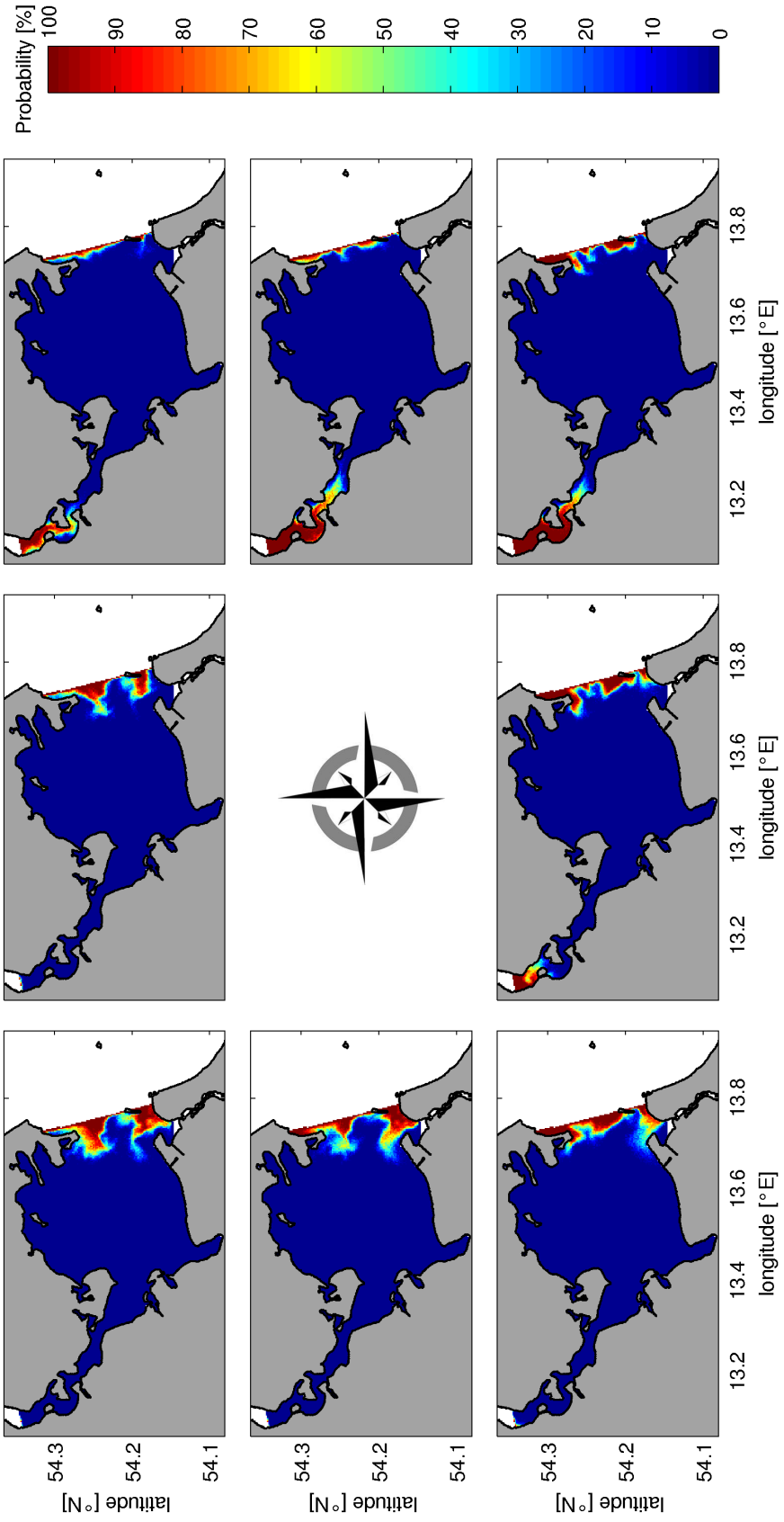

Figure 51: Spatially resolved probability to drift outside the lagoon, for particles exposed to wind speeds of 1 m s^{-1}. Plot orientation with respect to the compass rose corresponds to the forcing wind direction (e.g. upper left plot refers to north-westerly winds).

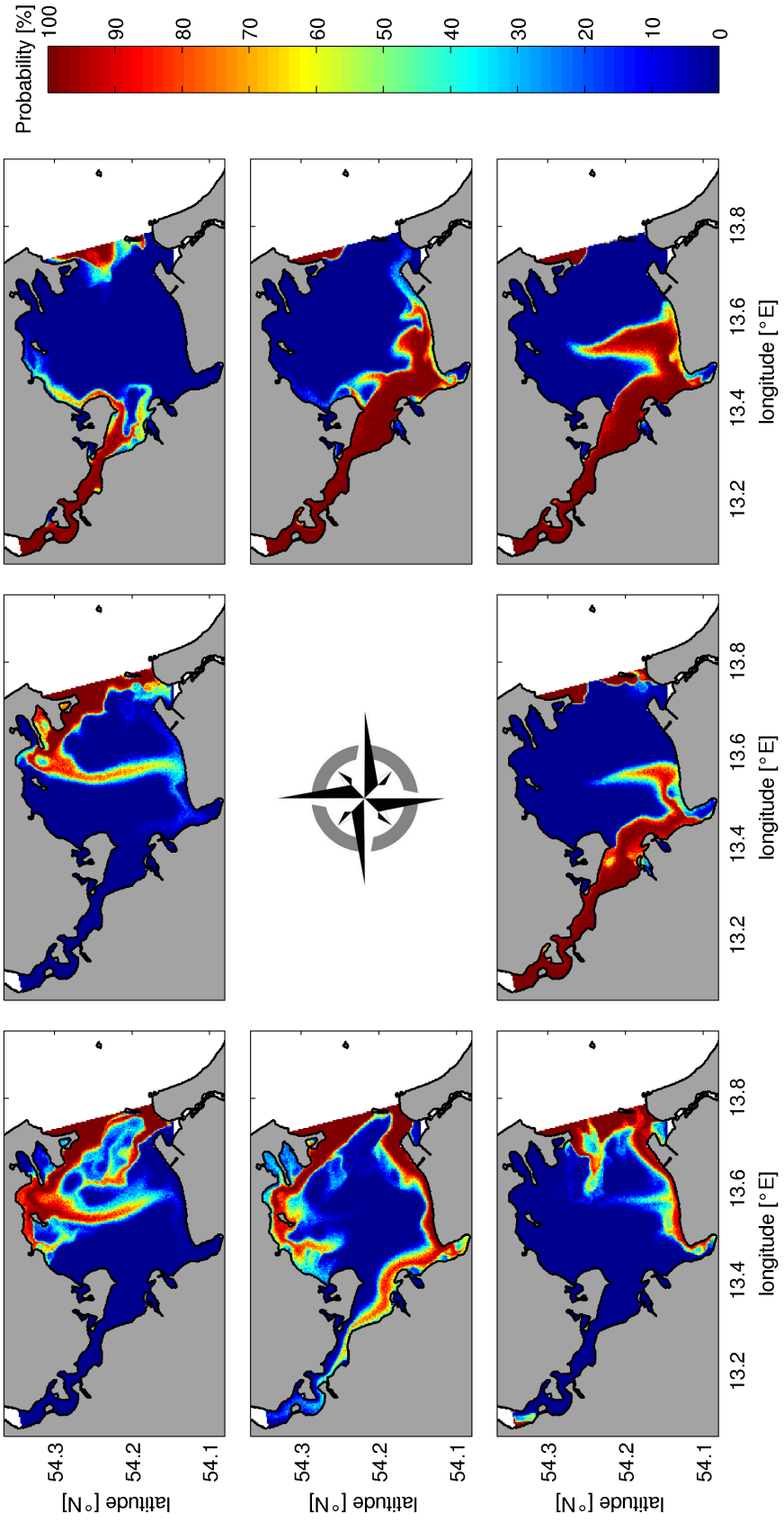

Figure 52: Spatially resolved probability to drift outside the lagoon, for particles exposed to wind speeds of 3 m s^{-1}. Plot orientation with respect to the compass rose corresponds to the forcing wind direction (e.g. upper left plot refers to north-westerly winds).

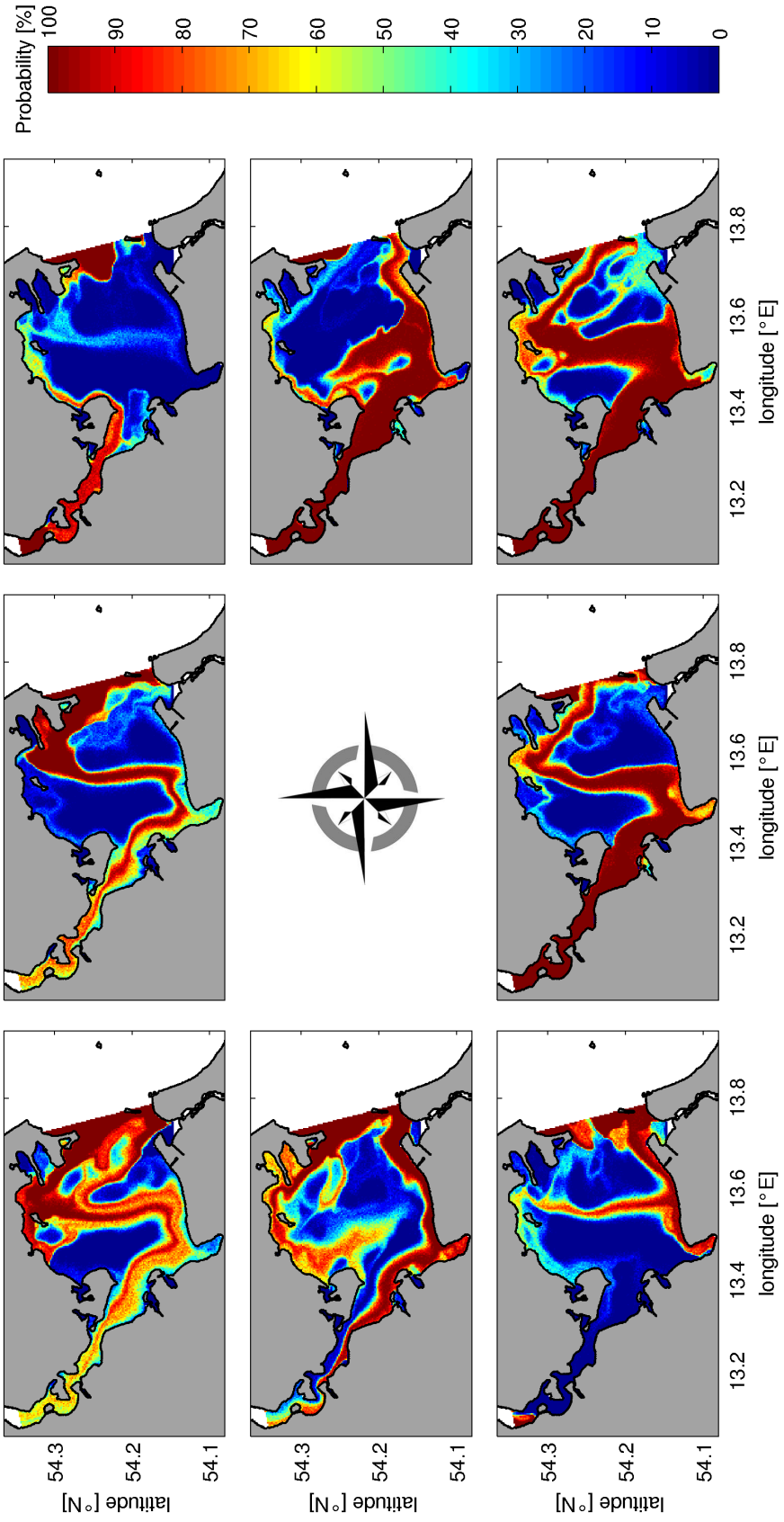

Figure 53: Spatially resolved probability to drift outside the lagoon, for particles exposed to wind speeds of 6 m s^{-1}. Plot orientation with respect to the compass rose corresponds to the forcing wind direction (e.g. upper left plot refers to north-westerly winds).

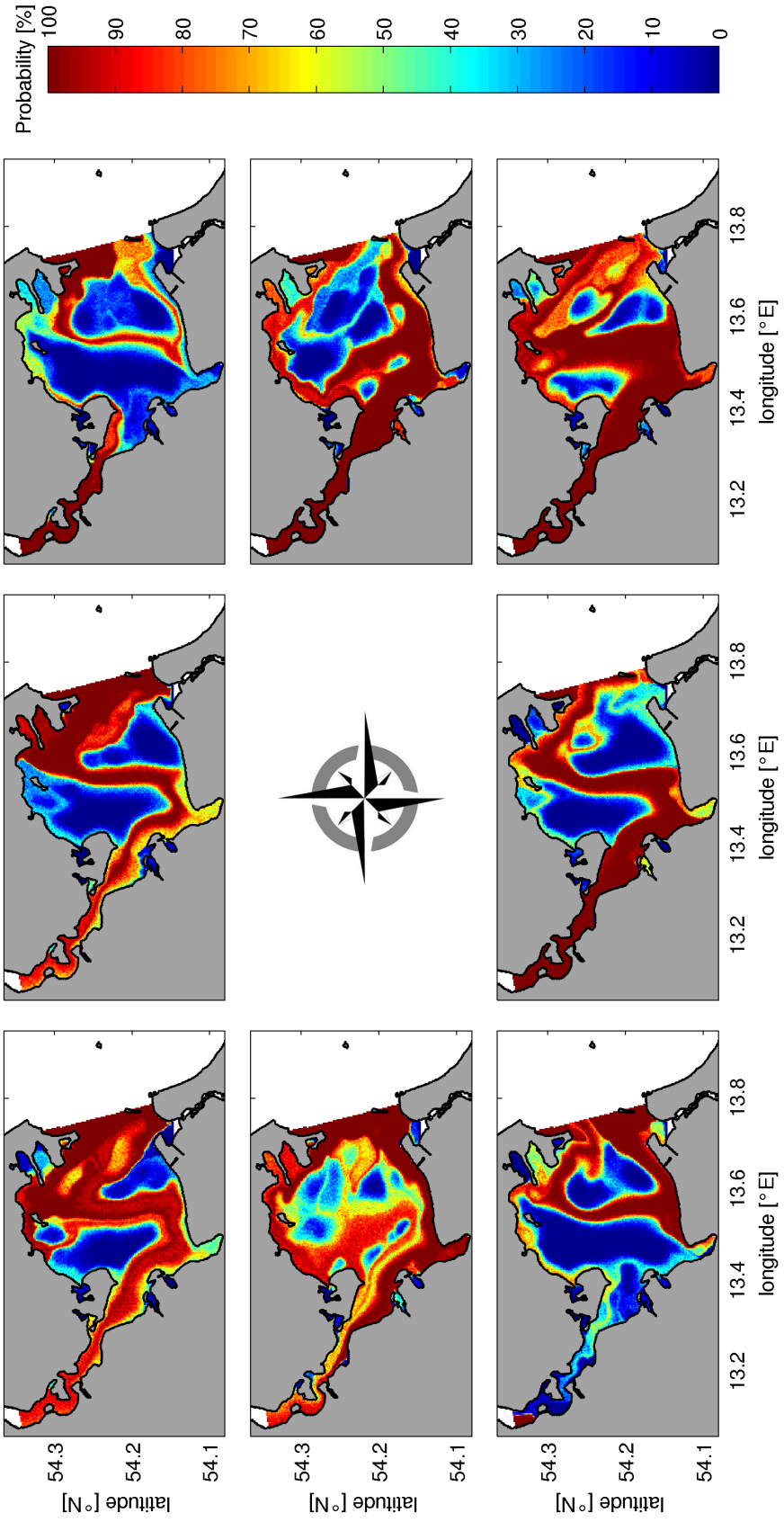

Figure 54: Spatially resolved probability to drift outside the lagoon, for particles exposed to wind speeds of 9 m s^{-1}. Plot orientation with respect to the compass rose corresponds to the forcing wind direction (e.g. upper left plot refers to north-westerly winds).

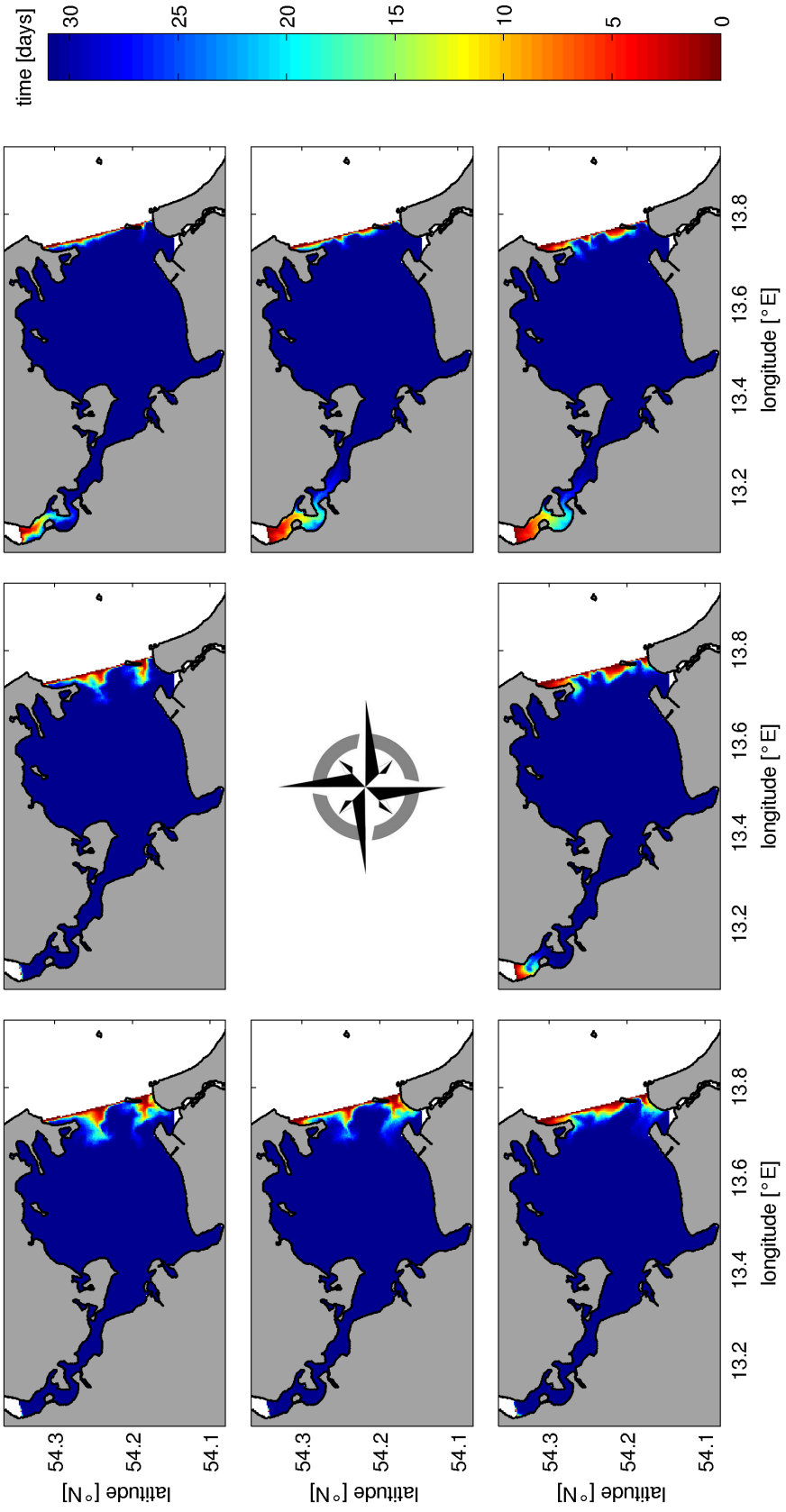

Figure 55: Spatially resolved residence time for particles exposed to wind speeds of 1 m s^{-1}. Plot orientation with respect to the compass rose corresponds to the forcing wind direction (e.g. upper left plot refers to north-westerly winds).

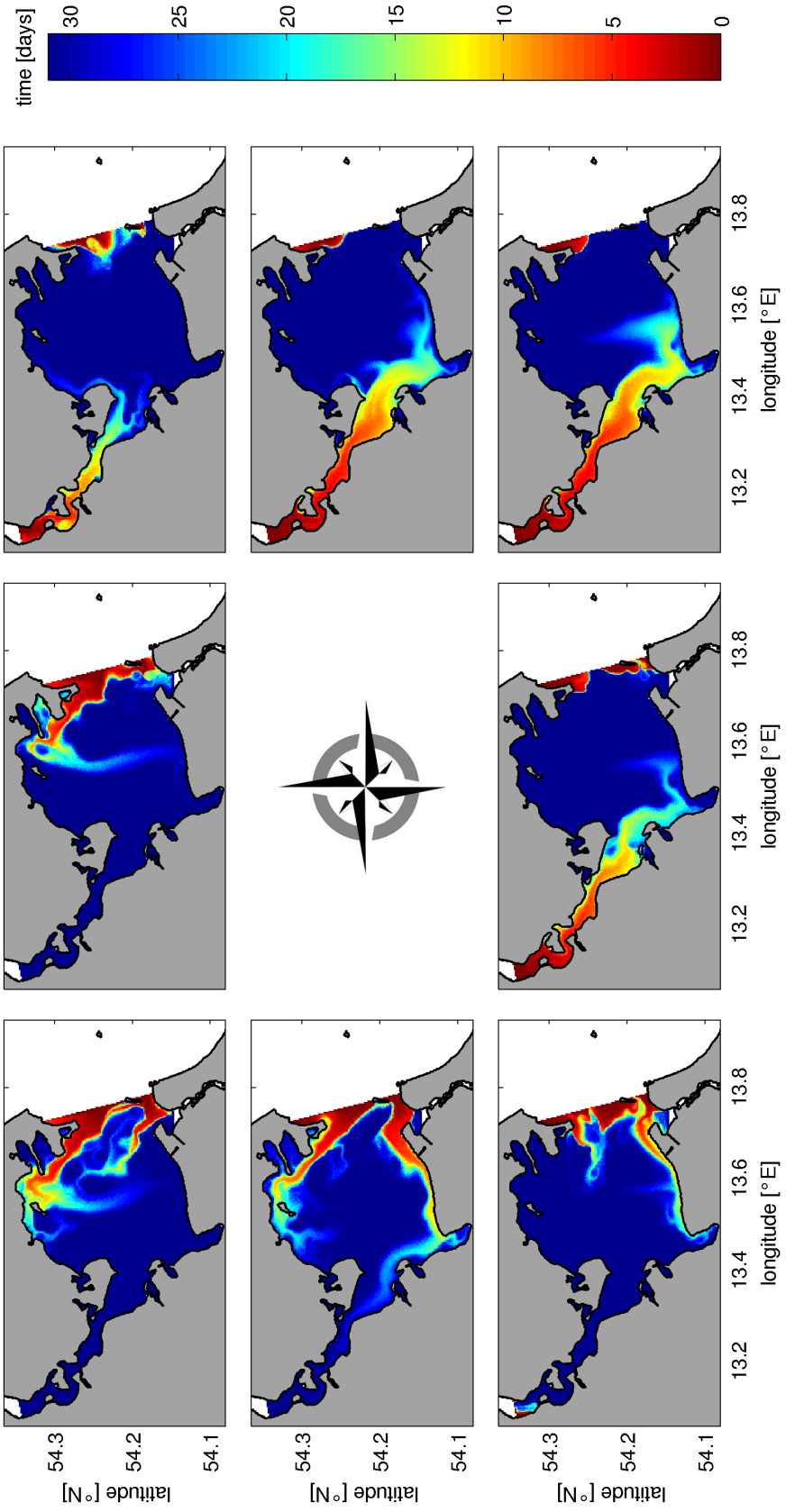

Figure 56: Spatially resolved residence time for particles exposed to wind speeds of 3 m s^{-1}. Plot orientation with respect to the compass rose corresponds to the forcing wind direction (e.g. upper left plot refers to north-westerly winds).

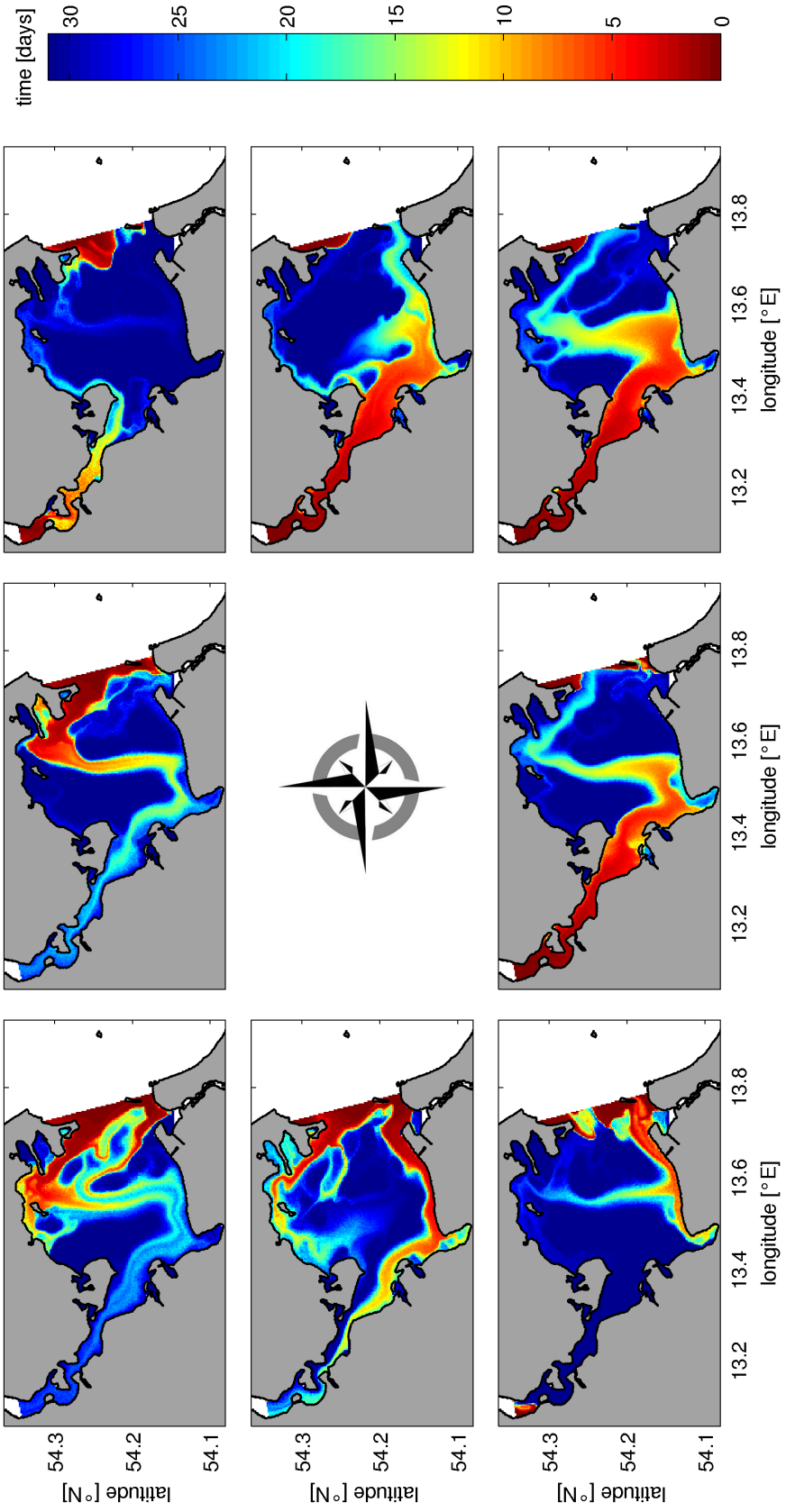

Figure 57: Spatially resolved residence time for particles exposed to wind speeds of 6 m s^{-1}. Plot orientation with respect to the compass rose corresponds to the forcing wind direction (e.g. upper left plot refers to north-westerly winds).

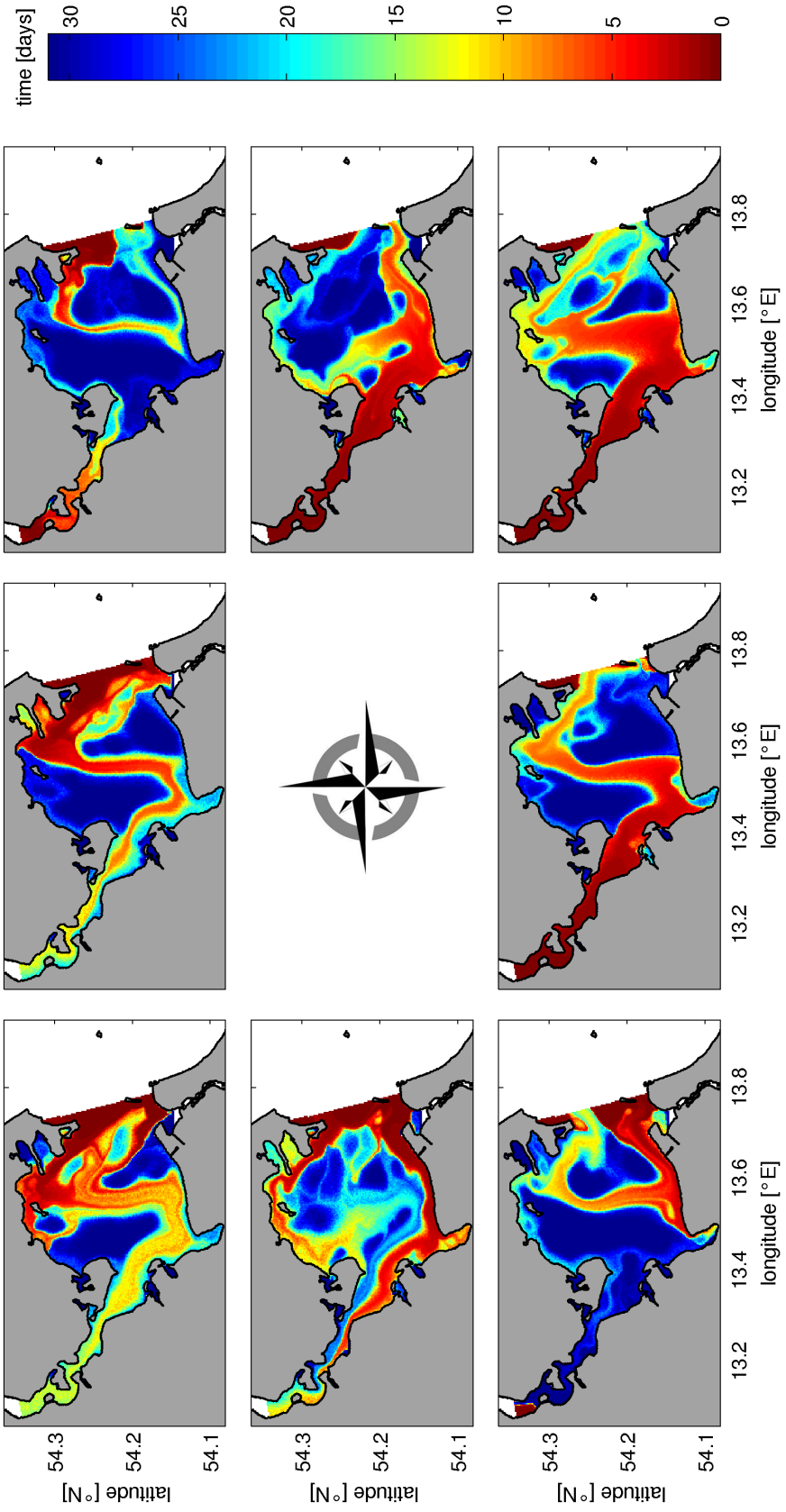

Figure 58: Spatially resolved residence time for particles exposed to wind speeds of 9 m s^{-1}. Plot orientation with respect to the compass rose corresponds to the forcing wind direction (e.g. upper left plot refers to north-westerly winds).

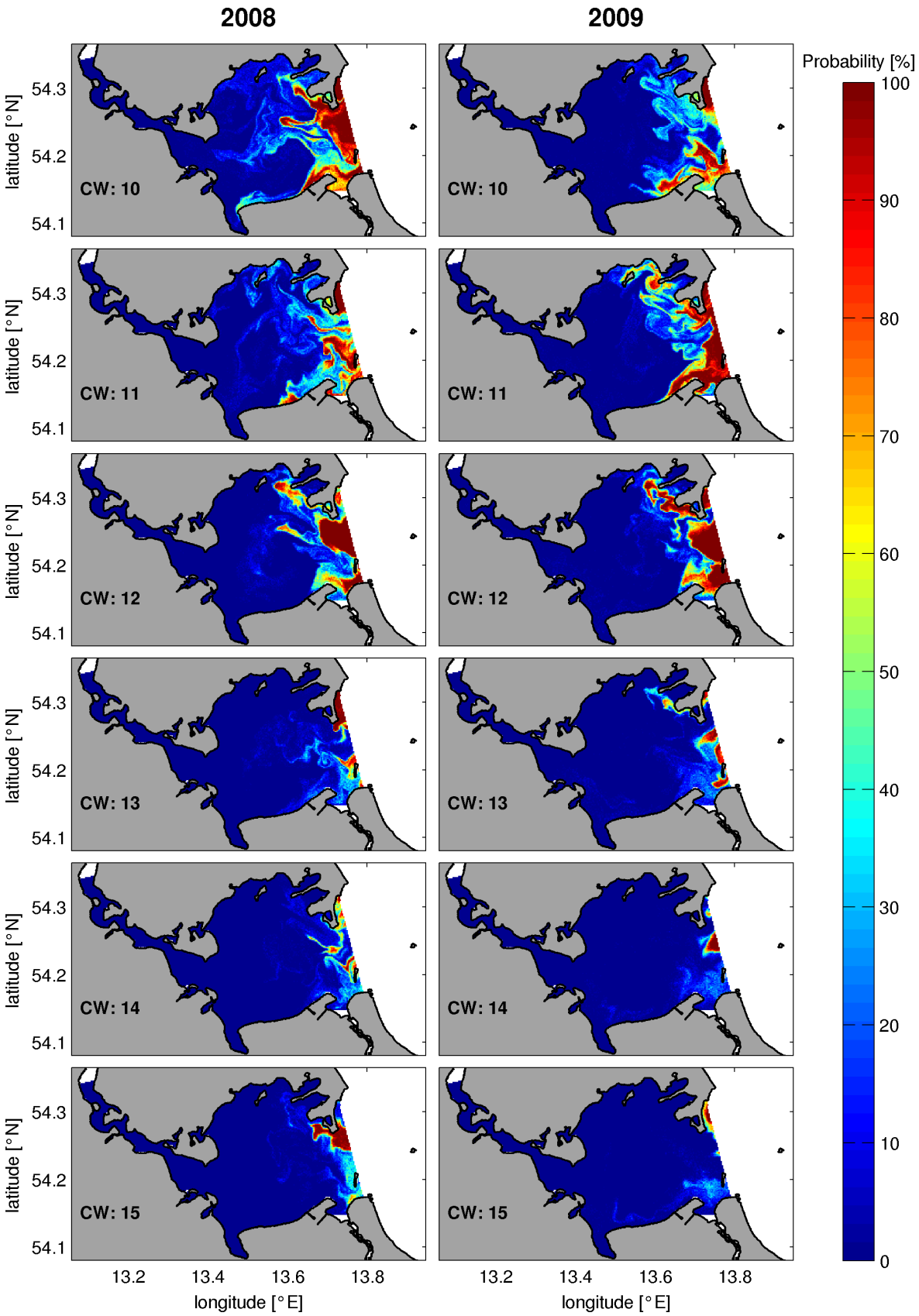

Figure 59: Spatially resolved probability to drift across the eastern sill, for particles which were seeded at the beginning of CW 10-15, given in percent.

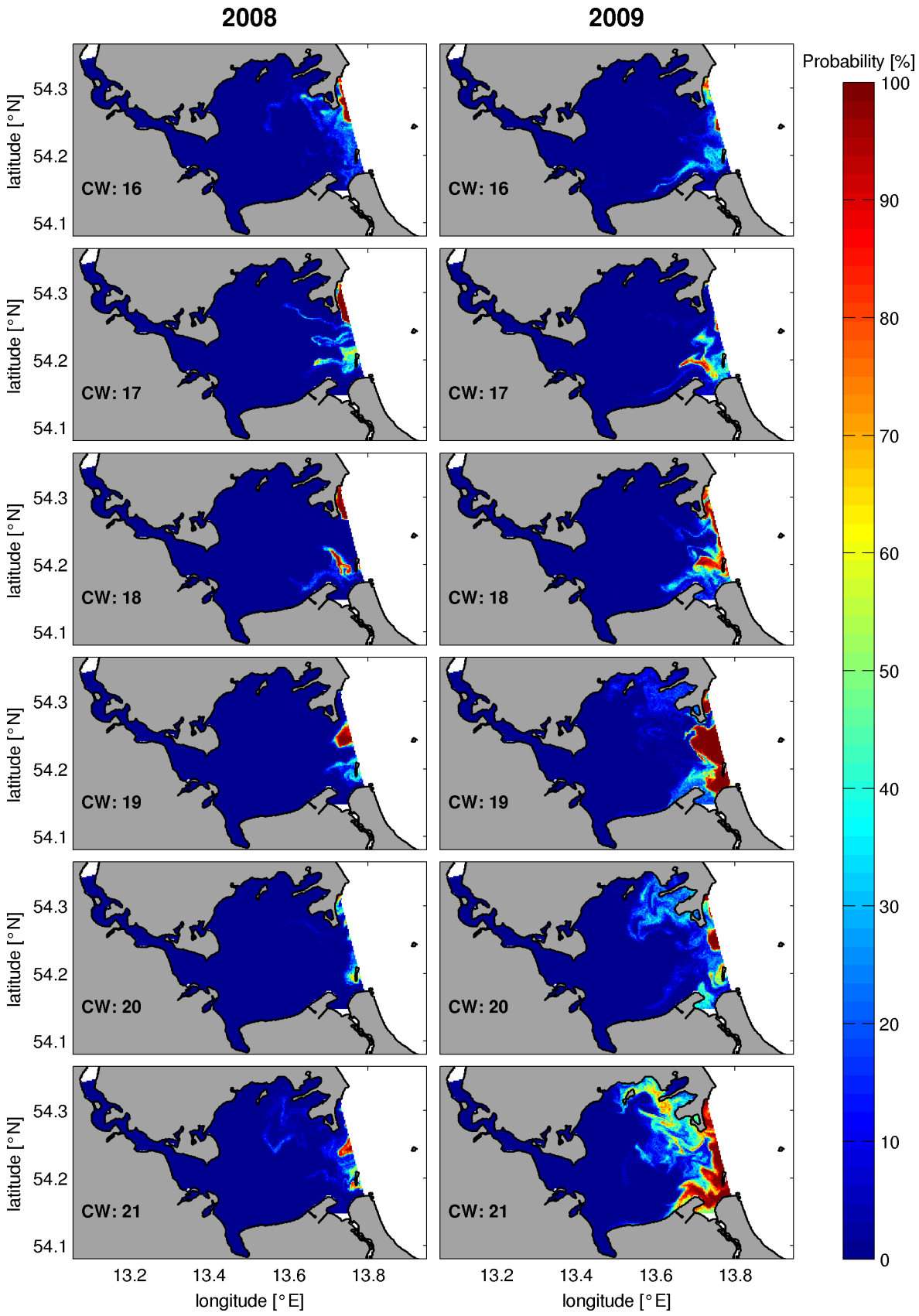

Figure 60: Spatially resolved probability to drift across the eastern sill, for particles which were seeded at the beginning of CW 16-21, given in percent.

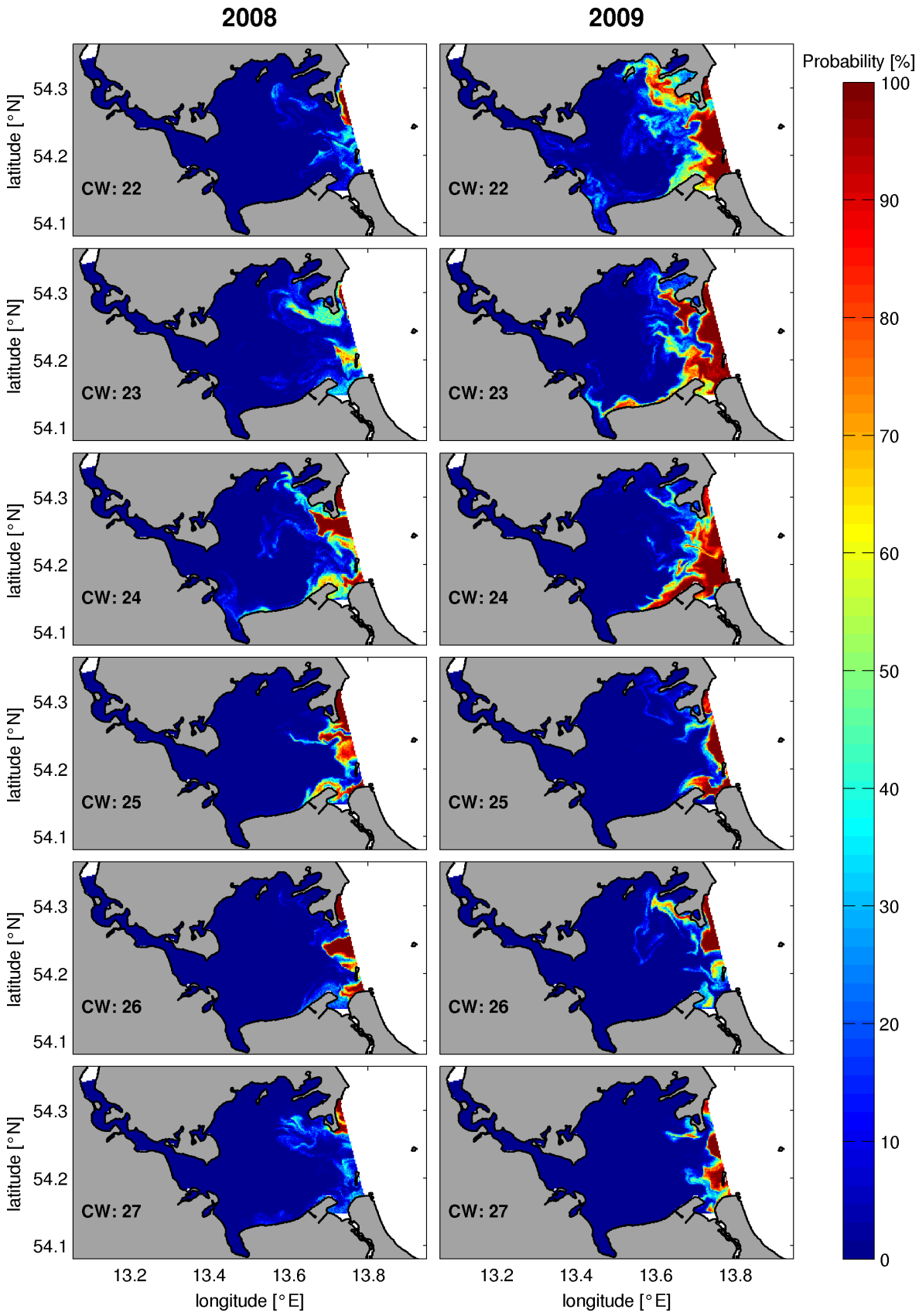

Figure 61: Spatially resolved probability to drift across the eastern sill, for particles which were seeded at the beginning of CW 22-27, given in percent.

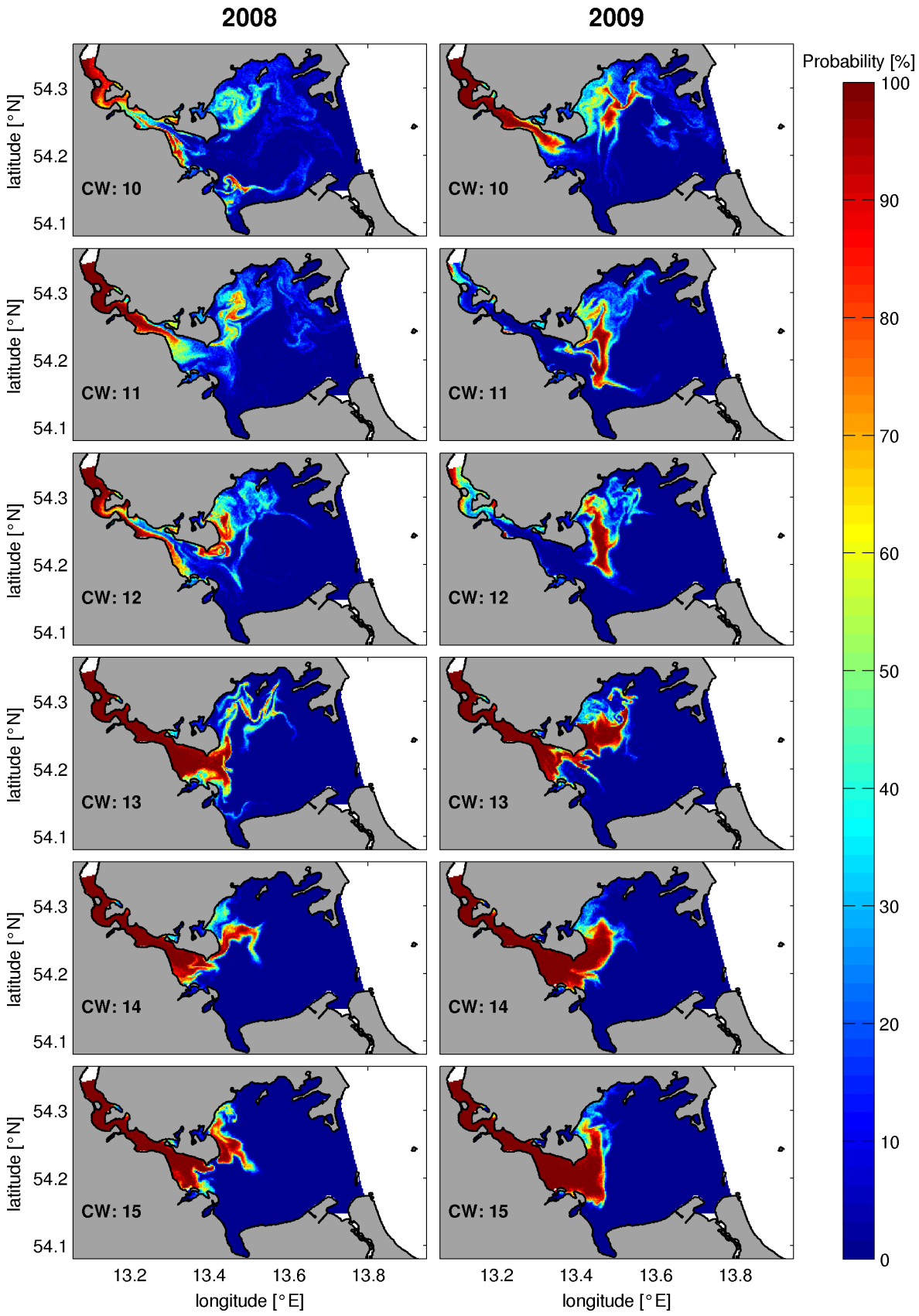

Figure 62: Spatially resolved probability to drift through the upper inlet of the Strelasund, for particles which were seeded at the beginning of CW 10-15, given in percent.

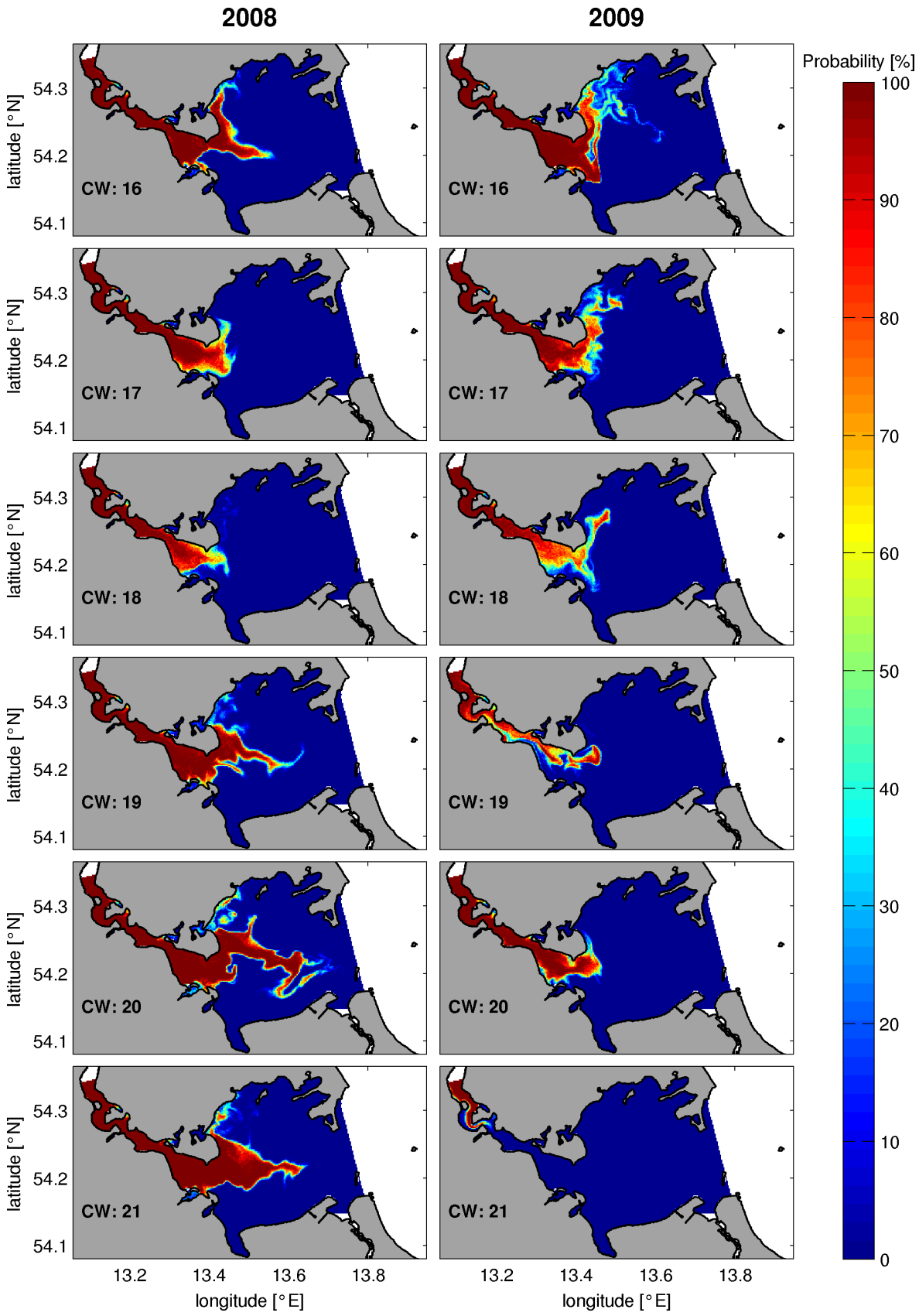

Figure 63: Spatially resolved probability to drift through the upper inlet of the Strelasund, for particles which were seeded at the beginning of CW 16-21, given in percent.

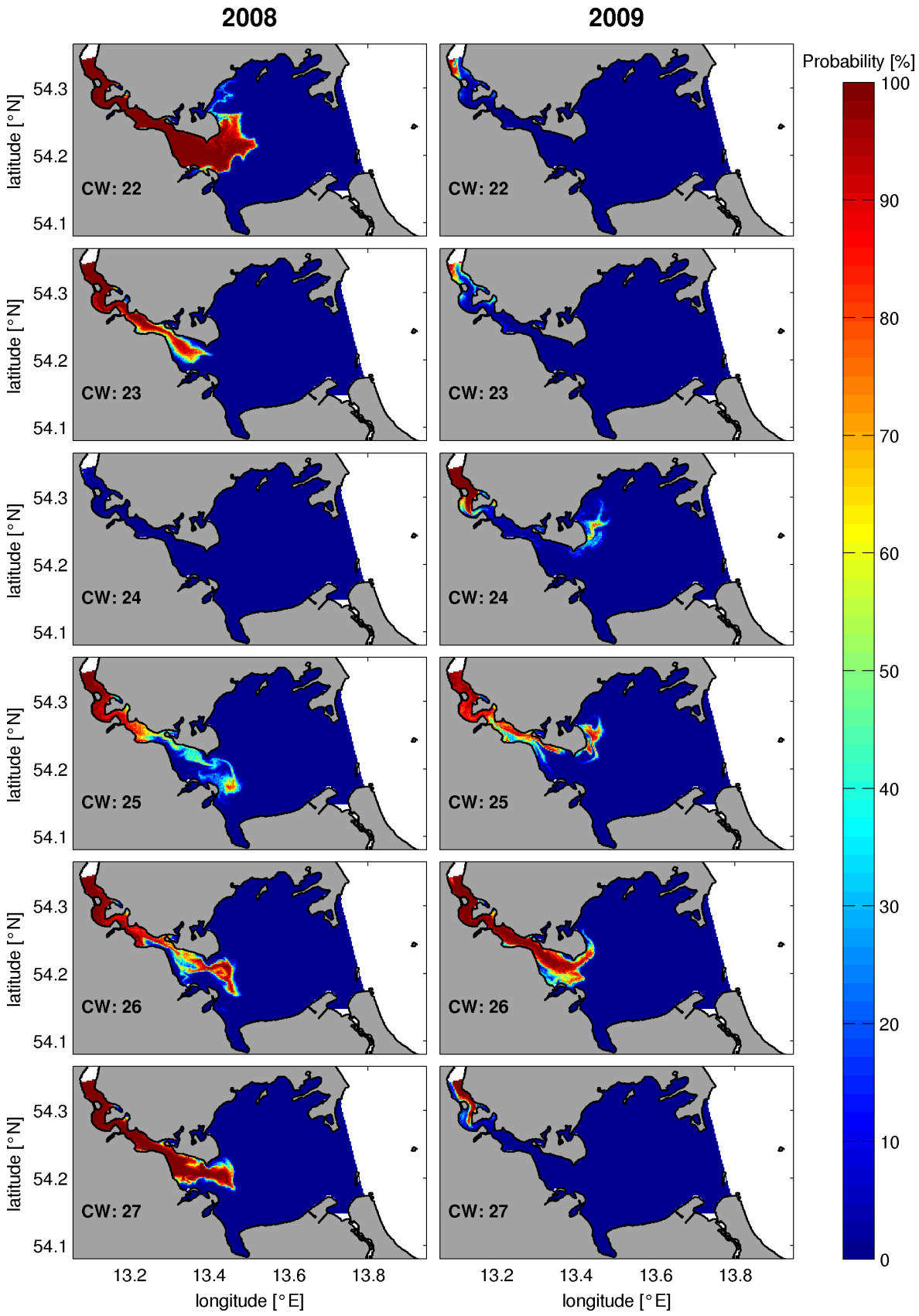

Figure 64: Spatially resolved probability to drift through the upper inlet of the Strelasund, for particles which were seeded at the beginning of CW 22-27, given in percent.

Acknowledgments

First of all, I would like to thank all the people who made this work possible, first of all Prof. Dr. Burchard and Dr. Ulf Gräwe who were quickly taken by idea of this interdisciplinary work. This thesis would not have been realized without their contribution and support. In particular, I would like to thank to Dr. Ulf Gräwe for his guidance, constructive criticism comments, ideas and constant willingness to help. The work with you has improved my skills in many ways. Thank you! I sincerely thank all of the members of the Physical Oceanography research group, especially Eefke van der Lee, Johannes Becherer, Peter Holtermann and Lennart Schüler. Their advice and help has made many things easier.

I am deeply thankful to Dr. Cornelius Hammer for supervising my work. My sincere thanks go to Dr. Christopher Zimmermann for providing input and ideas. I am very grateful to my mentor, Dr. Daniel Stepputtis, first because he came up with the idea of this study, but even more for his invaluable guidance and for devoting so much time and energy in pushing me forward. Daniel, it has been and it is still a real pleasure to work with you.

I would also like to thank all my friends. Their support means much to me.

Most of all, I would like to thank my family. Thank you for all your love and support!

Selbstständigkeitserklärung

Hiermit versiche ich, dass ich die vorliegende Arbeit selbständig verfasst und keine anderen als die angegebenen Quellen (siehe § 25, Abs. 7 der Diplomprüfungsordnung Biologie 2000) und Hilfsmittel verwendet habe. Mir ist bekannt, dass gemäß § 8, Abs. 3 der Diplomprüfungsordnung Biologie 2000 die Prüfung wegen einer Pflichtwidrigkeit (Täuschung u.ä.) für nicht bestanden erklärt werden kann.

Rostock, den 15.08.2011

Robert Bauer